CHARACTERIZATION OF CRICKET PARALYSIS VIRUS-HOST INTERACTION AND VIRAL PROTEIN SYNTHESIS

by

Anthony Khong

B.Sc., The University of British Columbia, 2008

A THESIS SUBMITTED IN PARTIAL FULFILLMENT OF

THE REQUIREMENTS FOR THE DEGREE OF

DOCTOR OF PHILOSOPHY

in

THE FACULTY OF GRADUATE AND POSTDOCTORAL STUDIES

(Biochemistry and Molecular Biology)

THE UNIVERSITY OF BRITISH COLUMBIA

(Vancouver)

August 2015

Abstract

Viruses are obligate parasites that have evolved strategies to recruit the translational machinery and inhibit antiviral defences. A relatively abundant family of positive-sense, monopartitate single stranded RNA viruses, dicistrovirus, remains relatively uncharacterized. Dicistroviruses are infectious to arthopods and have impacted a number of agricultural industries. Dicistroviruses, as indicated by their name, contain two open reading frames (ORFs). The 5'-untranslated internal ribosome entry site (5'-UTR IRES) directs translation of ORF1 which encodes non-structural proteins and the intergenic (IGR) IRES directs translation of ORF2 which encodes structural proteins. How dicistroviruses affect the host is not completely understood. My thesis focuses on several host pathways that are modulated during cricket paralysis virus (CrPV) infection, a model dicistrovirus. During CrPV infection, I discovered stress granule (SG) formation is inhibited but granules containing poly(A)$^{+}$ mRNAs form. Furthermore, I discovered a viral protein, CrPV 1A, that inhibits the SG pathway. Upon further characterization of CrPV 1A, I discovered the viral protein also stimulates 5'-dependent translation and 5'IRES dependent translation. Finally, I found IGR IRES-dependent translation is delayed compared to 5'-UTR IRES-dependent translation, thus providing a viral strategy of expressing non-structural proteins such as the replicase and protease prior to the synthesis of structural proteins for viral packaging. This thesis provides insights into the key strategies of dicistrovirus infection, its viral life cycle and the innate immune responses in insect cells.

Preface

A version of Chapter 2 has been published: Khong, A., Jan, E. (2010). Modulation of Stress Granules and P bodies during Dicistrovirus Infection. *Journal of Virology*. 85(4):1439-1451. I conducted all the experiments and data analysis. Dr. Jan, E. helped interpret and write the manuscript.

In figure 3.6A-B, Dr. Wang Q.S. performed these experiments and contributed data analysis.

In figure 4.4A-C, Dr. Jan E. performed these experiments and data analysis.

Copyrighted materials presented herein are adapted for this thesis.

Table of Contents

List of Tables

List of Figures

List of Symbols and Abbreviations

2C: superfamily 3 helicase

3C: chymotrypsin-like cysteine protease for processing viral proteins

4E-BP: eIF4E-binding protein

5'-UTR: 5'-untranslated region

ABPV: acute bee paralysis virus

Act D: Actinomycin D

Ago1: argonaute 1

Ago2: argonaute 2

Ars: arsenite

avSG: antiviral SG

CHICKV: chikungunga virus

CITE: 3'-cap independent translation element

CrPV: cricket paralysis virus

CSFV: classical swine fever virus

Cy3: cyanine dye 3

Cy5: cyanine dye 5

Cys: cysteine

DCP1: decapping protein 1

DCV: *drosophila* C virus

DENV: dengue virus

DMSO: dimethyl sulfoxide

dsAGO2: dsRNAs targeting Ago2 RNA

dsFL: dsRNAs targeting firefly luciferase RNA

dsGFP: dsRNAs targeting GFP RNA

dsRED: discosoma red fluorescent protein

dsRNA: double-stranded RNA

DTT: di-thiothreitol

EDTA: ethylenediaminetetraacetic acid

EMCV: encephalomyocarditis

FMDV: foot and mouth disease virus

FMR1: fragile X mental retardation protein 1

FRAP: fluorescence recovery after photobleaching

G3BP: GTPase binding protein

GADD34: growth arrest and DNA damage-inducible protein

GAPDH: glyceraldehyde 3-phosphate dehydrogenase

GCN2: general control nonderepressible 2

GFP: green fluorescent protein

GW182: glycine-tryptophan rich protein of 182kDa

HA: hemagluttinin

HAV: hepatitis A virus

HCV: hepatitis C virus

HDAC: histone deacetylase

HIV: human immunodeficiency virus

hpi: hours post infection

HRI: heme-regulated inhibitor kinase

IAPV: Israeli acute paralysis virus

IFN: interferon

IGR: intergenic

IRES: internal ribosome entry site

ITAFs: IRES transacting factors

ITIF: IRES transinactivating factor

KBV: Kashmir bee virus

Met: methionine

miRNA: microRNA

MOI: multiplicity of infection

mRNA: messenger RNA

mRNP: messenger ribonucleoprotein

OAS2: 2'-5'-oligoadenylate synthase 2

O-GlcNAc: O-linked N-acetylglucoasmine

ORF: open reading frame

PABP: poly(A) binding protein

PAGE: polyacrylamide gel electrophoresis

PatA: pateamine A

PBs: P-bodies

PBS: Phosphate buffered saline

PCR: polymerase chain reaction

PERK: protein kinase RNA-like endoplasmic reticulum kinase

PIC: preinitiation complex

PKI: pseudoknot 1

PKR: protein kinase R

PSIV: plautia stali intestine virus

PV: poliovirus

RdRp*, RdRp**, RdRp***: viral polyproteins containing unprocessed RdRp

RdRp: RNA-dependent RNA polymerase

RFP: red fluorescent protein

RhPV: rhapdosilum padi virus

RIG-1: retinoic acid-inducible gene 1

Rin: rasputin

RISC: RNA-induced silencing complex

RNAi: RNA interference

rRNA: ribosomal RNA

RT-PCR: Reverse transcription polymerase chain reaction

SBV: sindbis virus

SDS: sodium dodecyl sulfate

SFV: semliki forest virus

SG: stress granule

sgRNA: Subgenomic mRNA

SILAC: stable isotope labeling of amino acids in cell culture

siRNA: smal interfering RNA

SSM3: Shields and Sang M3 insect media supplemented with 10% fetal bovine serum

TC: ternary complex

TCV: turnip crinckle virus

TIA-1: T cell intracellular antigen 1

TIAR: TIA-1-related protein

TNFα: Tumor necrosis factor alpha

TSV: Taura syndrome virus

UV: ultraviolet

VacV: vaccinia virus

VSV: vesicular stomatis virus

WNV: west nile virus

ΔPK1: mutation that inactivates IGR IRES activity

Acknowledgements

I would like to thank Dr. Eric Jan for the past 7 years. His passion and drive is inspirational. In addition, I want to thank him for all his help with this thesis and our publications.

I would like to thank all the graduate students and post doctoral fellows: Dr. Julianne Garrey, Yun-Young Lee, Dr. Chris Jang, Qian Ren, Hilda Au, Julienne Jagdeo, Craig Kerr, and Dr. Qing Wang. The lab felt like a second home because of all these individuals. They are so friendly and their advice in the lab has helped me in my career.

I would also like to thank Dr. Michel Roberge and Dr. George Mackie for being my committee members and for reading and critiquing my thesis.

I would also like to thank UBC and NSERC for financial support.

Finally, I would like to thank a very special person in my life. She devoted so much financially and emotionally in my life and for my future. There is and never will be anyone like her. Thank you mom!

Chapter 1 Introduction

1.1 Overview

Despite a compact genome that encodes relatively few proteins, RNA viruses have evolved mechanisms to subvert the host translational machinery, dampen antiviral host responses and replicate their own genomes (Flint et al., 2009). All RNA viruses must rely on the host translational machinery to promote viral protein synthesis. Thus, RNA viruses have evolved many strategies to usurp the translational machinery. My thesis is focused on cricket paralysis virus (CrPV) as a model to study the interplay between the virus and host with a particular focus on how the virus hijacks the ribosome. In this Chapter, I provide a review of eukaryotic cap-dependent translation initiation, internal ribosome entry site (IRES) dependent translation, translational regulation, stress granules (SGs) and dicistroviruses. In addition, relevant examples of viruses targeting translation and affecting SGs are described.

1.2 Eukaryotic cap-dependent translation initiation

Most messenger RNAs (mRNAs) in eukaryotes are translated by a cap-dependent mechanism (reviewed in Hinnebusch and Lorsch, 2012; Jackson et al., 2010). Eukaryotic translation initiation can be further divided into a number of sub-steps: (i) eIF4F binding to the 5'-7-methylguanosine (m^7G) cap on the mRNA, (ii) recruitment of the 43S preinitation complex (PIC) to the mRNA, (iii) PIC scanning along the 5'-UTR to locate the start codon, and (iv) recruitment of the 60S subunit to form the 80S ribosome. Only translation initiation is described in depth as this is the focus of my thesis.

Cap-dependent translation begins when eIF4F (a complex including eIF4E, eIF4G, and eIF4A) binds to the m^7G cap on the mRNA (reviewed in Hinnebusch and Lorsch, 2012; Jackson et al., 2010). The m^7G cap is a modified guanine nucleotide that is linked through a 5'-5'-triphosphate bond to the first nucleotide (Meyer and Jaffrey, 2014). The cap binding protein eIF4E recognizes and binds to the m^7G cap. This interaction is enhanced by an eIF4E interacting partner, the scaffold protein eIF4G. eIF4G also interacts with eIF4A, poly(A) binding protein (PABP), and eIF3. The interaction of eIF4G and PABP promotes a stable closed loop structure that effectively circularizes the mRNA and subsequently synergizes translation (Figure 1.1) by enhancing recruitment of the PIC (Figure 1.1).

Another eIF4F component, eIF4A, is a DEAD-box RNA helicase that can be in an inactive 'open' or active 'closed' state (Hilbert et al., 2011; Nielsen et al., 2011; Oberer et al., 2005; Ozes et al., 2011; Schutz et al., 2008). eIF4G anchors eIF4A to the mRNA and promotes an active 'closed' state. Facilitated by ATP, eIF4B, and eIF4H, eIF4A unwinds secondary structures in the 5'-UTR to create a single stranded "landing pad" where the PIC can bind to the mRNA (Figure 1.1).

The mRNA is now primed to recruit the 43S PIC (Figure 1.1) (reviewed in Hinnebusch and Lorsch, 2012; Jackson et al., 2010). eIF4G binds to eIF3, a large protein complex consisting of 13 subunits (a-m). eIF3 is part of the 43S PIC which includes the 40S ribosomal subunit, eIF1, eIF1A and the ternary complex (TC). The TC is composed of the GTP-bound form of eIF2 and the initiator methionyl-tRNA (Figure 1.1).

After recruitment to the cap, the 43S PIC complex scans along the 5'-UTR for the start codon. Scanning is an ATP driven process that is facilitated by eIF1 and eIF1A. Specifically, eIF1 and eIF1A promote an "open" conformation within the PIC which is conducive for base-by-base inspection during scanning (Figure 1.1) (Passmore et al., 2007; Pestova and Kolupaeva, 2002). Supporting this model is a recent cryo-EM structure of a partial 43S complex in which the initiator Met-tRNA$_i$ is ~7 Å away from the ribosomal P site (Hashem et al., 2013). Unless the 5'-UTR is short and unstructured, scanning is also dependent on eIF4A or other helicases. For highly structured RNAs, DHX29, DeXH box protein 29, or DDX3, DEAD box protein 3, facilitate scanning (Berthelot et al., 2004; Pisareva et al., 2008).

Start codon recognition is mediated by eIF1, eIF1A, eIF2, and helix 44 of the 18S ribosomal RNA (rRNA) (Cheung et al., 2007; Fekete et al., 2007; Pisarev et al., 2006). For efficient translation initiation, the AUG start codon with an optimal context, Kozak consensus, is recognized by the PIC. Optimal context includes a purine at the -3 position and a guanosine at the +4 position relative to the adenosine (+1) of the AUG (Kozak, 1984, 1986). Recent cyro-EM structures suggest that the -3 position and +4 nucleotide are "sensed" by eIF2 and eIF1A (Hussain et al., 2014).

Following the identification of an AUG codon in a preferred context, the PIC undergoes a rearrangement driven by eIF5 (Maag et al., 2005). In this process, eIF1 is ejected from the complex and GTP bound to eIF2 is hyrolyzed (Algire et al., 2005; Kapp and Lorsch, 2004). After eIF1 ejection, the PIC assumes a "closed" conformation and the methionyl-tRNA is fully engaged within the P site of the 40S ribosome (Figure 1.1) (Hussain et al., 2014; Passmore et al., 2007). Once the PIC is in a "closed"

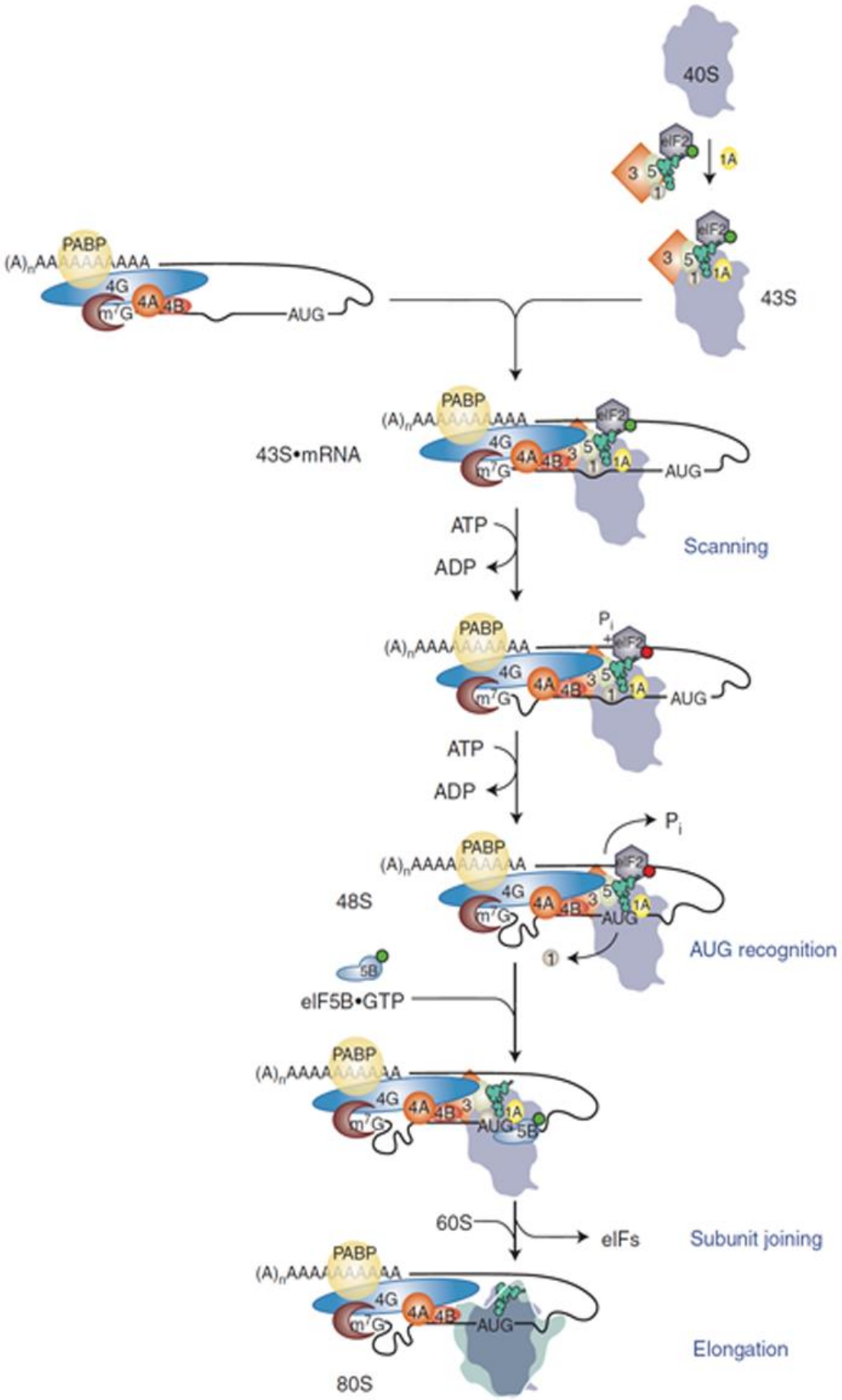
40S
eIF2
1A
3
5
1
PABP
(A)nAAAAAAAAAA
4G
4A
4B
m7G
AUG
43S
43S•mRNA
ATP
ADP
Scanning
Pi
48S
AUG recognition
5B
eIF5B•GTP
60S
eIFs
Subunit joining
80S
Elongation

Figure 1.1 Schematic of cap-dependent translation initiation in eukaryotes. Cap-dependent translation initiation can be grouped into three distinct steps: formation of 43S-mRNA complex, scanning, and recognition of authentic AUG codon and 60S subunit joining. The formation of 43S-mRNA complex occurs when the 40S ribosome, ternary complex (met-tRNAi and eIF2-GTP), eIF1, eIF1A, eIF5, and eIF3, bind to mRNAs containing eIF3, PABP, eIF4B, eIF4G, eIF4E, and eIF4A. Upon complex formation, guided by eIF1 and eIF1A, scanning occurs until the PIC finds an authentic AUG codon. Once an AUG codon is found, hydrolysis of eIF2-GTP occurs and eIF5 ejects eIF1 and promotes a "closed" conformation where the initiator met-tRNA is fully engaged within the P-site of the 40S ribosome. Structural rearrangements within the 40S and eIF5B-GTP joining facilitate 60S joining. Finally, eIF5B-GTP hydrolysis triggers structural rearrangements that alter the 80S from initiation to elongation mode. Adapted from Hinnebusch, A.G., and Lorsch, J.R. (2012).

---

confirmation, eIF2-GDP and other initiation factors within the PIC dissociate and the 60S subunit joins. Specifically, eIF5B-GTP binds to the 40S complex via eIF1A and facilitates 60S subunit joining and formation of the 80S ribosome (Pestova et al., 2000). Subsequently, energy provided by GTP hydrolysis from eIF5B alters the 80S structure from an initiation to an elongation mode (Figure 1.1)(reviewed in Aitken and Lorsch, 2012; Hinnebusch, 2011; Lorsch and Dever, 2011; Parsyan, 2011, Hinnebusch and Lorsch, 2012). At this stage, the ribosome is ready for the delivery of the next aminoacyl-tRNA and elongation begins.

1.3 Cap-independent translation initiation by internal ribosome entry sites

An alternative mechanism of translation initiation is through internal ribosome entry sites (IRES) (reviewed in Kieft, 2008; Komar and Hatzoglou, 2011). IRESs, which

are found in a subset of viral and cellular mRNAs, are generally highly structured, can recruit ribosomes independently of the m^7G cap and require fewer translation initiation factors than cap-dependent translation. Because of the decreased factor requirements, translation of mRNAs containing IRES elements is generally resistant or enhanced during cellular stress or viral infection.

The first IRESes were discovered in poliovirus (PV) and encephalomyocarditis virus (EMCV) (Jang et al., 1988; Pelletier and Sonenberg, 1988). The standard test for an IRES is the bicistronic assay. Specifically, the 5'-untranslated region (5'-UTR) of PV and EMCV RNA is inserted between two ORFs. Translation of the second ORF is only permitted if ribosomes can be recruited internally within the mRNA (Jang et al., 1988; Pelletier and Sonenberg, 1988). After the discovery of these two IRESs, many IRESs were found in other viruses and in a subset of cellular mRNAs (reviewed in Kieft, 2008). Since my thesis is focused on the CrPV IRESs (Chapter 4), I will place a greater emphasis on describing viral IRESs.

Viral IRESs can be distributed into four groups based on their translation initiation factor requirements and phylogenetic similarities. PV, hepatitis A virus, and rhinovirus IRESs are examples of Group IV IRESs (Borman and Jackson, 1992; Glass and Summers, 1992; Pelletier and Sonenberg, 1988). Group IV IRESs require the initiator met-$tRNA_i$, most canonical translation initiation factors and IRES trans-acting factors (ITAFs). ITAFs are factors that normally do not participate in translation but are recruited to viral IRESs to promote recruitment of translation initiation factors and ribosomes (Yu et al., 2011). For Group IV IRESs, a 43S PIC is recruited to the IRES and then scans a short distance to the AUG initiation codon. Alternatively, foot and

mouth disease virus (FMDV) and EMCV IRESs are examples of the Group III IRESs (Jang et al., 1988; Kuhn et al., 1990). Group III IRESs exhibit similar factor requirements as Group IV IRESs but Group III IRESs can recruit the ribosome directly to the initiation codon. On the other hand, Group II IRESs require minimal factors: initiator met-tRNA$_i$, eIF2, and eIF3. Examples of Group II IRESs are hepatitis C virus (HCV) and classical swine fever virus (CSFV) (Rijnbrand et al., 1997; Tsukiyama-Kohara et al., 1992). Lastly, the Group I IRESs use the most streamlined mechanism. These IRESs can directly recruit the ribosome without the aid of any translation factors. Examples include the intergenic (IGR) IRES in CrPV and plautia stali intestine virus (PSIV)(Sasaki and Nakashima, 1999; Wilson et al., 2000). (Figure 1.2). A detailed overview of the CrPV IGR IRES will be described in Section 1.5.

DNA based-bicistronic reporters are the classic tools used by many researchers to investigate if a viral or a cellular RNA contains an IRES. Nevertheless, there are some controversies with using these reporters *in vivo*. For example, researchers discovered some potential IRES elements have cryptic promoters or cryptic splice sites (reviewed in Kozak, 2003, 2005). Specifically, a cryptic promoter or a cryptic splice can generate a shorter separate monocistronic RNA that contains the second cistron (Riley et al., 2010), thus leading to expression of the second cistron through a cap-dependent mechanism. There are a number of control experiments that can eliminate the possibility of cryptic promoter or cryptic splice sites. For instance, qRT-PCR can be performed with appropriate primer sets that measure the levels of first and second cistron independently (reviewed in Thompson, 2012). If there are no cryptic promoters or cryptic splice sites, the levels of each cistron should be the same. Another control

experiment that can be performed is by utilizing siRNAs (Van Eden et al., 2004). Specifically, siRNAs are introduced into cells to target the first or second cistron. qRT-PCR is performed to measure the levels of each cistron independently. Both cistrons should be affected similarily if there are only intact bicistronic reporters. To avoid these labor intensive experiments, one can use RNA-based bicistronic reporters instead of DNA-based bicistronic reporters (reviewed in Thompson, 2012). A caveat with this approach is some IRES elements require a "nuclear experience" because the IRES element is only active if one or more nucleotides are modified or associated with a nuclear factor (Semler and Waterman, 2008; Stoneley et al., 2000). Nevertheless, I used RNA-based bicistronic reporters solely in my experiments (Chapters 3 and 4).

1.4 Translational control

Regulation of translation is critical for maintaining cellular homeostasis (reviewed in Sonenberg and Hinnebusch, 2009). Under acute stress, overall protein synthesis is strongly repressed in order to conserve energy and to provide time for the cell to adapt or in some cases when the stress is acute, induce apoptosis. Translation is controlled by many mechanisms. Most involve signaling pathways that sense and respond to a cellular stress and eventually lead to inhibition of one or more translation initiation factors. Several major translation controls act at the level of initiation. This makes sense as it is more efficient for the cell to regulate translation prior to spending energy and resources for protein synthesis. However, there are also mechanisms that control translation at the level of elongation and termination.

Two major pathways can impact cellular translation globally and these pathways are commonly targeted by a number of viruses (reviewed in Sonenberg and Hinnebusch, 2009). Therefore, I will provide a brief overview of these pathways.

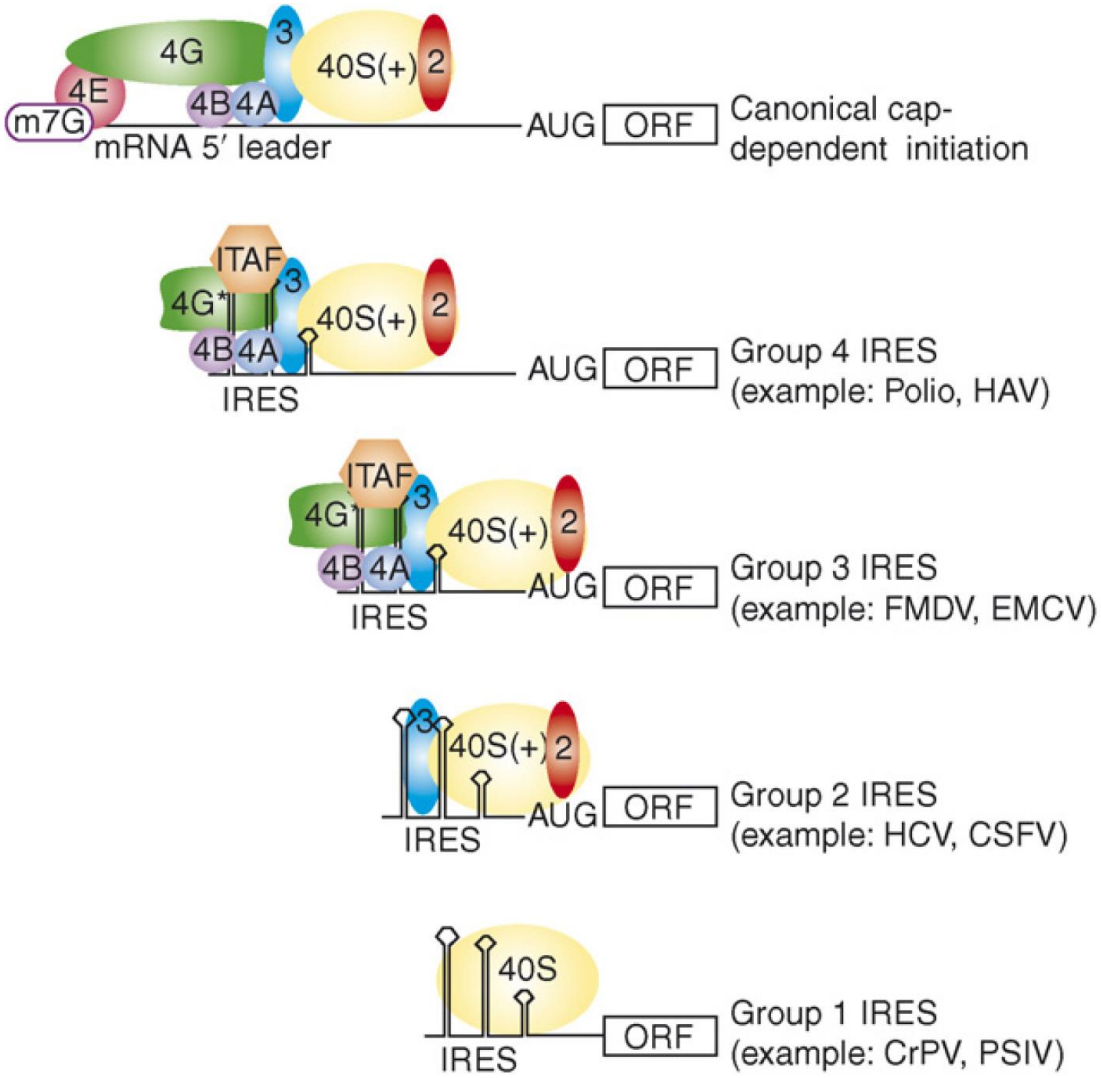

Figure 1.2 Cap-dependent translation versus four different viral IRES groups. There are four different viral IRES groups. Examples of group four are PV and HAV. Group four IRESs require some canonical initiation factors, initiator methionine tRNA, and IRES transacting factors (ITAFs). Additionally, 40S ribosome scanning is required in group four IRESs. In contrast, group three IRESs require no scanning and can recruit the ribosome directly to the start codon. Examples of group three IRESs are FMDV and

EMCV. Group two IRESs require fewer initiation factors. Examples include HCV and CSFV. Lastly, group one IRESs are the most streamlined IRESs. They require no translational initiation factors for ribosome assembly. CrPV and PSIV are examples of this group. Adapted from Kieft, J.S. (2008).

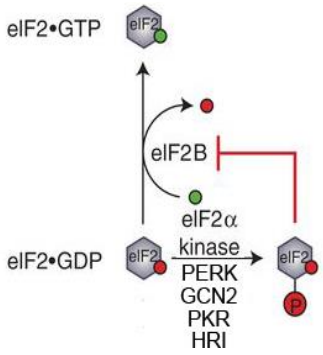

Figure 1.3 Control of translation by disrupting recycling of eIF2. During cellular stress, eIF2 recycling is disrupted and overall translation is inhibited. Specifically, disruption is triggered upon activation of eIF2α kinases that senses ER-stress (PERK), nutrient starvation (GCN2), the presence of long double-stranded RNA (PKR), or heme deficiency (HRI). Activated eIF2α kinases phosphorylate eIF2α and the phospho- form of eIF2α impedes eIF2B, a guanine exchange factor that recycles eIF2-GDP to eIF2-GTP. In insects, only PERK and GCN2 are present. Adapted from Hinnebusch, A.G., and Lorsch, J.R. (2012).

The first pathway involves eIF2α phosphorylation, which is a key global translational control mechanism that responds to cellular stress and viral infection. eIF2α is part of a three subunit complex of eIF2 consisting of alpha, beta and gamma subunits (reviewed in Sonenberg and Hinnebusch, 2009). eIF2 forms a ternary complex consisting of GTP and the initiator Met-tRNA$_i$. During translation initiation, after PIC complexes recognize the AUG codon, eIF2-GTP is hydrolyzed, leading to release of the

initiator Met-tRNA$_i$ and dissociation of eIF2 (section 1.1). eIF2-GDP is recycled back to eIF2-GTP by eIF2B, a guanine exchange factor. Under cellular stress or viral infection, the alpha subunit of eIF2 is phosphorylated at Ser51, which impedes recycling of eIF2-GDP to the GTP form. The phospho-form of eIF2 is a competitive inhibitor of eIF2B. Since eIF2B is in limiting quantities, a small increase in phospho-eIF2α can sequester eIF2B, leading to the inhibition of overall translation initiation (Rowlands et al., 1988). In mammalian cells, there are four known kinases specific for eIF2α: protein kinase RNA-like endoplasmic reticulum kinase (PERK), general control nonderepressible 2 (GCN2), heme-regulated inhibitor kinase (HRI) and protein kinase R (PKR). Each kinase is activated upon sensing a specific stress. PERK is a type I membrane protein that resides on the ER membrane and senses misfolded proteins. Amino acid starvation is sensed by GCN2 kinase through binding to uncharged transfer tRNA, which accumulates during amino acid starvation. Normally inactive in the presence of heme, HRI kinase is activated upon sensing heme deficiency. PKR kinase is activated by the presence of double stranded RNA which is normally present during viral replication. While mammals encode four such kinases, insects only express PERK and GCN2 (Figure 1.3).

Another well-studied global translation control mechanism is the regulation of the eIF4E-binding protein (4E-BP) (reviewed in Sonenberg and Hinnebusch, 2009). 4E-BP can interact with the cap-binding protein, eIF4E, and sequester it from the scaffold protein eIF4G. Biochemical and structural studies show that 4E-BP and eIF4G contain a common motif that binds to and competes for the same site on eIF4E (Mader et al., 1995). The phosphorylation status of 4E-BP controls its affinity for eIF4E. Specifically,

mTORC1, a conserved serine/threonine kinase, enhances translation by hyperphosphorylating 4E-BP and lowering 4E-BP's affinity for eIF4E. Conversely, inhibition of mTORC1 signaling leads to hypophosphorylation of 4E-BP, enhanced binding of 4E-BP to eIF4E, and inhibition of translation. mTORC1 is at a nexus of signaling pathways that includes the PI3K/AKT pathway which integrates four major signals in the cell: amino acid availability, oxygen levels, the presence of growth hormones and energy status.

1.5 Viruses targeting the host translational machinery

My thesis focuses on cricket paralysis virus (CrPV) infection in *Drosophila melanogaster* tissue culture cells (S2 cells). This model has been attractive because studying virus-host interactions in lower organisms can lead to better understanding of antiviral mechanisms in general. Moreover, given that many pathways are conserved between *Drosophila* and higher organisms, studies in *Drosophila* have paved the way to our fundamental understanding of key innate immune response pathways. For example, the Toll receptor, which was first discovered in *Drosophila*, is involved in innate immunity (Lemaitre et al., 1996). This finding led to the discovery of the Toll-like receptors, which are the mammalian versions of insect Toll (Medzhitov et al., 1997). These findings significantly altered the field of innate immunity and provided insights into how cells sense bacteria and viruses. A Nobel prize was awarded for this work in 2011 (reviewed in O'Neill et al., 2013). Therefore, a greater understanding between viral-host interactions in insects can provide insights into fundamental viral host mechanisms in mammals. Since my thesis focuses on viral translation strategies, I will

mention briefly some well studied examples of RNA viruses that target host translation. This is not an exhaustive list but to illustrate the diversity of translational targets.

I will briefly describe three different mechanisms, (i) viral elements that hijack translation initiation factors to facilitate viral translation, (ii) viral proteins that impair cap-dependent translation in order to increase the pool of ribosomes and translation factors available for viral translation, and (iii) viral proteins that block specific cell-induced cap-dependent translation repression. These mechanisms are not necessarily exclusive of each other and in many cases viruses have evolved multiple mechanisms to ensure optimal viral protein synthesis.

There are numerous examples of viral elements "hijacking" translation initiation factors to facilitate viral translation (reviewed in Walsh and Mohr, 2011). Viral IRESs are one example, which is explored in section 1.2. Another example is the 3'-cap independent translation element (CITE), which is found in the 3'UTR of plant RNA viruses. For example, Turnip crinckle virus (TCV) contains a CITE that binds translation factors eIF4E, eIF4G and the 60S ribosome in order to deliver them to the 5'end of the viral genome (Miller et al., 2007; Zuo et al., 2010) (Figure 1.4). Besides cis-acting RNA elements, viruses can use viral proteins to bind translation factors. The NS1 viral protein from influenza is a well-studied example. This protein can recruit eIF4G, deliver it to viral RNAs and promote viral translation (Burgui et al., 2007). This is beneficial because influenza virus can avoid relying on the cap-binding protein eIF4E which is a major target for translational regulation in the cell (Section 1.4).

Besides "hijacking" translation initiation factors to facilitate virus infection, a number of viruses inhibit cap-dependent translation to dampen host antiviral responses

and also increase the pool of available ribosomes for virus dependent translation. This strategy is adopted by viruses that require fewer initiation factors for viral translation as described earlier (IRESs, CITEs, viral proteins that interact with translation factors). I will highlight some of the strategies that viruses use to affect host translation. The PA subunit, an endonuclease, of influenza RNA polymerase, inhibits cellular translation by cleaving 10-15 nucleotides downsteam from the 5' cap of cellular mRNAs (Dias et al., 2009; Plotch et al., 1981). In addition, Vaccinia virus (VacV) also targets the 5' cap by expressing viral decapping enzymes that remove the m^7G cap from host mRNAs (Parrish and Moss, 2007; Parrish et al., 2007; Shuman, 1990). Besides the cap, viruses also target a number of translation factors to inhibit cap-dependent translation. For example, rabies and measles virus express eIF3 binding proteins that prevent eIF3 from facilitating cap-dependent translation (Komarova et al., 2007; Sato et al., 2007). In addition, FMDV inhibits host translation by degrading eIF3a and b subunits during infection (Rodriguez Pulido et al., 2007). Interestingly, PV inhibits cellular translation by cleaving eIF4G and PABP with viral proteases (Figure 1.4). Furthermore, EMCV, another enterovirus, activates 4E-BP1 in order to sequester eIF4E during infection (Gingras et al., 1996). Thus, within enteroviruses, several different mechanisms are observed. 4E-BP appears to be another common target for viruses. The M protein of vesicular stomatis virus (VSV) promotes 4E-BP hypophosphorylation by inhibiting the Akt signaling pathway (Connor and Lyles, 2002). In contrast, SV40 virus promotes 4E-BP hypophosphorylation by inhibiting the phosphatase that is responsible for regulating 4E-BP hypophosphorylation (Dunn and Connor, 2011) (Figure 1.4).

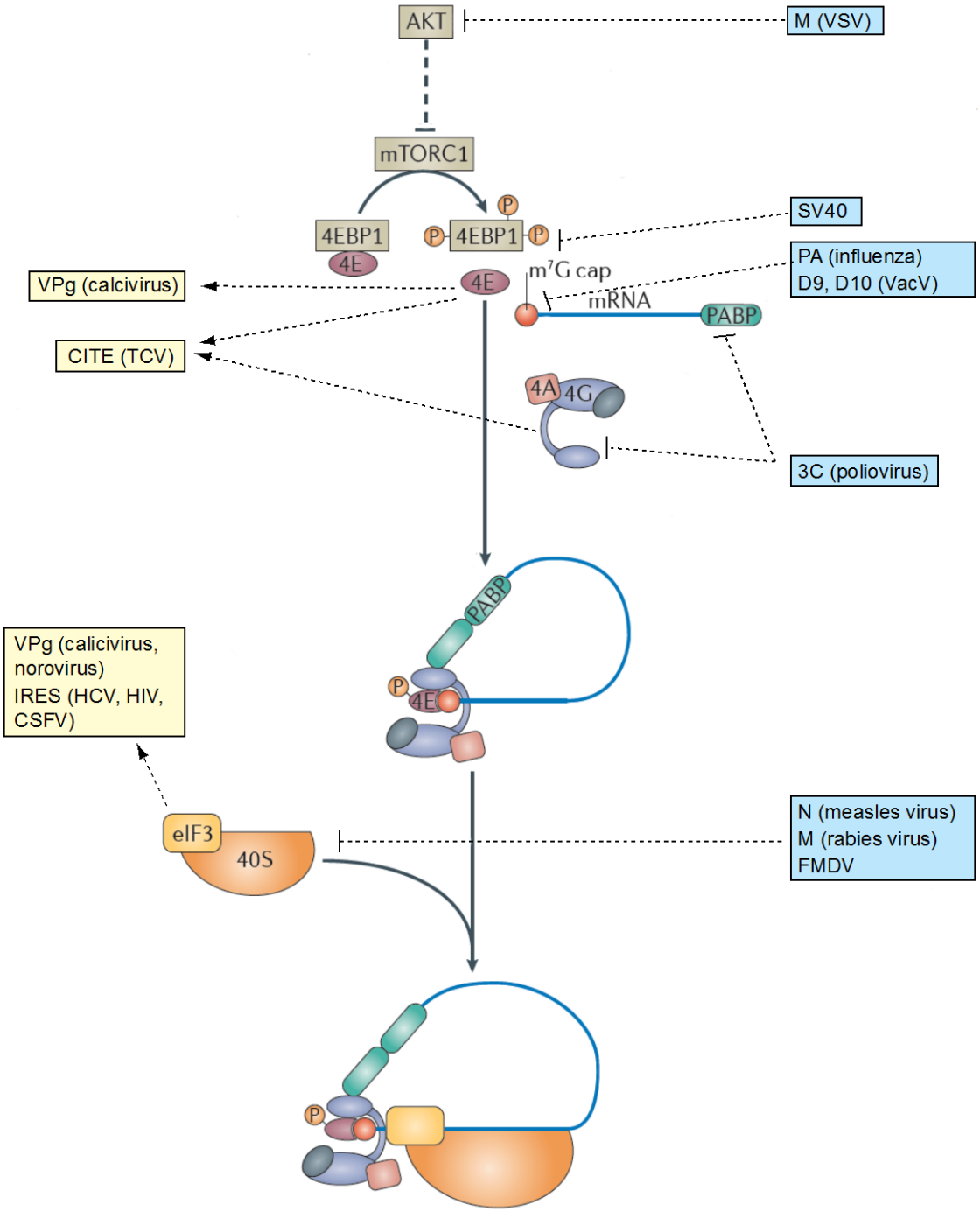

Figure 1.4 Viruses "hijacking" translation initiation factors and inhibiting cap-dependent translation. A number of translation initiation factors are required to form the PIC on the m^7G cap of mRNA. Viruses hijack some of these key factors to facilitate translation of viral RNA (light yellow). Examples listed in this illustration include VPg

from calicivirus that binds to eIF4E and eIF3. eIF3 is also hijacked by the VPg from norovirus and by a number of viral IRESs including HCV human immunodeficiency virus (HIV), and CSFV. CITE from TCV hijacks eIF4E and eIF4G. Besides "hijacking" translation factors, a number of viruses also inhibit cap-dependent translation (light blue). The M protein from VCV inhibits Akt signaling. Inhibition of this pathway will lead to 4E-BP binding to eIF4E and impairment of cellular translation. Similarily, SV40 infection suppresses the hyperphosphorylation of 4E-BP. The hypophosphorylated form strongly interacts with eIF4E and inhibits translation. The m^7G cap is targeted by a number of viruses. Influenza virus encodes an endonuclease that cleaves cellular mRNAs 10-15 nucleotides downstream of the m^7G cap and impairs cap-dependent translation. Vaccinia virus (VacV) encodes enzymes (D9, D10) that remove the m^7G cap from cellular mRNAs. On the other hand, 3C protease inhibits cap-dependent translation by cleaving translational initiation factors like eIF4G and PABP. In addition, rabies virus and measles virus inhibit cap-dependent translation by expressing eIF3 binding proteins which bind to eIF3. Finally, FMDV inhibits translation by degrading two subunits within eIF3. Adapted from Walsh, D., and Mohr, I. (2011).

Viruses have also evolved mechanisms to counteract translation repression induced by the host which can block viral translation. For example, replication intermediates or viral RNA structural elements such as IRES are sensed by the PKR kinase and are then activated to inhibit eIF2 (Section 1.3). Since a number of viruses require eIF2 for their translation, some express viral decoys that impede PKR activation. For example adenoviral VA RNA, Epstein-Barr virus EBERs, and influenza virus NS1 bind tightly to PKR and prevent its activation (Ghadge et al., 1994; Lu et al., 1995; Sharp et al., 1993). Other viruses can sequester dsRNAs from PKR. For example, E3L protein in VacV binds to dsRNA to prevent PKR recognition and activation (Chang and Jacobs, 1993). These examples illustrate the importance of subverting host-dependent translational repression during some viral infections.

Some viruses, on the other hand, thrive in conditions when eIF2α is phosphorylated. Examples include sindbis virus and HCV. These viruses do not rely on eIF2 for viral-dependent translation *in vivo* and may benefit from repression of cellular translation. *In vitro* experiments indicate that HCV IRES and Sindbis genomic RNA require eIF2 (section 1.2) for translation. However, eIF2α is phosphorylated during these viral infections but viral translation still occurs (Rivas-Estilla et al., 2002; Ventoso et al., 2006). It is possible that Sindbis RNA and HCV IRES use a number of mechanisms to ensure translation of viral proteins. For instance, ligatin or MCT1-DENR can be used instead of eIF2 to deliver initiator Met-tRNAi to viral RNA (Skabkin et al., 2010).

As described in this subchapter, there are diverse viral mechanisms that target host translation in order to promote viral replication and translation. My thesis explores how CrPV, an insect virus, hijacks the translation machinery.

1.6 Stress granules

My thesis also explores how CrPV interacts with stress granules (SGs). A review of what SGs are and examples of RNA viruses interacting with SGs are provided in the next two subchapters.

SGs are cytoplasmic foci containing stalled translation initiation complexes whose formation is triggered upon global translational repression by stresses like oxidative stress and heat shock. SGs are not required for global translational repression (Buchan et al., 2008; Kwon et al., 2007; Loschi et al., 2009; Mokas et al., 2009; Ohn et al., 2008) or regulation of global mRNA stability (Buchan et al., 2008; Hilgers et al.,

2006) but are thought to be sites where the increased local concentration of proteins and mRNA allows for remodeling and redistribution of messenger ribonucleoproteins (mRNPs) (reviewed in Buchan and Parker, 2009). In addition, specific proteins can be selectively sequestered to or away from SGs, thus affecting biochemical processes in the cell. For example, RACK1, an apoptotic factor, is recruited to SGs during mild stress and prevents premature activation of the apoptotic pathway (Arimoto et al., 2008).

One of the better described pathways for SG induction is eIF2α phosphorylation (Kedersha et al., 2002; Kedersha et al., 1999). For example, viral infection can activate PKR and trigger eIF2α phosphorylation (sections 1.2,1.3) and SG formation. Additionally, SGs can be induced in an eIF2-independent manner. For instance, treatment of cells with hippuristanol or pateamine A (PatA), which alter the activity of the helicase, eIF4A, also induces SG formation (Dang et al., 2006; Mazroui et al., 2006). In general, inhibition of translation will trigger SG assembly. However, there are exceptions. In one study, preventing 60S subunit joining with the 40S subunit does not lead to SG assembly, suggesting that translational repression can be uncoupled from SG induction (Mokas et al., 2009). Thus, SGs may form only through the inhibition of specific translation factors or within a defined window during translation initiation (reviewed in Buchan and Parker, 2009) (Figure 1.5).

SGs are nonmembranous dense complexes composed of several proteins and RNA. In addition to stalled initiation complexes composed of translation initiation factors such as eIF4E, eIF2, eIF3, PABP and the small 40S ribosomal subunit, SGs contain hallmark protein markers such as T cell intracellular antigen 1 (TIA-1), TIA-1-related

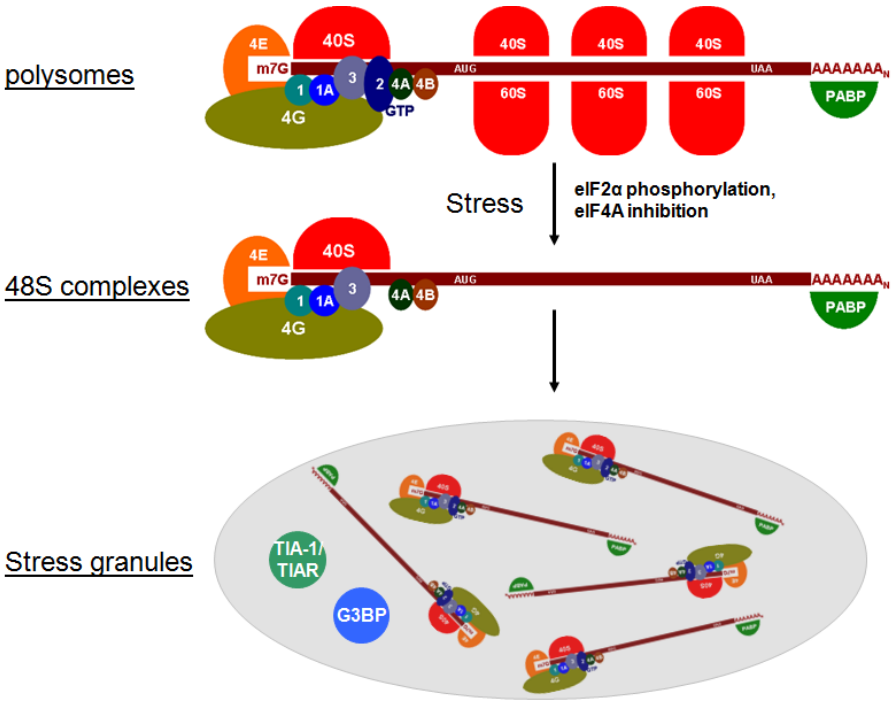

Figure 1.5 Stress granule induction. Stress granules (SGs) are formed during inhibition of protein synthesis when cells limit the availability of translation initiation factors for mRNA translation in response to some environmental stress (eIF2α phosphorylation) or when cells are treated with drugs (PatA) that disrupt the action of specific translation initiation factors (eIF4A). These instances of translational repression promote accumulation and aggregation of 48S complexes (40S subunit, translation initation factors and mRNAs) in the cell. The aggregation is facilitated by RNA binding proteins like TIA-1 and G3BP and by the microtubule network.

---

protein (TIAR), and GTPase (Src homology 3 [SH3] domain) binding protein (G3BP) (Kedersha et al., 2000; Tourriere et al., 2003). TIA-1 and TIAR are closely related proteins that contain RNA recognition motifs and are implicated in RNA metabolism (Tian et al., 1991). G3BP, a member of the Ras signaling pathway, was discovered by its ability to bind to the SH3 domain of RasGAP and has since been implicated in a

number of biological processes including RNA metabolism (reviewed in Irvine et al., 2004). All three proteins contain domains that are important for the aggregation and formation of SGs. For example, TIA-1 and TIAR lacking the QN-rich prion-like domain, which allows for self-aggregation, can no longer form SGs (Gilks et al., 2004). Currently more than 50 proteins are associated with SGs (reviewed in Anderson and Kedersha, 2009; Buchan and Parker, 2009). Furthermore, a small interfering RNA (siRNA) screen identified more than 100 genes involved in promoting the assembly and disassembly of SGs (Ohn et al., 2008).

SG assembly is reversible. Under stress, stalled initiation complexes are shuttled to SGs (Kedersha et al., 2002; Kedersha et al., 1999; Kimball et al., 2003). Upon recovery from the stress, SGs disassemble, and stalled initiation complexes can now re-enter the translation cycle and assemble onto polyribosomes. Inhibiting mRNA release from translating ribosomes by treating cells with translation elongation inhibitors such as emetine or cycloheximide block aggregating RNA-binding proteins from binding to non-translating mRNAs and forming SGs (Kedersha et al., 2000). Moreover, fluorescence recovery after photobleaching (FRAP) studies have shown that proteins shuttle in and out of SGs rapidly (Fujimura et al., 2008; Guil et al., 2006; Kedersha et al., 2000; Kedersha et al., 2005; Mollet et al., 2008). Thus, SG assembly and disassembly are in equilibrium with translating polysomes, and this process is likely regulated. Interestingly, a study reported that dynein and kinesin motors are required for SG assembly and disassembly, indicating that RNPs are delivered to SGs on microtubule tracks (Loschi et al., 2009).

The mechanism that drives mRNP aggregation into SGs has not been well understood until recently. A leading theory is SGs and other RNA granules form through a process called "phase seperation" where RNA molecules and proteins above a certain concentration condense to form a liquid droplet. (Han et al., 2012; Li et al., 2012; Weber and Brangwynne, 2012). Specific ribonucleoproteins (RNP) in the cell can promote this liquid phase transition into liquid-like droplets. The main feature of these RNPs that promotes liquid-like droplets is their propensity to promote weak multivalent interactions with other proteins. Typically, these RNP, contain SH3 domains, proline-rich motifs and other low complexity amino acid sequences. Examples of RNPs with this propensity include the classical SG markers G3BP and TIA-1. This insight demonstrates that SGs and other RNA granules form through similar processes.

Currently, the most common method to study SGs is observation via immunofluorescence with confocal microscopy. For example, antibodies that recognize key SG markers like TIA-1 and G3BP can be detected by indirect immunofluorescence. Another approach is to express recombinant SG markers that are tagged with fluorescent markers such as GFP. To confirm that the observed granules are indeed SGs, a number of other markers are examined in conjuction with TIA-1 or G3BP. These include translation initiation factors and mRNAs (reviewed in Anderson and Kedersha, 2009; Buchan and Parker, 2009). In general, visualization of SGs is the main approach to studying SG assembly because their biochemical isolation is difficult (Souquere et al., 2009).

1.7 Viruses targeting stress granules

Since viruses target many aspects of RNA biology including translation (section 1.3), it is not surprisingly that a number of viruses also perturb SGs (reviewed in Lloyd, 2013; Reineke and Lloyd, 2013). In general, viruses inhibit SG formation (Figure 1.6 and 1.7). However it is not clear from many studies describing virus-SG interactions except for recent work in influenza and enteroviruses that the inhibition of SG itself is important for virus life cycle (Khaperskyy et al., 2012; Onomoto et al., 2012)(Reineke and Lloyd, 2015). Viruses perturb SGs in a number of different ways but can be grouped into common mechanisms: (i) viral proteases cleave essential SG proteins to inhibit SG formation, ii) viruses inhibit signaling pathways that lead to SG induction, and iii) viruses compete for essential SG markers like G3BP and TIA-1.

Poliovirus is one of the first virus that describes the relationship between SGs and virus infection. Poliovirus infection stimulates G3BP1-containing SG formation early in infection. Later in infection, G3BP1- containing SGs dissociate. The dissociation is caused by viral 3C protease-mediated cleavage of G3BP1. SG formation can be rescued during infection by overexpressing a recombinant cleavage-resistant form of G3BP1, in which the cleavage site was mutated. Furthermore, poliovirus-infected cells expressing this cleavage-resistant mutant form of G3BP1 exhibited decreased viral yield (White et al., 2007). These results suggest that cleaving G3BP is important for the poliovirus life cycle. However, in an alternate study, it was shown that TIA-1-containing SGs form during poliovirus infection and do not dissociate later in the infection unlike G3BP1-containing SGs. The authors suggest that these TIA-1 containing SGs are compositionally unique compared to canonical SGs (Piotrowska et al., 2010). A later

study claims that these TIA-1-containing granules are not classical SGs because they lack translation factors eIF3, eIF4G, eIF4E and poly(A) mRNA (White and Lloyd, 2011). These studies emphasize the importance of testing for a number of canonical SG markers (Figure 1.6). Moreover, these studies suggest that multiple classes of granules differing in composition can occur depending on the stress.

Influenza infection exemplifies another common SG disruption strategy, which is to block its induction. Influenza virus encodes three viral proteins that disrupt SG assembly via different mechanisms. NS1 blocks PKR-mediated SG induction (Khaperskyy et al., 2012). Infection by a mutant influenza deleted for NS1 leads to SG induction and lower viral yield. The same authors discovered two other viral proteins, NP and PA-X,that also disrupt SG formation (Khaperskyy et al., 2014). NP inhibits SG formation independent of eIF2α phosphorylation. On the other hand, PA-X is responsible for the repression of host translation during influenza infection. This protein is produced by a ribosomal frameshift from the PA gene and inhibits SG accumulation by degrading a significant portion of cytoplasmic poly(A) mRNAs. Mutations that disrupt PA's ability to interfere with host translation also inhibit its ability to disrupt SG induction (Khaperskyy et al., 2014). These studies demonstrate that influenza adopts a multi-pronged approach to disrupt SG formation (Figure 1.6).

Some viruses inhibit SG formation by competing for key SG components since SG proteins may contribute directly to viral replication. Alphaviruses like Semliki Forest virus (SFV), Chikungunga virus (CHICKV) and Sindbis virus (SBV) induce SGs early in infection but then disrupt them later in infection. Specifically, non-structural viral proteins sequester G3BP1, thereby disrupting SGs, and recruit it to replication complexes. How

G3BP1 facilitates viral replication is unclear but virus replication is reduced when viruses express a mutant form of nsp3 that cannot bind to G3BP1 (Cristea et al., 2010; Fros et al., 2012; Panas et al., 2012). The SG markers TIA-1 and TIAR are also "hijacked" by a number of viruses such as West Nile virus (WNV) and Dengue virus (DENV). Like GEBP, TIA-1 and TIAR are co-opted to the viral replication machinery. It

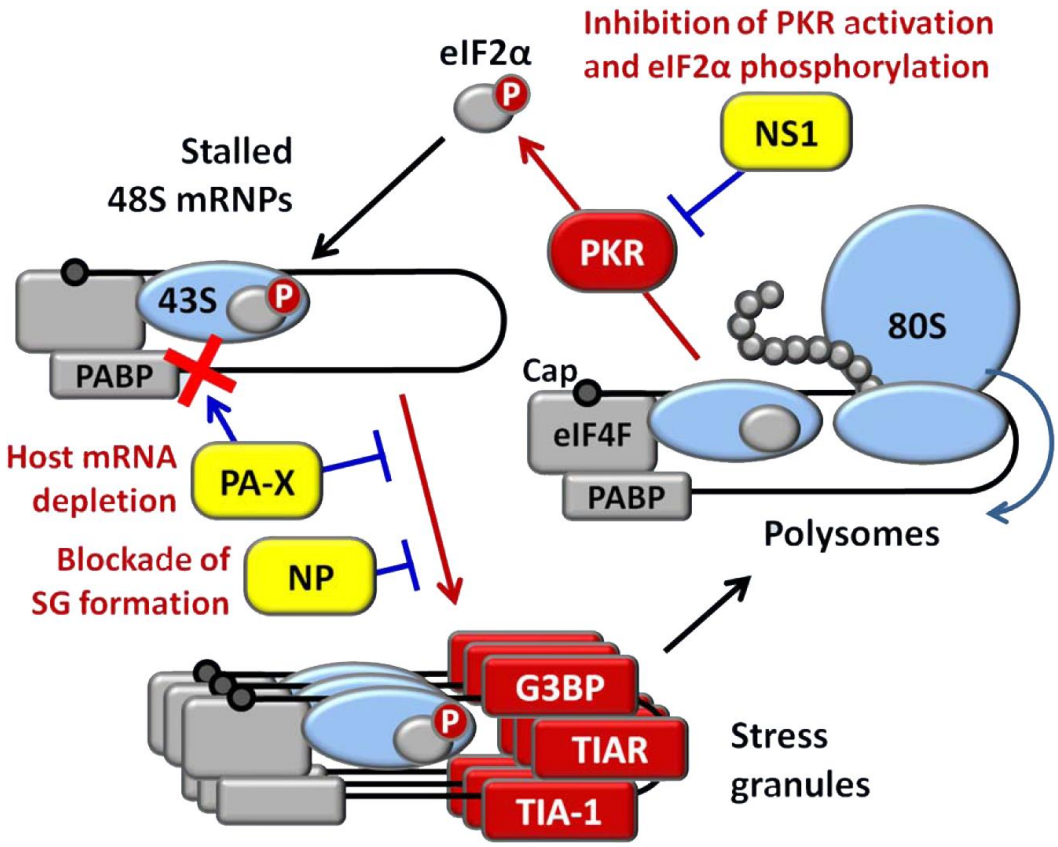

Figure 1.6 Three viral influenza proteins block stress granule formation. NS1 inhibits PKR-mediated SG induction. Alternatively, NP, the structural protein, and PA-X blocks SG induction in an eIF2α phosphorylation-independent manner. PA-X encodes a ribonuclease that degrades cytoplasmic RNA and inhibits host translation. This domain is crucial for blocking SG formation. Adapted from Khaperskyy, D.A., *et al*. (2014).

is currently unclear how these proteins facilitate viral replication but it is known that the 3' stem loop of the viral RNA, which is the promoter for minus strand RNA synthesis binds to TIA1 and TIAR (Emara and Brinton, 2007). Another example of SG factors hijacked by viruses occurs during Junin virus infection. Junin N protein inhibits SGs by binding to G3BP1, eIF4A, and eIF4G and sequestering them to replication complexes (Baird et al., 2012; Linero et al., 2011) (Figure 1.7). HCV is another example of a virus that sequesters G3BP to replication compartments (Ariumi et al., 2011; Garaigorta et al., 2012; Pager et al., 2013; Ruggieri et al., 2012). These studies showed that HCV infection affects SGs quite differently than other virus infections; HCV infection induces a dynamic assembly/disassembly of SGs. The SG assembly/disassembly is dependent on phosphorylation and dephosphorylation of eIF2α respectively. During phases when SGs are diassembled, cellular translation is restored and viral translation is enabled. This oscillation supports chronic infection in HCV. Nevertheless, like the other viruses, it remains to be determined how G3BP1 facilitates HCV RNA replication (Figure 1.7). These examples suggest that sequestration of SG components to viral replication factories disrupts SGs.

Despite all these diverse strategies of disrupting SGs, it's not well understood if disrupting SGs is important for viruses in general. Recent exciting work from a number of labs suggest SG disruption is important. New insights are starting to show that SGs are important in innate immunity. When cells are infected with a mutant influenza virus that is unable to inhibit SGs, retinoic acid-inducible gene 1 (RIG-I)-like receptors and PKR can bind to viral RNA and enter SGs (Khaperskyy et al., 2012; Onomoto et al., 2012). Depletion of G3BP disrupted these granules and resulted in diminished

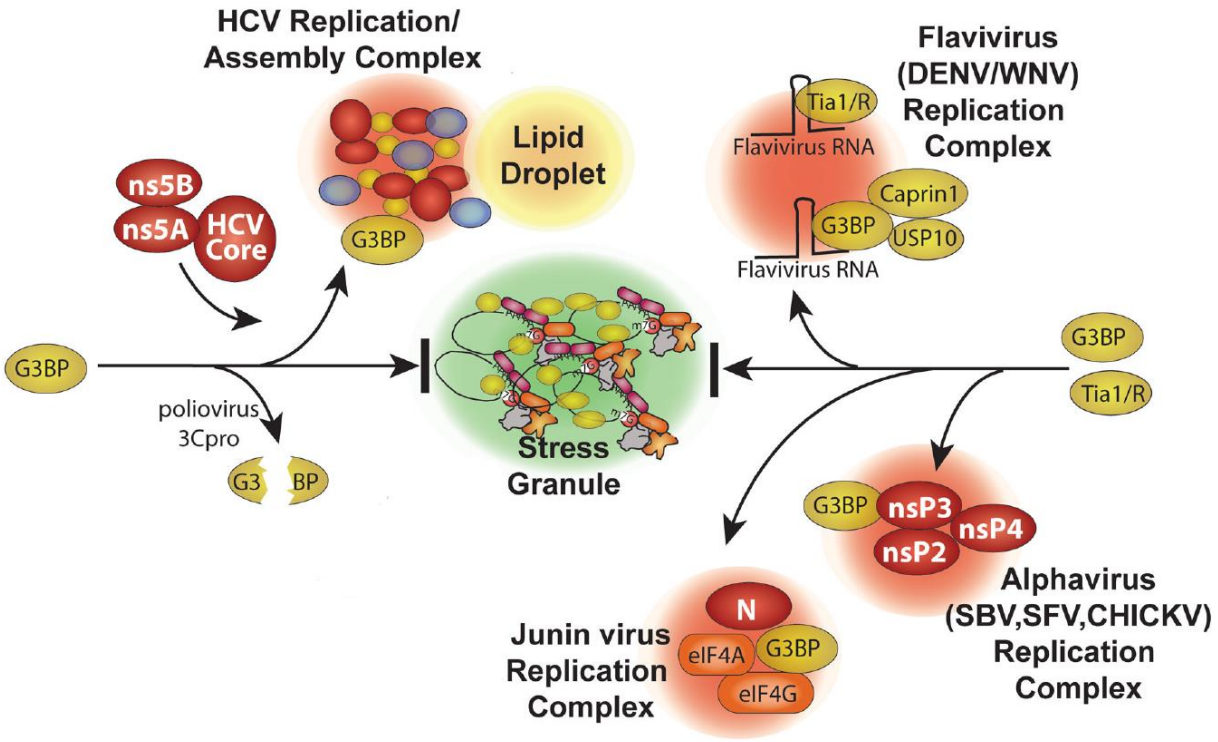

Figure 1.7 G3BP1 is targeted by a number of viruses. SGs are inhibited by a number of viruses "hijacking" G3BP1. Examples include DENV, WNV, SFV, CHICKV, SBV, and Junin Virus. HCV also "hijacks" G3BP1 but SGs do form during infection. G3BP1 is recruited to the replication complex of all the viruses noted. How G3BP1 facilitates viral replication is unknown. Adapted from Lloyd, R.E. (2013).

---

interferon production and higher viral yield. The authors called these granules antiviral SGs (avSGs). A recent publication shows that this strategy is not influenza-specific. Reineke and Lloyd (2015) demonstrated that G3BP is required for recruiting PKR and innate response factors like 2'-5'-oligoadenylate synthase 2 (OAS2) and RNase L to SGs in several enterovirus infections. Furthermore, they showed that G3BP-1 induced SGs are associated with NF-kB-dependent activation of innate immune response

(Reineke and Lloyd, 2015). These results suggest that SGs are intimately linked to the innate immune response and disruption of SGs may facilitate virus infection.

1.8 Thesis

Dicistroviruses are positive-sense, single-stranded RNA viruses. They are classified in the order Picornavirales which includes notable virus families including Comoviridae, Iflavirus, Picornaviridae, Potyviridae, and Sequiviridae. Isolated from Austrialian field crickets by Carl Reinganum, CrPV was the first dicistrovirus discovered at the Victorian Plant Research Institute in 1970 (Reinganum, 1975). Key characteristics of CrPV infection in crickets are paralysis and significant mortality (>95%). Since its discovery, 15 other dicistroviruses have been identified (Table 1.1)(reviewed in Bonning and Miller, 2010; Guo et al., 2013). Notable dicistroviruses include Taura syndrome virus (TSV) which has devastated Shrimp farms in America and Taiwan and Israeli acute paralysis virus (IAPV) which has been associated with colony collapse disorder in honey bees (Cox-Foster et al., 2007; Lightner, 1996; Lightner et al., 1997). In addition, recent metagonomic surveys suggest that Dicistroviruses are ubiquitous and prevalent in many ecosystems (Culley et al., 2006; Ng et al., 2012; Victoria et al., 2009).

The Dicistroviruses were classified initially as insect "picornaviruses" but detailed genome analysis determined that they comprise a new family (reviewed in Bonning and Miller, 2010). While a picornavirus contains a single open reading frame, a dicistrovirus contains two open reading frames. Another key difference is the arrangement of structural and nonstructural proteins: the structural proteins are encoded at the 3' end of the Dicistrovirus genome whereas they are found at the 5' end of picornaviruses.

However, comparison between the two families suggests significant similiarites at the protein sequence level. Specifically, there are significant similarities in sequence of the supergroup type I RNA-dependent RNA polymerase (RdRp) and chymotrypsin-like cysteine protease for processing viral proteins (3C). In addition, the arrangement of non-structural proteins within the dicistrovirus and picorniavirus genomes is the same: from the N- to the C-terminus, a superfamily 3 helicase (2C), VPg for priming RNA replication, the 3C protease and the RdRp replicase (Figure 1.8)

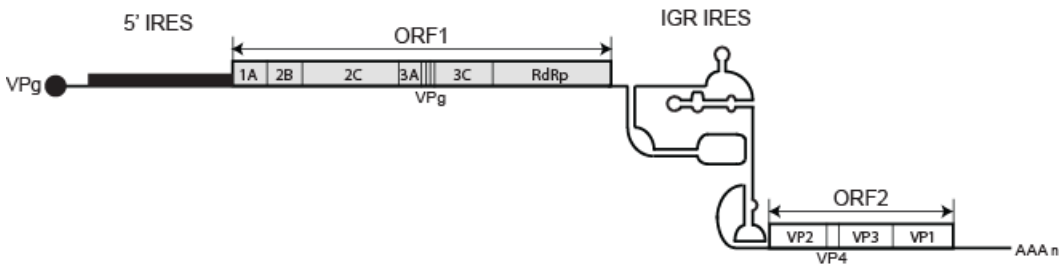

Figure 1.8 Dicistrovirus genomic organization. Dicistroviruses are single-stranded, positive sense RNA viruses. Approximately nine kilobases in length, there are two ORFs. Each ORF is translated by a distinct internal ribosome entry site (IRES). The 5' IRES is responsible for the translation of the ORF1 and the IGR IRES is responsible for the translation of the ORF2. ORF1 encodes non-structural proteins and ORF2 encodes structural proteins. 3C is the chymotrypsin-like cysteine protease responsible for processing viral proteins and RdRp is the RNA-dependent RNA polymerase responsible for viral replication.

Translation of the non-structural proteins (open reading frame 1 (ORF1)) and structural proteins (ORF2) is directed by independent IRESs. The intergenic (IGR) IRES has been extensively studied and is quite remarkable compared to other IRES (Costantino et al., 2008; Jan, 2006; Jan and Sarnow, 2002; Spahn et al., 2004). The

IGR IRES directly recruits the ribosome without the aid of any translation initiation factor and initiates translation at a non-AUG codon (Deniz et al., 2009; Jan and Sarnow, 2002; Wilson et al., 2000) (Figure 1.9). Biochemical and structural studies have revealed that the IGR IRES adopts structural domains that occupy regions of the ribosome normally bound by tRNAs (Costantino et al., 2008; Jang et al., 2009; Pfingsten et al., 2006; Schuler et al., 2006; Spahn et al., 2004). In fact, the pseudoknot I domain (PKI) of the IGR IRES structurally mimics the anticodon loop of a tRNA (Costantino et al., 2008; Fernandez et al., 2014; Jan, 2006; Jan and Sarnow, 2002; Koh et al., 2014)(Figure 1.10). In contrast, studies on the 5'-UTR IRES have been limited; Reconstitution experiments have shown that the 5'-UTR IRES of rhapdopsilum padi virus (RhPV) requires eIF1, eIF2 and eIF3 for translation initiation and is stimulated by eIF1A, eIF4F, and eIF4A (Terenin et al., 2013).

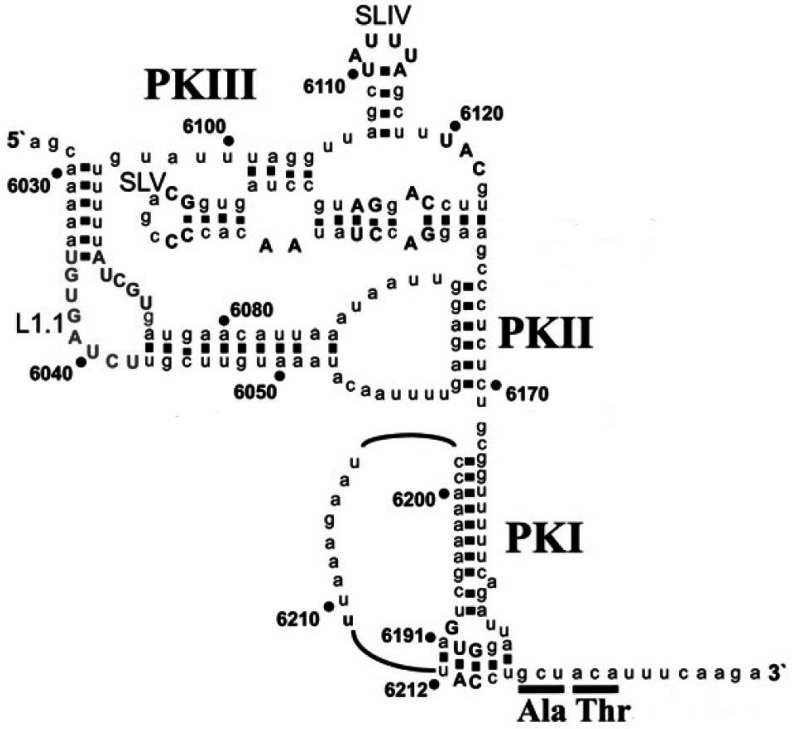

Figure 1.9 Secondary structure of CrPV IGR IRES. Shown is a predicated secondary structure of the CrPV IGR IRES. There are three pseudoknots (PK) which is a structure where the loop of one stem is base pairing with another section of the RNA. Chemical probing was used to deduce the secondary structure of the IGR IRES. The sequences underlined indicate the first two codons of ORF2. Adapted from Jang, C. and Jan, E. (2010).

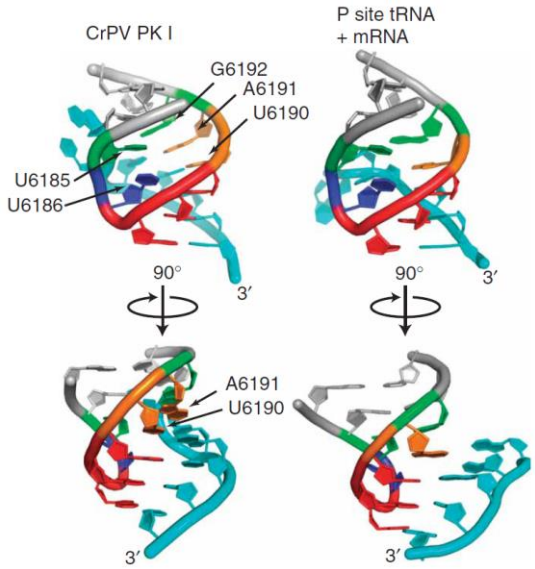

Figure 1.10 CrPV pseudoknot 1 (PK1) mimics authentic tRNA-mRNA interactions. The left two images are the structure of PK1 of CrPV. The right two images are the structure of initiator tRNA anticodon (rainbow coloured) engaged in anticodon-mRNA (cyan) interaction in the P site of the ribosome. Adapted from Costantino, D.A., *et al.* (2008).

There are two genera within dicistroviruses: cripaviruses and aparaviruses (reviewed in Bonning and Miller, 2010). Phylogenetic distance between dicistrovirus genomes and distinct structural differences in the IGR IRES are used to distinguish members of each genus (reviewed in Bonning and Miller, 2010). Specifically, cripaviruses contain a conserved bulge sequence (UGAUCU and UGC) in the IGR IRES and aparaviruses contain an extra stem-loop in the 3'-proximal region of the IGR

IRES (Figure 1.9). CrPV is an example of a cripavirus and IAPV is an example of an aparavirus (Table 1.1).

The crystal structure of CrPV virion was solved by John Tate *et al.* (1999). Sixty copies of VP1, VP2, and VP3 are used to form the capsid. The structure is 30 nm in diameter and exhibits pseudo-T3 symmetry. Each viral structural protein contains a beta-barrel arrangement of eight beta-sheets forming a jelly roll structure. VP1, VP2, VP3, and VP4 form a pentamer and 60 pentamers are used to form the capsid (Figure 1.11). VP4, encoded between VP2 and 3, is packaged as a fusion with the N terminus of VP3 before it is cleaved to form the mature VP3 (Tate et al., 1999). The receptor used by CrPV to gain access into the cell is not known. However, it has been shown that CrPV viral entry depends on clathrin-mediated endocytosis (Cherry and Perrimon, 2004).

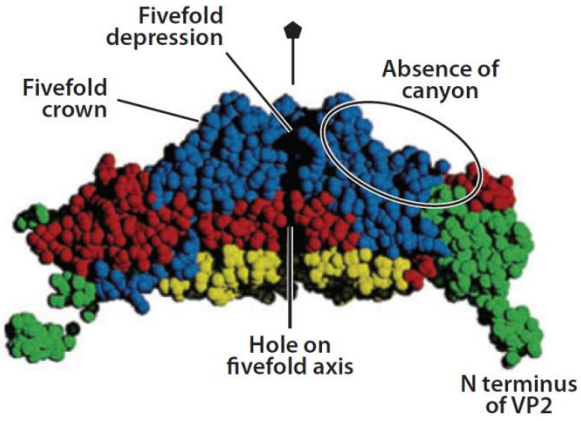

Figure 1.11 A pentamer of the CrPV virion. VP1, VP2, VP3, and VP4 are blue, green, red, and yellow respectively. 60 pentamers are used to form the CrPV virion. Adapted from Tate, J., *et al.* (1999).

Most studies on the molecular mechanisms of the Dicistrovirus life cycle have used CrPV and *Drosophila* C Viruses (DCV) as models (Garrey et al., 2010; Khong and

Jan, 2011; Nayak et al., 2010; van Rij et al., 2006). Infection of *Drosophila* S2 cells with CrPV or DCV leads to a rapid repression of host translation concomitant with an increase in viral protein synthesis (Garrey et al., 2010; Moore et al., 1980; Wilson et al., 2000). A correlation was observed between cap-dependent translational repression during CrPV infection and dissociation of eIF4G from eIF4E in Garrey et al. (2010), thus suggesting that eIF4G dissociation may contribute to translational repression. Phosphorylation of eIF2α is observed during infection but Garrey et al. (2010) demonstrated that this phosphorylation is not important for CrPV-dependent repression of host translation.

1.9 Thesis investigation

Despite significant research into the IGR IRES, little is known about the viral life cycle of dicistroviruses. Moreover, the function of each viral protein in this family is not well understood. I speculate that one or more viral proteins affects host processes to facilitate virus infection. First, I hypothesize that one or more viral proteins are responsible for host cap-dependent repression during CrPV infection. Second, I hypothesize that the SG pathway is disrupted to aid in virus infection and one or more viral proteins are responsible for this disruption (section 1.7). These hypotheses form the basis of my thesis. Chapter 2 explores how CrPV affect SGs. In Chapter 3, I identified a viral protein that stimulates reporter RNA translation and blocks SGs. Finally, in Chapter 4, I explored the relevance of dicistroviruses possessing two distinct IRESs *in vivo.* In summary, my thesis characterizes different aspects of CrPV-host interaction.

Table 1.1 Dicistroviruses and natural hosts

Dicistroviruses	Acronym	Orders of natural hosts
Genus: Cripavirus		
Aphid lethal paralysis virus	ALPV	Hemiptera
Black queen cell virus	BQCV	Hymenoptera
Cricket paralysis virus	CrPV	Diptera, Hemiptera, Hymenoptera, Lepidoptera, Orthopetra
Drosophila C virus	DCV	Diptera
Himetobi P virus	HiPV	Hemiptera
Homalodisca coagulata virus-1	HoCV-1	Hemiptera
Plautia stali intestine virus	PSIV	Hemiptera
Rhopalosiphum padi virus	RhPV	Hemiptera
Triatoma virus	TrV	Hemiptera
Genus: Aparavirus		
Acute bee paralysis virus	ABPV	Hymenoptera
Israeli acute paralysis virus	IAPV	Hymenoptera
Kashmir bee virus	KBV	Hymenoptera
Mud crab dicistrovirus	MCDV	Decapoda
Solenopsis invicta virus-1	SINV-1	Hymenoptera
Taura syndrome virus	TSV	Decapoda

Chapter 2: Stress granules and Dicistroviruses

2.1 Introduction

The importance of SGs has been highlighted by observations that several viruses from diverse taxonomies inhibit the formation of these aggregates (Lloyd, 2013). In addition, recent publications suggest that formation of SGs reprograms the cell to an anti-viral state (Khaperskyy et al., 2012; Onomoto et al., 2012; Reineke et al., 2012; Reineke et al., 2015; Reineke and Lloyd, 2015). Nevertheless, the mechanisms that lead to this reprogramming are still not well described. Furthermore, since the reprogramming is partly dependent on PKR which is not present in insects, it is not known if insect-induced SGs are anti-viral. I used CrPV as a model to investigate if insect viruses disrupt SGs in insect cells. I demonstrate that SGs are inhibited in both CrPV- and DCV infected cells, suggesting that disruption of these RNA granules is important for virus replication. I also show that the CrPV 3C protease is sequestered in SGs under cellular stress but becomes dispersed during viral infection. I propose that CrPV inhibits SG formation to keep viral proteins and RNA available for viral replication and translation.

2.2 Materials and methods

2.2.1 Cell culture and virus

S2 cells (*Drosophila* Schneider 2) were maintained and passaged in Shields and Sang medium containing 10% fetal bovine serum. CrPV and DCV production in *Drosophila* S2 cells has been previously described. A total of 3 X 10^9 cells was infected with 1 mL of virus suspension for 30 min at an MOI of 10. S2 cells were subsequently

incubated in 60 mL medium for 14 h at 25°C. The cells were pelleted, resuspended in PBS, and subjected to four freeze-thaw cycles. Viral titers and yields were determined as described (Garrey et al., 2010). UV-irradiated CrPV was produced as described (Garrey et al., 2010). The lack of replication of the UV-irradiated CrPV was confirmed by infecting S2 cells and probing for the viral RNA by Northern blot analysis.

2.2.2 Plasmids and transfection

pAc5.1 GFP-PABP and pAc5.1 V5-eIF3 S9 were generously provided by Dr. Pam Silver (Harvard, Cambridge). GFP-DCP1a and GFP-GW182 were gifts from Dr. Elisa Izaurralde (Max Planck, Munich). GFP-Ago1 and RFP-Ago2 were gifts from Dr. Andrew Simmonds (University of Alberta, Edmonton). Full-length Rox8, FMR1, and CrPV viral proteins were RT-PCR-amplified from RNA extracted from S2 cells infected with CrPV. Full-length Rin (Rasputin) cDNA was PCR-amplified from a clone obtained from the *Drosophila* Genomics Resource Center. Rox8 and Rin were fused with GFP by PCR amplification and ligated into pAc5.1 cleaved with Kpn1 and Xba1 to produce Rox8-GFP and Rin-GFP. FMR1 and the viral 3C protein were PCR amplified and ligated into pAc5.1 fused in-frame with the V5 tag to produce FMR1-V5 and 3C-V5. For transient transfections, 1 X 10^7 cells were transfected with 20 µg of plasmid DNA using Lipofectamine 2000™ (Invitrogen) according to the manufacturer's protocol. Cells were incubated for 18 hours at 25°C. S2 cells were infected with CrPV or DCV at a MOI greater or equal to 10. In detail, S2 cells were centrifuged and washed once with PBS. Cells were infected with virus for 30 min followed by adding medium. Cells were treated with 50 nM PatA (generous gift of Dr. Jerry Pelletier, McGill University, Montreal), 500

μM arsenite, or incubated at 42°C to induce SGs. In preparation for microscopy, a total of 1 X 10^6 S2 cells was plated on coverslips pre-coated with concanavalin A 0.5 mg/ml (Calbiochem) for 1 h. Cells were subsequently fixed with 3% paraformaldehyde in PBS and permeablized in 0.5% Tween in PBS.

2.2.3 *In situ* hybridization

In preparation for *in situ* hybridization, S2 cells were incubated in hybridization buffer (2X SSC, 20% formamide, 0.2% BSA, 1μg/uL yeast tRNA) for 15 min at 37°C. Subsequently, S2 cells were hybridized with 1 mg/mL DNA probes, oligo(dT)(40) conjugated to Cy-3 or Cy-5, antisense CrPV RNA conjugated to Cy-5, or antisense 18S rRNA conjugated to Cy-3 overnight at 46°C in hybridization buffer (IDT). The next day, S2 cells were washed with 2X SSC with 20% formamide twice for 5 min each at 37°C, 2X SSC twice for 5 min each at 37°C, and 1X SSC once for 5 min. If needed, cells were co-stained by indirect immunofluorescence.

18S rRNA probe sequence: 5'-GTCCTAGATACTACCACAAAAGTTGATAG

Antisense CrPV RNA probe sequence: 5'-ACTAAATAAAATATACAATAAAT

2.2.4 Indirect immunofluoresence assays

After *in situ* hybridization, S2 cells were washed with 2 mL PBS and incubated with antibodies in 50 μL PBS containing 5% horse serum for one hour at 25°C. The antibodies included 1:200 rabbit-anti-deIF4E (generous gift from Dr. Paul Lasko, McGill University, Montreal), 1:500 rabbit anti-V5 IgG (Sigma), 1:200 anti-dsRNA (English & Scientific Consulting limited liability corporation), and 1:500 mouse anti-O-GlcNAc IgG

(Covance). Cells were subsequently washed with 2 mL PBS 3 times and incubated with 50 µL PBS containing secondary antibodies for one hour at 25°C: 1:300 goat anti-rabbit Texas Red IgG (Invitrogen) and 1:500 goat anti-mouse Alexa Fluor 568 IgG (Invitrogen). Cells were then washed 3 times with 2 mL PBS. Coverslips were mounted on slides with Prolong Gold Antifade Reagent (Invitrogen). Images were acquired by a confocal microscope (Olympus FV1000 using Olympus Fluoview Ver.2.0a) with a 60X oil immersion lens. Images shown are a representative single Z-section. Photoshop CS2 software was used to process the images. Quantitation of percent cells with SGs or P-bodies (PBs) was measured by manually counting the number of cells with ≥3 or ≥10 visible foci per cell.

2.2.5 Western blots

5 x 10^6 S2 cells were lysed in 50 µL lysis buffer (20mM HEPES, 150 mM NaCl, 1% Triton X-100, 10% glycerol, 1mM EDTA, 10mM tetrapyrophosphate, 100mM NaF, 17.5 mM β-glycerophosphate, and a protease inhibitor cocktail (Roche)). Equal masses (in micrograms) of lysates were loaded and separated on a 10-15% acrylamide SDS-PAGE gel and then transferred to a polyvinylidene difluoride Immunobilon-FL membrane (Millipore). The membrane was blocked for 30 min in 20 mL of 5% skim milk in TBST (20mM Tris, 150mM NaCl, 0.1% Tween) and incubated at 4°C overnight with the following antibodies: 1:1,000 mouse anti-GFP (Roche), 1:5,000 rabbit anti-V5 (Sigma), and 1:1000 rabbit-anti-deIF4E (generous gift from Paul Lasko, McGill University) in 5mL of 5% skim milk in TBST. Membranes were washed with 20 mL TBST three times and incubated with IRDye 800CW goat-anti-rabbit IgG (LI-COR

biosciences) or IRDye 680CW goat anti-mouse 1:10,000 for one hour at room temperature in 5 mL of 5% skim milk in TBST. The membranes were washed 3 times with 20 mL of TBST, and scanned on an Odyssey imager (LI-COR Biosciences). In some experiments, a 1:30,000 dilution of donkey anti-rabbit IgG-horseradish peroxidase (Amersham) or a 1:10,000 dilution of goat anti-mouse IgG-horseradish peroxidase (Santa Cruz Biotechnology) was also used to detect proteins by chemiluminescence (Millipore).

2.3 Results

2.3.1 Induction of stress granules in *Drosophila* S2 cells

Previous reports demonstrated that SGs can be induced in *Drosophila* S2 cells under oxidative or heat shock stress, conditions that inhibit translation initiation in an eIF2α phosphorylation-dependent or -independent manner, respectively (Farny et al., 2009; Loschi et al. 2009). To further provide a comprehensive analysis of SG formation in *Drosophila* cells, I monitored the formation of mRNA granules by *in situ* hybridization using an oligo(dT)-Cy3 probe in S2 cells treated with arsenite (oxidative stress), heat shock (42°C), or pateamine A (PatA). PatA inhibits translation initiation by sequestering eIF4A from the cap-binding complex, which results in the assembly of SGs in mammalian cells (Dang et al., 2006; Mazroui et al., 2006). In untreated S2 cells, the poly(A)$^+$ RNA was diffusely distributed in the cytoplasm. Treatment of cells with arsenite or heat shock for one hour induced poly(A)$^+$ RNA granules in ~100% of cells (Figure 2.1). Similarly, treatment of cells with PatA also induced poly(A)$^+$ RNA granules (~100% of cells), demonstrating that the induction of RNA granules when eIF4A activity is

inhibited is a conserved process from *Drosophila* to mammals (Figure 2.1). To determine whether these poly(A)$^+$ RNA granules are SGs, I monitored the subcellular localization of a panel of SG protein markers. Because antibodies to several *Drosophila* SG markers are not yet available, I transiently transfected expression vectors containing SG markers fused with either GFP or V5. As observed previously with some of the markers (Farny et al., 2009), expression of the fusion SG markers was cytoplasmically diffuse in untreated cells (Figure 2.1). In contrast, in all stressed cells tested, exogenously expressed Rox8-GFP, GFP-PABP, FMR1-V5, and Rin-GFP were recruited to granules that colocalized with poly(A)$^+$ RNA granules (Figure 2.1A to C and E). Rox8 and Rasputin (Rin) are the *Drosophila* homologues of the mammalian TIA-1 and G3BP, respectively, which are classic markers of SGs (Kedersha et al., 2000; Tourriere et al., 2003). Other signature SG markers include translation initiation factors and the small ribosomal subunit (Kedersha et al., 2002; Kedersha et al., 1999; Kimball et al., 2003). I monitored the subcellular localization of a subunit of the translation factor eIF3 (fusion V5-eIF3 S9) and the endogenous cap binding protein, eIF4E, by indirect immunofluorescence. I also detected the small ribosomal subunit by fluorescent *in situ* hybridization using probes that hybridize to the 18S rRNA. Under all stress conditions, V5-eIF3 S9, endogenous eIF4E, and the 18S rRNA colocalized with poly(A)$^+$ RNA granules, consistent with previous reports that stalled translation complexes are recruited to SGs (Figure 2.1D, F, and G). In addition, it has been shown that a subset of O-linked N- acetylglucosamine (O-GlcNAc)-modified proteins colocalizes with SG markers (Ohn et al., 2008). In untreated cells, O-GlcNAc staining by immunofluorescence showed punctate foci that did not colocalize with poly(A) granules.

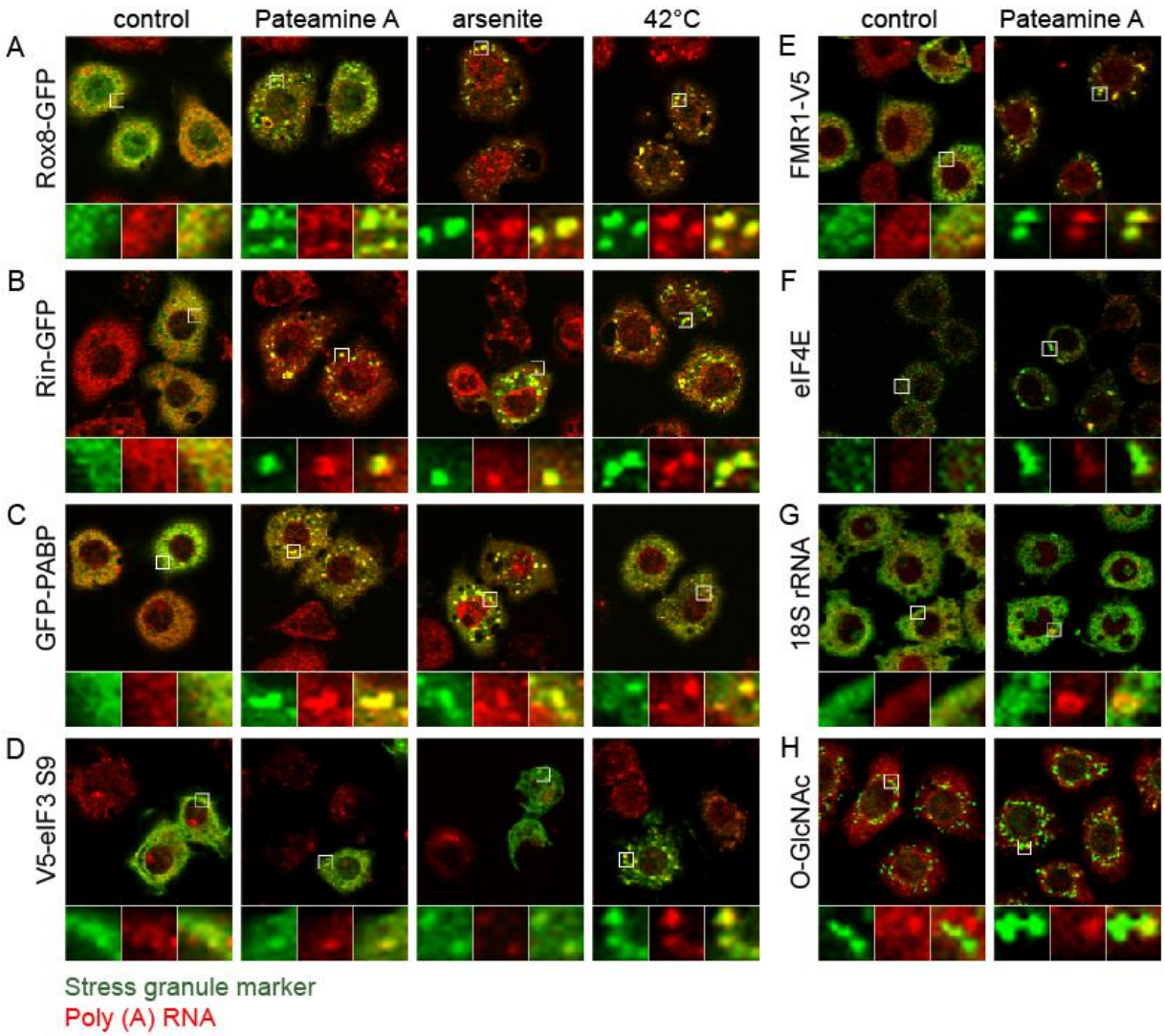

Figure 2.1 Stress granule markers colocalize with poly(A)$^+$ RNA granules in stressed *Drosophila* S2 cells. S2 cells were transiently transfected with expression vectors containing Rox8-GFP (A), Rin-GFP (B), GFP-PABP (C), V5-eIF3 S9 (D), or FMR1-V5 (E) as described in section 2.2.2. A day later, S2 cells were either left untreated (control) or were treated with 50 nM PatA or 500 µM arsenite or heat-shocked at 42°C for one hour. Poly(A)$^+$ RNA was detected by fluorescence *in situ* hybridization using Cy3- or Cy5-oligo d(T)40 (red fluorescence) as described in section 2.2.3. S2 cells were subsequently costained with antibodies to V5 (D and E), eIF4E(F), or *O*-GlcNAc (H) or cohybridized with Cy3-antisense 18S rRNA (G) as described in 2.2.3 and 2.2.4. All SG markers except for poly(A)$^+$ RNA are shown in the green channel. Enlarged views of the boxed areas highlight different channels and merged views.

In PatA-treated cells, a small fraction of O-GlcNAc staining colocalized with the poly(A)$^+$ RNA granules, suggesting that, as in the mammalian cells, the GlcNAc modification may be important for assembly of SGs in *Drosophila* cells (Figure 2.1H). In summary, I had established that SGs can be induced in *Drosophila* cells under a number of stresses using a comprehensive panel of SG protein markers.

2.3.2 Modulation of stress granules during cricket paralysis virus infection

In CrPV-infected S2 cells, significant repression of host translation occurs by three to four hours post infection, concomitant with phosphorylation of eIF2α; thus, I would predict that SGs would form during this time (Garrey et al., 2010). For this analysis, cells with three or more visible foci were counted as SG-containing cells. I found that this approach provided a reproducible and stringent assessment of a cell containing SGs. In uninfected cells, only ~3 to 11% of transfected cells exhibited punctate foci containing Rox8-GFP, Rin-GFP, or PABP-GFP (Figure 2.2A to C). Although significant host translation repression occurs by four hours post infection (hpi), only ~15 to 20% of transfected cells at four and six hpi showed recruitment of Rox8-GFP and Rin-GFP to SGs, compared to ~ 9 to 11% of mock-infected cells (Figure 2.2A and B). Similarly, staining of V5-eIF3 S9 and FMR1-V5 by indirect immunofluorescence was primarily diffuse in both mock-infected cells and at 6 hpi (Figure 2.2D and F). Also, no change in O-GlcNAc staining was observed in mock and CrPV-infected cells, and there was a lack of colocalization between O-GlcNAc staining and poly(A)$^+$ granules at 6 hpi (Figure 2.2E). In summary, these results indicate that SG assembly as defined by these SG protein markers is inhibited during CrPV infection. However, unlike results for

the SG markers above, the number of transfected cells exhibiting foci that contain GFP-PABP increased to 21% and 43% by four and six hpi, respectively, compared to ~ 3% in mock-infected and at two hpi (Figure 2.2C). This suggests that the assembly of SGs composed of GFP-PABP during CrPV infection is distinct from that of other SG markers. Interestingly, the percentage of cells containing three or more poly(A)$^+$ RNA granules increased during CrPV infection from ~20% of mock-infected cells to ~90% of cells by eight hpi (Figure 2.2G). By using a more stringent analysis, the number of cells exhibiting 10 or more foci containing poly(A)$^+$ RNA granules also increased from ~20% in mock-infected cells to ~70% in CrPV-infected cells by eight hpi (Figure 2.2G). In general, I found that the poly(A)$^+$ RNA granules appeared smaller and more numerous than those observed in cells treated with PatA, heat shock, or arsenite. In every case, all SG markers (Rox8- GFP, Rin-GFP, V5-eIF3, FMR1-V5, and O-GlcNAc staining) except for GFP-PABP failed to colocalize with poly(A)$^+$ RNA granules (Figure 2.2A, B, and D to F). Although primarily diffuse, a fraction of GFP-PABP colocalized with the poly(A)$^+$ RNA granules during infection (Figure 2.2C). Thus, CrPV infection inhibits SG formation but not GFP-PABP-containing SGs or poly(A)$^+$ RNA granule formation in S2 cells.

In poliovirus-infected cells, the inhibition of G3BP-containing SGs late in infection is due to cleavage of G3BP by the viral 3C protease(White et al., 2007). To rule out the possibility that the diffuse localization of SG proteins in CrPV-infected cells may be due to degradation or cleavage, I monitored the status of these proteins by Western blot analysis. The SG markers, Rin-GFP, eIF4E, Rox8-GFP, FMR1-V5 and V5-eIF3 S9, remained intact and stable in mock- and CrPV-infected cells at six hpi (Figure 2.2H).

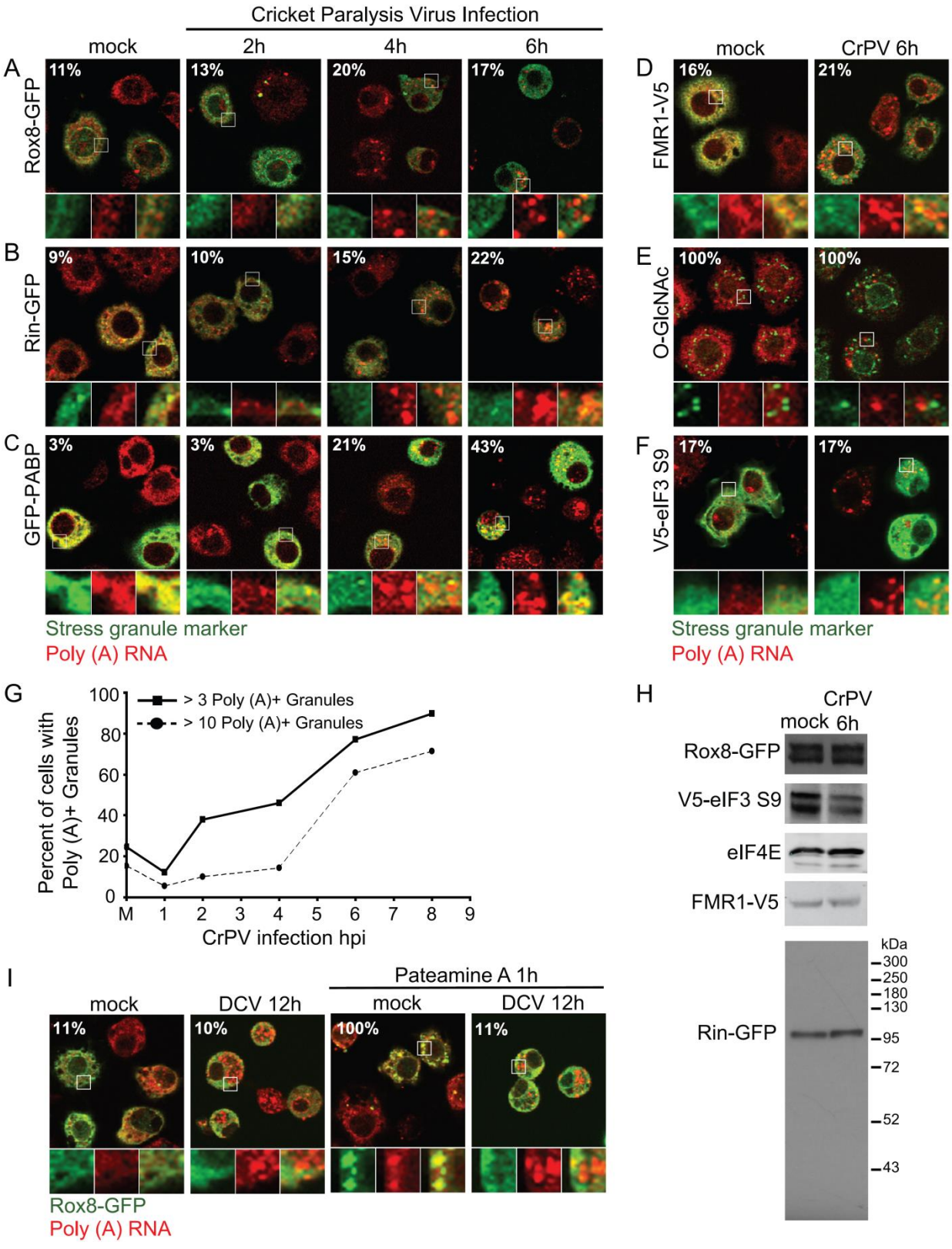
Cricket Paralysis Virus Infection
mock
2h
4h
6h
A
Rox8-GFP
11%
13%
20%
17%
B
Rin-GFP
9%
10%
15%
22%
C
GFP-PABP
3%
3%
21%
43%
Stress granule marker
Poly (A) RNA
mock
CrPV 6h
D
FMR1-V5
16%
21%
E
O-GlcNAc
100%
100%
F
V5-eIF3 S9
17%
17%
Stress granule marker
Poly (A) RNA
G
Percent of cells with Poly (A)+ Granules
100
80
60
40
20
0
> 3 Poly (A)+ Granules
> 10 Poly (A)+ Granules
M
1
2
3
4
5
6
7
8
9
CrPV infection hpi
H
CrPV
mock
6h
Rox8-GFP
V5-eIF3 S9
eIF4E
FMR1-V5
kDa
300
250
180
130
Rin-GFP
95
72
52
43
I
Pateamine A 1h
mock
DCV 12h
mock
DCV 12h
11%
10%
100%
11%
Rox8-GFP
Poly (A) RNA

Figure 2.2 Granules containing PABP and poly(A)$^+$ RNA but not Rox8-GFP or Rin-GFP are formed in CrPV-infected cells. As described in section 2.2.2, S2 cells transiently transfected with expression vectors containing Rox8-GFP (A), Rin-GFP (B), GFP-PABP (C), FMR1-V5 (D), or V5-eIF3 S9 (F) were mock infected or infected for two, four, or six hours with CrPV at an MOI of 10. The V5 fusion proteins and *O*-GlcNAc-modified proteins (E) were detected by staining using anti-V5 and anti-GlcNAc antibodies, respectively, as described in section 2.2.4. (G) Quantitation of the percentage of cells containing poly(A)$^+$ granules as described in section 2.2.4. (H) Western blot analysis of the indicated SG protein markers in mock- and CrPV-infected cells at 6 hpi as described in section 2.2.5. (I) Inhibition of SGs in *Drosophila* C virus-infected cells. S2 cells transiently transfected with the expression vector containing Rox8-GFP were mock-infected or infected for twelve hours with DCV at an MOI of 10. Poly(A)$^+$ RNA was detected by *in situ* hybridization using Cy3-oligo d(T)40 (red fluorescence) as described in section 2.2.3. Percentages represent the proportion of transfected cells containing at least three granules expressing GFP or staining with V5 or *O*-GlcNAc. Enlarged views of the boxed areas highlight different channels and merged views. More than 100 cells were analyzed in multiple fields for each experiment. The average of three independent experiments is shown.

Similarly, it has been shown that PABP is not cleaved or degraded during CrPV infection (Garrey et al., 2010). Thus, the lack of SG induction in CrPV-infected cells is not due to loss of these SG markers.

To determine whether SG assembly is actively inhibited during CrPV infection, cells were challenged with PatA treatment for one hour prior to fixation at different times of infection. PatA treatment of cells, either mock-infected or two hpi, induced SGs, as demonstrated by colocalization of poly(A)$^+$ RNA granules with Rox8-GFP, Rin-GFP, and GFP-PABP (Figure 2.3A to C), indicating that the pathway leading to SG assembly is intact during the first two hours of infection (83 to 100% of cells contained SGs). By four

and six hpi, only 9 to 15% of PatA-treated cells showed foci containing Rox8-GFP and Rin-GFP while the rest of the cells exhibited diffuse GFP expression (Figure 2.3A and B). In contrast, close to ~100% of infected cells at four and six hpi exhibited 3 or more poly(A)$^+$ RNA granules per cell (Figure 2.3). Moreover, as was observated during CrPV infection alone, these poly(A)$^+$ RNA granules did not colocalize with Rox8-GFP and Rin-GFP (Figure 2.3A and B). In the case of GFP-PABP, only a fraction of GFP-PABP colocalized with poly(A)$^+$ RNA granules in PatA-treated cells at 4 and 6 hpi, which is also similar to observations in CrPV-infected cells (Figure 2.2C and 3C). To determine whether CrPV infection can inhibit other SG assembly pathways, I challenged infected cells with arsenite and heat shock. As was seen in PatA-treated cells, Rox8-GFP remained diffuse and did not colocalize with poly(A)$^+$ RNA granules late in infection (Figure 2.3D and E). In summary, these results demonstrate that the assembly of Rox8-GFP and Rin-GFP SGs but not poly(A)$^+$ RNA granules is inhibited in CrPV-infected cells.

2.3.3 *Drosophila* C virus infection inhibits stress granule formation

I next asked whether the related Dicistrovirus, DCV, also inhibits SG formation. Like CrPV infection, DCV infection also leads to host translation repression but at a later time point than in CrPV-infected cells (Cherry et al., 2005). At twelve hpi in DCV infected cells, poly(A)$^+$ RNA granules accumulated in visible foci which did not contain Rox8-GFP (Figure 2.2I). The Rox8-GFP remained cytoplasmically diffuse. When challenged with PatA for one hr at twelve hpi, DCV-infected cells still displayed diffuse Rox8-GFP which did not colocalize with poly(A)$^+$ RNA granules (Figure 2.2I). Given that

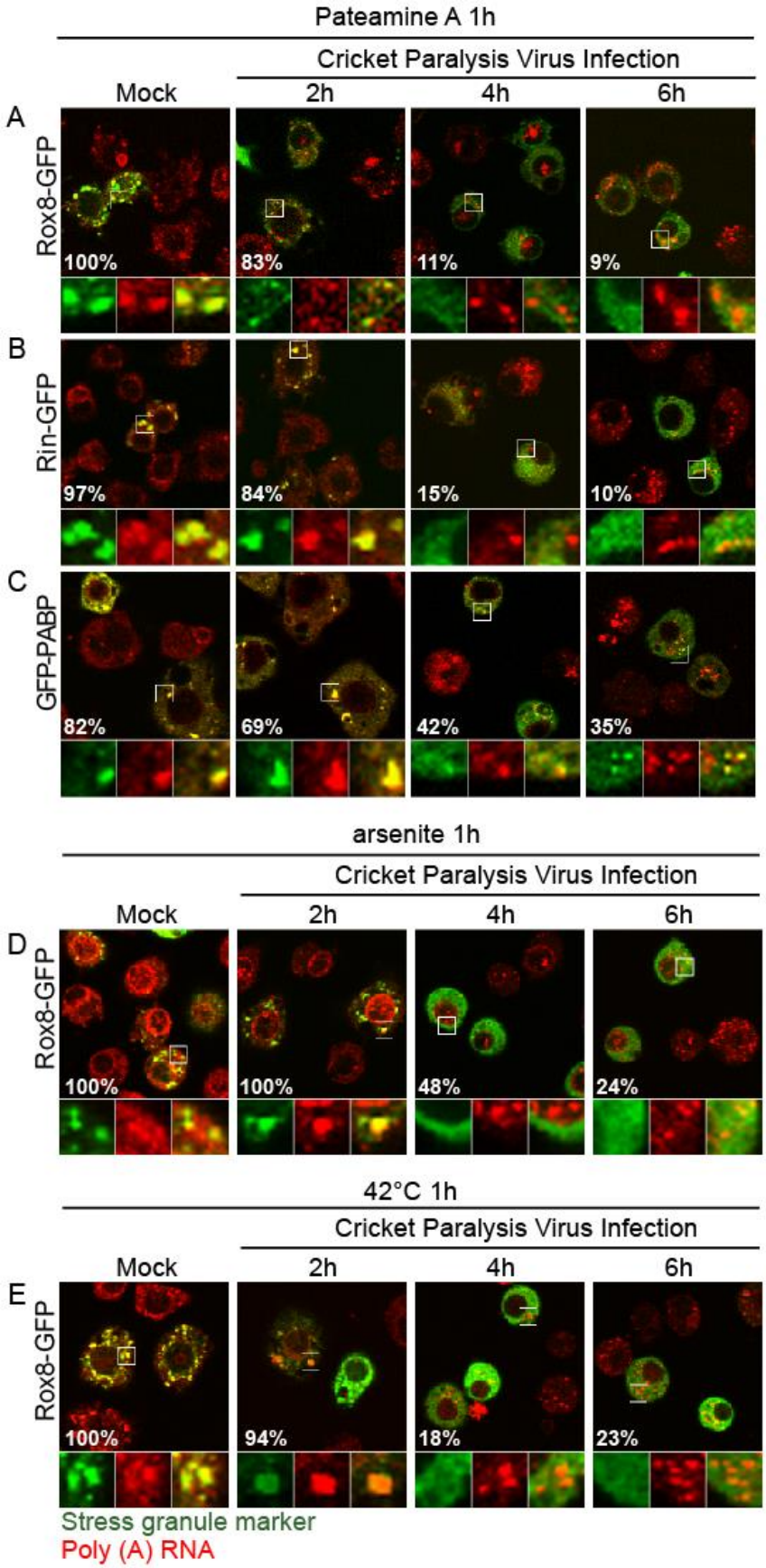
Pateamine A 1h
Cricket Paralysis Virus Infection
Mock
2h
4h
6h
A
Rox8-GFP
100%
83%
11%
9%
B
Rin-GFP
97%
84%
15%
10%
C
GFP-PABP
82%
69%
42%
35%
arsenite 1h
Cricket Paralysis Virus Infection
Mock
2h
4h
6h
D
Rox8-GFP
100%
100%
48%
24%
42°C 1h
Cricket Paralysis Virus Infection
Mock
2h
4h
6h
E
Rox8-GFP
100%
94%
18%
23%
Stress granule marker
Poly (A) RNA

Figure 2.3 CrPV infection inhibits stress granule formation in response to PatA, arsenite, and heat shock treatment. S2 cells transiently transfected with expression vectors containing Rox8-GFP (A), Rin-GFP (B), or GFP-PABP (C) were either mock infected or CrPV infected (MOI of 10) for two, four, or six hours and treated with 50nM PatA (A to C) or 500µM arsenite (D) or heat shocked at 42°C (E) for one hour prior to fixation as described in section 2.2.2. Poly(A)$^+$ RNA was detected by *in situ* hybridization using Cy3-oligo d(T)40 (red fluorescence) as described in section 2.2.3. Enlarged views of boxed areas highlight different channels and merged views. Percentages of transfected cells containing at least three GFP-containing granules are shown. More than 100 cells were analyzed in multiple fields for each experiment. The average of three independent experiments is shown.

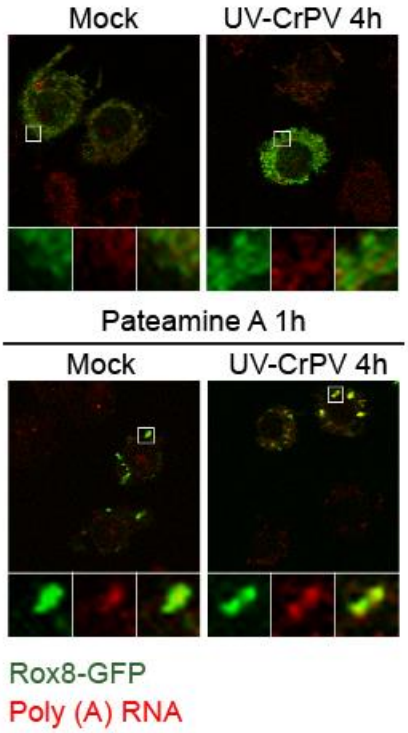

Figure 2.4 UV-inactivated CrPV does not inhibit stress granule formation. Transiently transfected S2 cells expressing Rox8-GFP as described in section 2.2.2 were mock infected or infected with UV-inactivated CrPV. Where indicated, cells were treated with PatA for one hour prior to fixation. Poly(A)$^+$ RNA was detected by *in situ*

hybridization using a Cy3-oligo d(T)40 (red fluorescence) as described in section 2.233. Enlarged views of boxed areas highlight different channels and merged views.

---

both CrPV and DCV infection lead to inhibition of Rox8-containing SGs and induce poly(A)$^+$ RNA granules, this may suggest a general property of dicistrovirus infections in general.

2.3.4 CrPV replication is required for modulation of stress granules

To determine whether CrPV replication is required for the inhibition of SGs, S2 cells were infected with UV-inactivated CrPV. UV-inactivated CrPV was replication-defective and did not produce viral proteins in S2 cells (data not shown). UV-inactivated CrPV failed to induce foci containing Rox8-GFP or poly(A)$^+$ granules at four hpi, a time when poly(A)$^+$ granules are normally detected in CrPV-infected cells (Figure 2.4). When challenged with PatA for one hour at four hpi, cells infected with UV-inactivated CrPV exhibited foci that contained both Rox8-GFP and poly(A)$^+$ granules (Figure 2.4), thus demonstrating that viral replication is necessary for inhibition of SG formation during CrPV infection.

2.3.5 Stress granules are not maintained in CrPV-infected cells

Our experiments indicate that the formation of SGs containing markers such as Rox8 and Rin is inhibited after four hpi in CrPV-infected cells (Figure 2.2 and 2.3). It is possible that CrPV infection may not only inhibit the assembly of SGs but also promote their disassembly. To address this, after SGs were induced by the addition of PatA to infected cells at one hpi, Rox8-GFP-containing SGs were monitored at two or four hpi.

The four hpi time point was chosen because this is when Rox8-containing SGs are inhibited during CrPV infection (Figure 2.3). Whereas PatA treatment for one hour at 2 hpi led to punctate Rox8-GFP granules that colocalized with poly(A)$^+$ RNA (Figure 2.5C), PatA treatment for 3 hour at 4 hpi resulted in diffuse Rox8-GFP and poly(A)$^+$ RNA granules (Figure 2.5D). The lack of Rox8-GFP-containing SGs is not due to the dynamic property of SGs as uninfected cells treated with PatA for 1 or 3 hours still displayed foci containing Rox8-GFP that colocalized with poly(A)$^+$ RNA granules (Figure 2.5A and B). These results indicate that Rox8-GFP-containing SGs cannot be maintained during the course of infection.

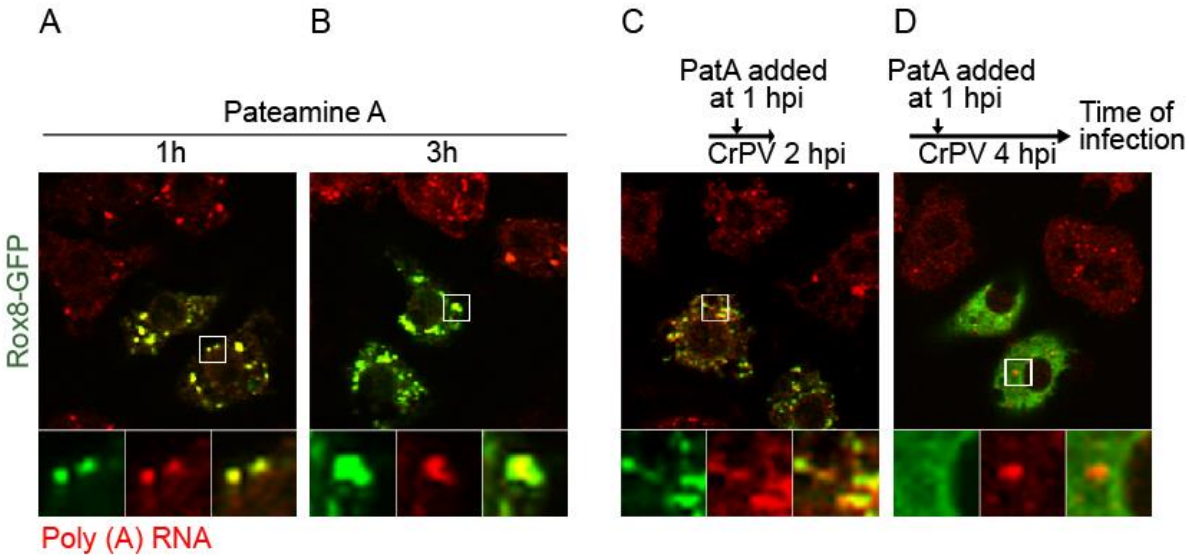

Figure 2.5 CrPV infection leads to disassembly of stress granules. Transiently transfected cells expressing Rox8-GFP as described in section 2.2.2 were infected with CrPV for two hours or four hours (C,D). At one hpi, 50nM PatA was added. As controls, uninfected cells were treated with 50nM PatA for one hour or three hours (A,B). Cells were subsequently fixed, and poly(A)$^+$ RNA was detected by *in situ* hybridization using a Cy3-oligo d(T)40 (red fluorescence) as described in section 2.2.3. Enlarged views of boxed areas highlight different channels and merged views.

2.3.6 Characterization of poly(A)$^+$ RNA granules in CrPV-infected cells

The lack of colocalization of several SG markers with poly(A)$^+$ RNA granules in CrPV-infected cells suggests that the poly(A)$^+$ RNA granules may represent atypical RNA granules. One possibility is that these poly(A)$^+$ RNA granules are P-bodies (PBs). To monitor PBs, cells were transfected with plasmids expressing GFP-GW182 (glycine-tryptophan protein of 182kDa), GFP-DCP1 (decapping protein 1), GFP-Ago1 (argonaute 1), or RFP-Ago2 (argonaute 2). Expression of these reporter proteins resulted in distinct punctate GFP or RFP expression, indicative of basal PB formation (Figure 2.6A). PBs containing GFP-DCP1 or GFP-GW182 were present in 100% of transfected cells, whereas those containing GFP-AGO1 or RFP-AGO2 were present in ~ 50% of cells (cells with > 3 foci per cell were counted as PB-containing cells). As shown in this study, at four and six hpi, poly(A)$^+$ RNA granules were induced in CrPV-infected cells. However, these granules did not colocalize with the GFP-GW182, GFP-DCP1, GFP-AGO1, or RFP-AGO2 foci, indicating that these poly(A)$^+$ RNA granules are not PBs. Interestingly, the number of cells that contained GFP-GW182 and GFP-DCP1 PBs moderately decreased at late times of infection (Figure 2.6A). Compared to mock-infected cells (100% of transfected cells), only ~ 60% of CrPV-infected cells at six hpi displayed > 3 foci containing GFP-GW182 or GFP-DCP1 (Figure 2.6A). This decrease was not due to degradation or cleavage of the PB markers (Figure 2.6B). In contrast, the percentage of cells with PBs containing GFP-AGO1 or RFP-AGO2 remained constant throughout infection (Figure 2.6A). Thus, these results demonstrate that formation of PBs containing GFP-GW182 or GFP-DCP1 but not GFP-AGO1 or RFP-AGO2 is inhibited in CrPV-infected cells. Since the CrPV viral RNA genome has a

poly(A)$^+$ tail (Eaton and Steacie, 1980), we next investigated the possibility that the poly(A)$^+$ RNA granules contain CrPV RNA or viral replicative RNA intermediates. By *in situ* hybridization using a probe specific to the sense strand of CrPV RNA, fluorescence increased during the course of CrPV infection, strongly indicating that the increase in viral RNAs was specifically detected (Figure 2.7). As a control, a probe containing a randomized sequence did not result in fluorescence signal over background (data not shown). Despite the increase in viral RNA, the detectable fluorescence signal did not colocalize with the poly(A)$^+$ RNA granules (Figure 2.7). To determine whether the poly(A)$^+$ RNA granules may be sites of replicative intermediates, I used an antibody that specifically recognizes double-stranded RNA (dsRNA) (62). Whereas mock-infected cells displayed basal immunofluorescence, the dsRNA staining increased over time in CrPV-infected cells, consistent with an increase in replicative viral intermediates (Figure 2.7). The dsRNA staining was punctate, indicating that CrPV replication is localized. However, the dsRNA staining did not colocalize with the poly(A)$^+$ RNA granules in CrPV-infected cells (Figure 2.7, compare green and red channels). From these results, I concluded that the virally induced poly(A)$^+$ RNA granules are not PBs and do not contain viral RNA.

2.3.7 The CrPV 3C protease is sequestered to stress granules

Our results suggest that CrPV replication is required for the inhibition of SG formation (Figure 2.4). One possibility is that a CrPV protein may be mediating this effect. To begin testing this hypothesis, I subcloned individual CrPV non-structural and structural proteins. Of the CrPV proteins tested so far, none can inhibit the formation of

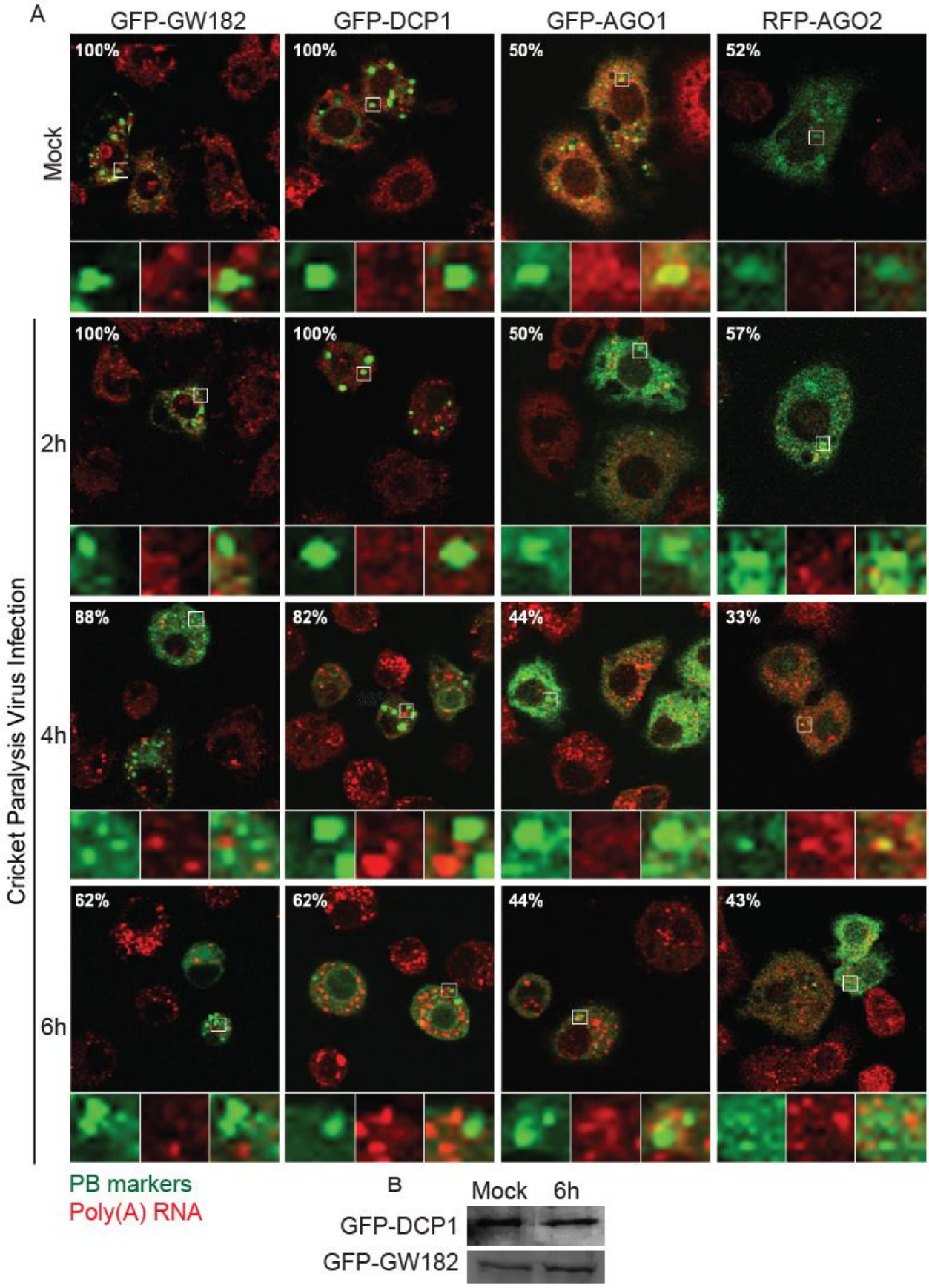
A
GFP-GW182
GFP-DCP1
GFP-AGO1
RFP-AGO2
Mock
Cricket Paralysis Virus Infection
2h
4h
6h
100%
100%
50%
52%
100%
100%
50%
57%
88%
82%
44%
33%
62%
62%
44%
43%
PB markers
Poly(A) RNA
B
Mock
6h
GFP-DCP1
GFP-GW182

Figure 2.6 Virus-induced poly(A)$^+$ RNA granules do not contain P body markers. (A) S2 cells transiently transfected with expression vectors containing GFP-AGO1, RFP-AGO2, GFP-DCP1, or GFP-GW182 as described in section 2.2.2 were either mock or CrPV infected for two, four, or six hours with CrPV at an MOI of 10. PB markers are shown in green. Poly(A)$^+$ RNA was detected by *in situ* hybridization using Cy3-oligo d(T)40 (red fluorescence) as described in section 2.2.3. Percentages represent the proportion of transfected cells containing at least three GFP- or RFP-containing granules. Enlarged views of boxed areas highlight different channels and merged views. (B) Western blot analysis of the indicated PB protein markers in mock- and CrPV-infected cells at six hpi as described in section 2.2.5.

Rox8-GFP-containing SGs in cells treated with PatA. However, through our analysis, I noticed that in cells expressing the V5- tagged 3C protease, the staining of V5 by indirect immunofluorescence colocalized with SGs containing Rox8-GFP and poly(A)$^+$ RNA under PatA treatment (Figure 2.8, middle panel). I next tested whether the tagged 3C protease may be colocalizing with the poly(A)$^+$ RNA granules that are induced in CrPV-infected cells. As shown previously in CrPV-infected cells, the Rox8-GFP remained diffuse, and poly(A)$^+$ RNA granules assembled in CrPV-infected cells (Figure 2.8, right panel). However, the tagged 3C protease was not recruited to the poly(A)$^+$ granules during CrPV infection and remained cytoplasmically diffuse. Because the viral 3C protease may be being sequestered to SGs, one possible outcome of inhibiting SG assembly during CrPV infection is that the 3C protease remains available for viral processing.

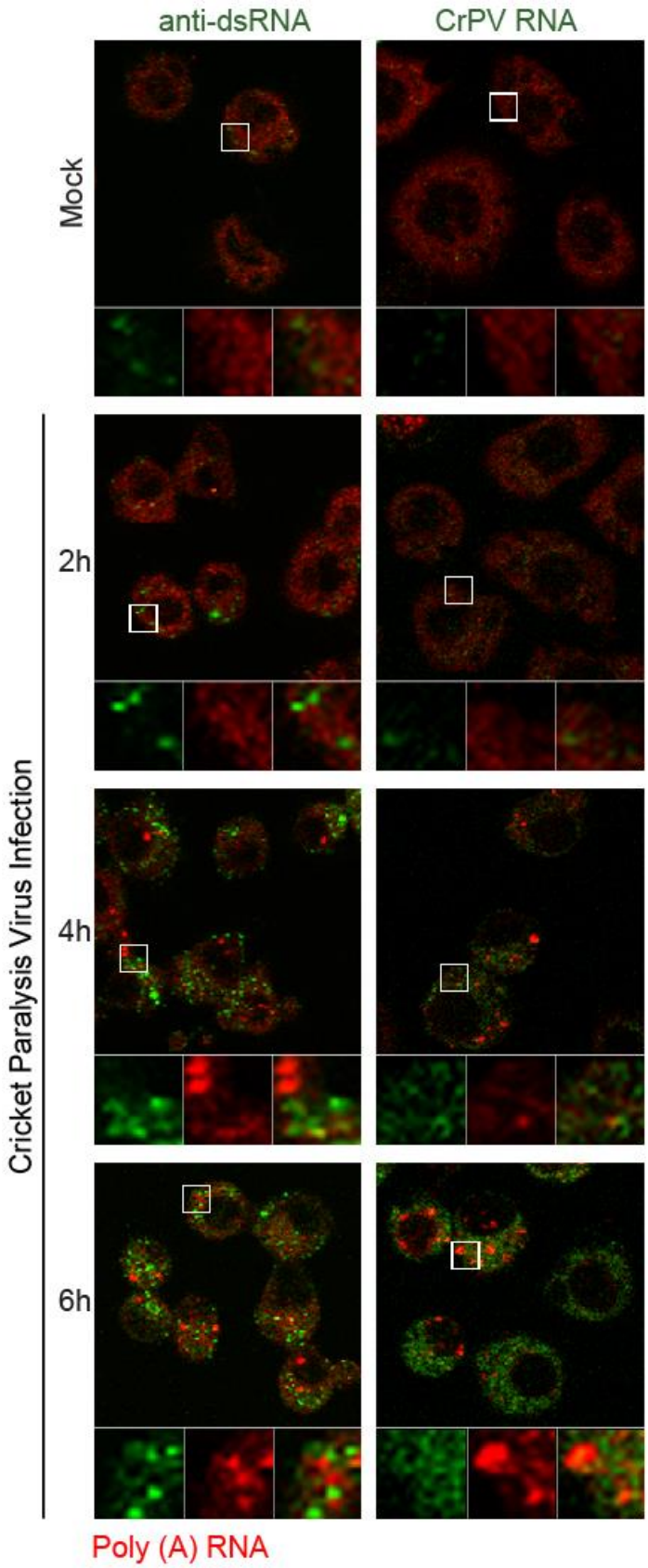
anti-dsRNA
CrPV RNA
Mock
2h
4h
6h
Cricket Paralysis Virus Infection
Poly (A) RNA

Figure 2.7 Virus-induced poly(A)$^+$ RNA granules do not contain CrPV RNA. S2 cells were mock or CrPV infected (MOI of 10) for two, four, or six hours and then processed for *in situ* hybridization. Poly(A)$^+$ RNA was detected by *in situ* hybridization using a Cy5- or Cy3-oligo d(T)40 (red) as described in section 2.2.3. Viral dsRNA intermediates were detected by indirect immunofluorescence using an anti-dsRNA antibody (green) as described in section 2.2.4. CrPV RNA was detected by using a Cy5-conjugated antisense probe that hybridized to the sense strand of CrPV RNA (green) as described in section 2.2.3. Enlarged views of boxed areas highlight different channels and merged views.

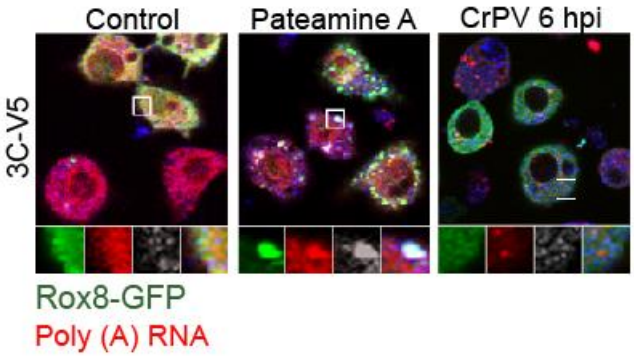

Figure 2.8 The CrPV 3C-like protease is sequestered to SGs under cellular stress. S2 cells transiently cotransfected with expression vectors containing Rox8-GFP and CrPV 3C protease-V5 as described in section 2.2.2 were left untreated (control), treated with 50nM PatA for one hour, or infected with CrPV for six hours. Fusion V5 viral proteins were detected by costaining with anti-V5 antibody (gray) as described in section 2.2.4, and poly(A)$^+$ RNA was detected by *in situ* hybridization using Cy5-oligo d(T)40 (red) as described in section 2.2.3. Expression of Rox8-GFP is shown in green. Enlarged views of boxed areas highlight different channels and merged views.

2.4 Discussion

Viruses have evolved unique mechanisms to evade the host antiviral response and to usurp host factors for viral translation and replication. There is increasing evidence that viruses can modulate SG and PB formation, suggesting that they can

impact virus infection and yield (Lloyd, 2013). Here, I have demonstrated that infection by the dicistroviruses CrPV and DCV inhibits the assembly of SGs, as defined by a set of SG protein markers, but not of granules containing poly(A)$^+$ RNA. My results suggest that the inhibition of SG formation may keep viral 3C protein available for CrPV polypeptide processing.

This Chapter expands on previous reports on SGs in *Drosophila* cells, and I have now demonstrated several SG markers that aggregate and colocalize with poly(A)$^+$ RNA under a number of cellular stress conditions (Farny et al., 2009; Loschi et al., 2009). SGs are induced in cells treated with heat shock, arsenite, and PatA, indicating that SG assembly is conserved in *Drosophila* and that these SGs are compositionally similar to those in mammalian cells (Figure 2.1). Using this panel of SG markers, I explored the relationship of SG formation during dicistrovirus infection. In CrPV- and DCV-infected cells, despite a rapid loss of host protein synthesis, the majority of the classic SG markers do not aggregate and remain dispersed (Figure 2.2). This was surprising as I monitored signature SG markers such as Rox8, Rin, and eIF3. Only the SG marker PABP partially aggregated and colocalized with poly(A)$^+$ RNA granules. My results showed that infected cells challenged with potent SG inducers such as heat shock, arsenite, or PatA could not induce aggregation of SG markers after four hpi but could at earlier times of infection (Figure 2.3). This suggests that the inhibition of SG formation in CrPV-infected cells likely targets a general pathway of SG formation at late times of infection. My results also indicate that Rox8-containing SGs are not maintained during CrPV infection when SGs are induced early in infection (Figure 2.4). Taken together, these results indicate that CrPV infection promotes the disassembly of SGs at late times

of infection. Despite the lack of aggregation of most SG markers, poly(A)$^+$ RNA granules were still induced in CrPV-infected cells (Figure 2.5). This observation highlights the importance of monitoring both SG protein markers and poly(A)$^+$ RNA and serves as an example that distinct SGs and RNA granules may be differentially regulated under specific cellular conditions. Moreover, given that there is more evidence that compositionally distinct SGs exist and may be differentially regulated, as I have observed in our studies, it is imperative to monitor as many SG markers as possible during a given cellular stress (Piotrowska et al., 2010; Stoecklin et al., 2004).

The percentage of cells containing poly(A)$^+$ RNA granules increased during infection, which correlated with viral replication (Figure 2.1). To my surprise, using two approaches to detect viral RNA by *in situ* hybridization and by indirect immunofluorescence using an anti-dsRNA antibody, I found that these poly(A)$^+$ RNA granules do not contain viral RNA (Figure 2.7). I also showed that these poly(A)$^+$ RNA granules do not colocalize with PB markers (Figure 2.6). Currently, I do not know if these poly(A)$^+$ RNA granules represent novel RNA granules or are distinct SGs that do not colocalize with known classic SG markers but, rather, with a yet to be discovered aggregating protein complex. A report showed that in poliovirus-infected cells, the induction of poly(A)$^+$ RNA granules requires ongoing host transcription (Piotrowska et al., 2010). In CrPV-infected cells, addition of actinomycin D did not affect the induction of poly(A)$^+$ RNA granules or lead to the inhibition of SG marker aggregation (data not shown). In CrPV-infected cells, overall translation is shut off by four hpi, which is approximately the same time when poly(A)$^+$ RNA granules are induced (Garrey et al., 2010). It is likely that these poly(A)$^+$ RNA granules represent inactive mRNAs that are

released from polysomes during infection. An outstanding question is whether a subset of mRNAs or all nontranslating mRNAs are localized to these poly(A)$^+$ RNA granules in infected cells.

What is dissociating SGs during CrPV infection? UV-inactivated CrPV does not mediate the inhibition of SG assembly, indicating that CrPV replication is required (Figure 2.4). Furthermore, the inhibition of SG formation occurred after four hpi, suggesting that a viral protein may be mediating this effect (Figure 2.2 and 2.3). SGs can assemble through the action of aggregating proteins such as TIA-1 and G3BP (Kedersha et al., 2002; van Rij et al., 2006). However, during CrPV and DCV infection, these and other SG proteins tested in this study do not aggregate and are not cleaved or degraded (Figure 2.2). Another possibility is one or more of the SG proteins are recruited by CrPV and DCV and the loss of this protein destabilizes SGs during infection. There are many examples of this in other viruses (section 1.7). However, the viruses that do interact with SG markers require these proteins for viral replication. Besides "hijacking" SG factors, CrPV infection might affect a posttranslational modification pathway and that might affect SG assembly. For example, it has been reported that the deacetylase activity of histone deacetylase (HDAC) is required for SG assembly (Kwon et al., 2007). Moreover, a siRNA screen identified several genes (>100) involved in the assembly and disassembly of SGs, suggesting that multiple factors may mediate SG assembly (Ohn et al., 2008). One interesting outcome from this previous study was the discovery that the O-GlcNAc modification of proteins may be important for the assembly of SGs (Ohn et al., 2008). In my experiments, the staining of O-GlcNAc by immunofluorescence was localized to SGs under cellular stress but not

during CrPV infection, suggesting that CrPV infection does not affect this pathway of SG assembly. My data suggest that SGs may be actively disrupted during CrPV infection (Figure 2.5). The factors Staufen 1 and eIF5A have been shown to disrupt SGs by maintaining ribosomes bound to mRNAs, thus preventing initiation complexes from shuttling to SGs (Li et al., 2009; Thomas et al., 2009). It is unlikely that these factors are responsible for the inhibition of SGs during CrPV infection since host translation is shut off, and the majority of polysomes is disassembled (Garrey et al., 2010).

My results demonstrated that PBs containing GW182 and DCP1 disassemble late during CrPV infection (Figure 2.6). PBs are thought to be sites to which translationally stalled mRNPs are shuttled either for degradation or for reorganization of mRNPs. Moreover, PBs are normally found adjacent to SGs during cellular stress, and proteins and mRNAs may be exchanged between PBs and SGs (Kedersha et al., 2005). In general, GW182, DCP1, Ago1, and Ago2 interact with each other to form cytoplasmic PB foci containing mRNA and miRNAs (Behm-Ansmant et al., 2006; Eystathioy et al., 2002; Ingelfinger et al., 2002; Schneider et al., 2006). However, not all PBs contain the full complement of PB markers, and many PB markers are in other types of RNA granules. For instance, PBs containing DCP1 and Ago2 do not colocalize under certain cellular stress conditions (Leung et al., 2006). In addition, some classical PB markers like GW182 and AGO2 are also in other granules that is different from the DCP1-containing P bodies (Gibbings et al., 2009). Supporting this, CrPV infection affects only granules containing DCP1 and GW182 but not Ago1 and Ago2 (Figure 2.6). During CrPV infection, the virus may inhibit DCP1- and GW182-containing PBs specifically in order to keep viral RNAs from being degraded. Alternatively, given that

GW182 is a key component in miRNA-dependent translational control, it is possible that a miRNA that is normally shuttled to PBs may be required for CrPV infection (Eulalio et al., 2007; Liu et al., 2005; Rehwinkel et al., 2005). It has been shown that Ago2-deficient flies are hypersensitive to CrPV and DCV infection, indicating that Ago2 is an antiviral factor in *Drosophila* (van Rij et al., 2006). Moreover, the CrPV silencing suppressor 1A protein targets and inhibits Ago2 activity, thereby antagonizing RNA interference (Nayak et al., 2010). Because Ago2 remains punctate during CrPV infection, it remains to be seen whether this process may contribute to the suppression of Ago2 activity and affect viral yield. I observed that the V5-tagged 3C protease colocalized with Rox8-GFP and poly(A)$^+$ RNA granules under PatA-induced stress, suggesting that this viral protein has a tendency to be sequestered to SGs (Figure 2.7). Under viral infection, the 3C protease remained disperse and did not colocalize with the poly(A)$^+$ RNA granules. Thus, I propose that one purpose of inhibiting SG formation during infection is to keep the CrPV 3C protease available and free for viral protein processing. Alternatively, given that SGs may sequester specific proteins to regulate apoptosis (Arimoto et al., 2008), it is possible that the inhibition of SGs in CrPV-infected cells affects other cellular processes.

Even though SGs are disrupted to prevent viral proteins from being "trapped," there may be other potential reasons why dicistroviruses would want to disrupt SGs. Recently, new evidence has emerged that suggests that SGs activate the innate immune response (Reineke and Lloyd, 2015). For example, PKR activation can be triggered in SGs by overexpressing G3BP. Specifically, Reineke and Lloyd (2015) showed that G3BP can recruit inactive PKR to SGs and by some undetermined

mechanism, PKR becomes activated and leaves SGs. This novel activation is dependent on G3BP interacting protein Caprin 1 (Reineke et al., 2015). Since activation of PKR leads to interferon (IFN) production, G3BP overexpression in cells inhibited enterovirus replication. This novel link between SGs and innate immunity is likely not present in *Drosophila* because *Drosophila* lacks PKR and IFN. Nevertheless, it will be interesting to test if G3BP overexpression activates an innate immune response in *Drosophila*.

Another enticing reason why dicistrovirus might benefit from disrupting SGs is to recruit cellular factors that would have been "trapped" in SGs. For example, a recent paper by Majzoub *et al.* (2014) demonstrates that RACK1, a protein that is normally enriched in SGs during cellular stress, interacts with CrPV and DCV 5'-UTR IRES. In addition, RACK1 is important for 5-'UTR IRES translation because depletion of this factor led to 10-fold decrease in IRES activity (Majzoub et al., 2014). More experiments will be needed to determine whether there is a link between SG disassembly and recruitment of RACK1 by the 5'-UTR IRES.

Chapter 3: CrPV-1A stimulates 5'-dependent translation and inhibits the stress granule pathway

3.1 Introduction

Viruses have evolved several strategies to manipulate the host cell to facilitate viral replication and translation. In CrPV-infected S2 cells, a number of cellular processes are affected including repression of cellular transcription (Chapter 4) and translation (Garrey et al., 2010), inhibition of the RNAi silencing pathway (Nayak et al., 2010) and inhibition of the SG pathway (Chapter 2)(Khong and Jan, 2011). How some of these pathways are perturbed by CrPV infection and contribute to the life cycle of the virus is not well understood. I hypothesize that one or more viral non-structural and structural proteins are responsible for the disruptions in these cellular processes. Since a least 13 viral proteins are produced during CrPV infection, I subcloned and expressed each viral protein in *Drosophila* S2 cells and monitored cell viability and the effects on reporter gene expression (Appendix)(Figure 3.1C)(Moore et al., 1980). I identified one candidate, viral protein CrPV 1A, that inhibited gene expression and induced cell death. This Chapter focuses on the role of CrPV 1A on specific cellular processes.

To counteract the RNAi antiviral response, a number of viruses have evolved RNAi suppressors that inhibit specific steps of the RNAi pathway (Bronkhorst et al., 2014; Lu et al., 2005; Schnettler et al., 2012; Sullivan and Ganem, 2005; van Mierlo et al., 2014; van Rij et al., 2006). Briefly, the *Drosophila* RNAi pathway is activated upon recognition of long dsRNA, which is typically generated as a viral intermediate during viral replication. Dicer2, an RNase III-like enzyme, 'dices' the dsRNA into 21-23 bp siRNAs (reviewed in Sabin et al., 2010). siRNAs are then loaded into the RNA-induced

silencing complex (RISC), which contains a second RNase III-like enzyme, Ago2. One strand of the siRNA guides the RISC complex to viral genomic RNA by perfect complementary base pairing and Ago2 cleaves the viral RNA (Figure 3.1). Illustrating the importance of this pathway, Ago-2-deficient flies are hypersensitive to viruses like DCV and CrPV and succumb earlier than wild-type flies (van Rij et al., 2006; Wang et al., 2006). Furthermore, a number of viruses block this pathway (Bronkhorst et al., 2014; Lu et al., 2005; Schnettler et al., 2012; Sullivan and Ganem, 2005; van Mierlo et al., 2014; van Rij et al., 2006). For example, Flock house virus (FHV) encodes a viral protein called B2 that binds to dsRNA with high affinity and inhibits Dicer2 processing (Lu et al., 2005; Sullivan and Ganem, 2005). Dicistroviruses have also evolved mechanisms to also inhibit RNAi. The 1A protein of CrPV suppresses the RNAi response by interacting with Ago2 and inhibiting the cleavage of target RNA directly (Nayak et al., 2010). Interestingly, protein 1A of DCV, which is related to CrPV, suppresses the RNAi pathway by binding to dsRNA and sequestering the viral RNA from the RNAi machinery (van Rij et al., 2006) (Figure 3.1). The fact that dicistroviruses have evolved multiple mechanisms to inhibit RNAi further demonstrates the significance of these pathways in antiviral responses in *Drosophila*.

Besides suppressing RNAi, a recent paper by Besnard-Guerin *et al.* (2015) discovered that 1A also affects microRNA (miRNA) silencing. Unlike siRNAs, miRNAs are small endogenously encoded RNAs that mediate silencing by binding imperfectly to target RNAs (reviewed in Ameres and Zamore, 2013). The authors found that CrPV-1A inhibits Ago2-dependent miRNA-mediated silencing in S2 cells and in flies (Besnard-Guerin et al., 2015).

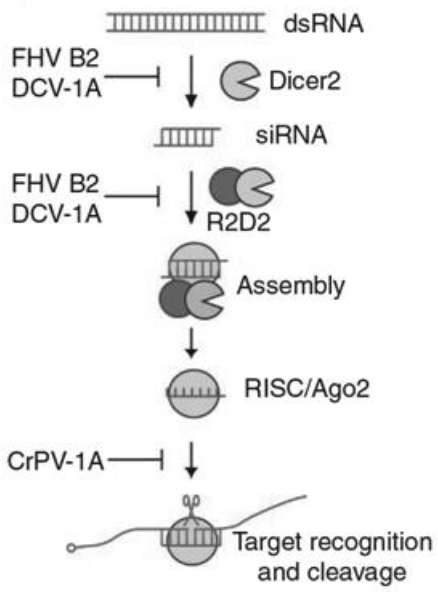

Figure 3.1 CrPV-1A, DCV-1A, and FHV-B2 suppress the RNAi pathway in insects. RNAi silencing is a major insect immunity pathway. Specifically, long dsRNAs from viral replication intermediates or structured RNA are recognized and processed by Dicer2, a RNase-III enzyme, into siRNAs. Once loaded into the RISC complex, one strand of the siRNAs guide the RISC complex to viral genomes by complementary base pairing. Ago2, an RNase III enzyme, within the RISC complex cleaves the viral RNA which marks it for further degradation. CrPV, DCV, and FHV encode RNAi suppressors. DCV-1A and FHV-B2 impede RNAi silencing by binding to long dsRNA and siRNA. CrPV-1A blocks RNAi silencing by binding to Ago2. Adapted from Nayak *et al.* (2010)

In this Chapter, I discovered that CrPV 1A has other functions besides suppressing siRNAs and miRNAs. Notably, 1A stimulates 5'-end-dependent translation in an Ago2-dependent manner. I showed that deletion of the C-terminal domain of 1A disrupted this activity and that amino acid residue (R146) within 1A is important specifically for this activity but not for RNAi suppression. Lastly, expression of 1A in cells can suppress SG induction by PatA and arsenite. Together, these results suggest that CrPV-1A exhibits multiple functions to facilitate virus infection.

3.2 Materials and methods

3.2.1 Cell culture and virus infection

Drosophila S2 cells were maintained as described in section 2.2.1.

3.2.2 Plasmids

CrPV 1A (NC_003924, nt:709-1200), KBV 1A (NC_004807, nt:609-1127), ABPV 1A (NC_002548, nt:605-1096), and CrPV 1AΔ128 (NC_003924, nt:709-1092) were cloned into the pAct5.1-HA expression plasmid. pAc5.1-HA was constructed by inserting the 3xHA oligo (synthesized by IDT) using restriction sites Xba1 and Apa1. The 3xHA oligo sequence is 5'-TCTAGATACCCGTACGACGTCCCGGACTACGCTGG CTATCCCTATGATTGCCCGATTATGCGTATCCTTACGATGTTCCAGATTATGCCTAA TGAGGGCCC-3'. The following steps were used to generate the pAct-CrPV-1A-HA expression plasmid. 1) RNA was extracted from CrPV-infected S2 cells with Trizol (invitrogen). 2) cDNA was generated from the RNA by reverse transcriptase with an oligo dT(20) primer. 3) Primers with Kpn1 and Xba1 (5'-ACTG GGTACC ATGTCTTTTCAACAAACAAACAACAACG-3' and 5'-ACTG TCTAGA ATTAGATTCGACATCACCACTCATCAAA-3') flanking sequences respectively were used to amplify 1A from the cDNA. 4) The PCR-derived 1A was then digested with Kpn1 and Xba1 and inserted into pAct5.1-HA plasmid lineard with Kpn1 and Xba1. 5) Following transformation of ligation products, bacterial colonies were picked and plasmids were extracted and purified by miniprep. 6) Finally, ligation was confirmed by sequencing the plasmids. pAct-KBV-1A-HA, pAct-ABPV-1A-HA, pAc5-CrPV-1AΔ128

were constructed similarily except the PCR-derived KBV-1A, ABPV-1A, and CrPV1AΔ128 were generated from full length genomic KBV or ABPV (synthesized by IDT), and pAct-CrPV-1A-HA respectively.

The CrPV minigenome reporter was constructed stepwise using the pGEM3 plasmid as a backbone. 1) The CrPV IGR IRES including a short region of ORF2 (AF218039, nt:6217 to 6373) was PCR-amplified and ligated between the EcoR1 and Nco1 sites of pGEM3. 2) The firefly luciferase gene was PCR-amplified and ligated between the Nco1 and Xba1 sites. 3) The 3'UTR of CrPV (synthesized by IDT) was ligated between Xba1 and BamH1 sites. 4) Finally, the 5'-UTR CrPV and Renilla luciferase gene, generated by overlapping pcr, were inserted between the HindIII and EcoR1 sites.

The GAPDH bicistronic reporter was constructed using the CrPV minigenome reporter described above as a backbone by Gibson Assembly (NEB), a single isothermal reaction that combines an 5' exonuclease, a DNA polymerase, and a DNA ligase for the joining of multiple overlapping DNA fragments. The following steps were used to create this construct. 1) RNA was extracted from S2 cells with Trizol (invitrogen). 2) cDNA was generated from the RNA by reverse transcriptase with oligo dT(20) primer. 3) Primers with overlaps were used to amplify GAPDH from the cDNA (5'-ACGACTCACTATAGGGTTTTTAAGGCGCTTATATAATCAAACC-3' and 5'-CATAAACTTTCGAAGTCATGGCTGAGTTCCTGCTGTC-3'). 4) Overlapping reverse complement primers were used to amplify the entire CrPV minigenome reporter minus the 5'-UTR IRES. 5) After cleanup by phenol chloroform extraction and ethanol precipitation, the PCR-derived 5'-UTR GAPDH DNA (NM_080369, nt:1-260) was

incubated with the PCR-derived CrPV minigenome lacking the 5'-UTR IRES in a 3:1 molar ratio with 1X Gibson assembly mix for one hour. 6) After assembly, 2 uL was used for transformation. 7) Several bacterial colonies were picked, purified, and sequenced to confirm that the 5'-UTR of GAPDH had replaced the 5'-UTR IRES in the minigenome construct. The CrPV minigenome and the GAPDH bicistronic plasmids were linearized with BamHI before proceeding to RNA synthesis by *in vitro* transcription.

3.2.3 DNA transfection, luciferase assay, and trypan blue assay

DNA transfections (Figure 3.2) were performed using Xtreme-GENE HP DNA transfection reagent (Roche). 1ug of pAct expression plasmid (CrPV-1A-HA, KBV-1A-HA, ABPV-1A-HA, or dsRED) were cotransfected with 1ug of pAct firefly luciferase construct into S2 cells (1.5 X 10^6 cells per mL; 6-well plates) as described by the manufacturer (Roche). Cells were harvested with passive lysis buffer (Promega) forty eight hours after transfection and assayed for luciferase activity (Promega) using a microplate luminometer (Berthold Technologies, Centro LB 960). Trypan blue assay was performed as described by the manufacturer (Thermo Fisher).

3.2.4 Scanning alanine mutagenesis

Site-directed mutagenesis was performed on pAct-CrPV-1A-HA at specific nucleotide positions to introduce an alanine at specific amino acids within CrPV 1A. The constructs were verified by sequencing.

3.2.5 *In vitro* transcription

1A-HA, 1AΔ128-HA, 1Amutants-HA, dsRED, and GFP were PCR amplified from reporter plasmids (Section 3.2) by using a reverse primer and a forward primer with a T7 promoter.

In vitro transcription reactions using T7 RNA polymerase were performed as described previously (Wang and Jan, 2014). RNA were capped and polyadenylated (CellScript), purified (RNeasy kit, Qiagen) and the integrity of the RNA was determined by visualization on an agarose gel. The quantity of the RNA was determined by Nanodrop (Thermo Scientific).

3.2.6 dsRNA-mediated knockdown

~400-500bp PCR products of GFP, firefly luciferase and dAgo2 were amplified using primers that contain the T7 promoter at both ends. The PCR products were used as templates in *in vitro* transcription reactions using T7 RNA polymerase. dsRNA was purified and its integrity was verified by denaturing gel analysis. dsRNA (13 μg/million cells) was incubated with S2 cells in serum-free SSM3 media for one hour, followed by the addition of complete SSM3 media. S2 cells were incubated with firefly luciferase and Ago2 dsRNAs for two and five days respectively.

3.2.7 RNA transfection and luciferase assay

Luciferase reporter RNAs (0.5 μg) were co-transfected with indicated RNAs (0.5 μg) (lipofectamine 2000, Invitrogen) into S2 cells (1.5 X 10^6 cells per mL; 12-well plates) as described by the manufacturer (Invitrogen). All RNAs were capped and

polyadenylated. Cells were harvested with passive lysis buffer (Promega) four hours after transfection and assayed for luciferase activity (Promega) using a microplate luminometer (Berthold Technologies, Centro LB 960).

3.2.8 Western blot analysis with Ago2, HA and Tubulin

The westerns were performed as described in section 2.2.5. In this Chapter, the primary antibodies used were α-Ago2 (1:500 dilution, Andrew Simmonds from the University of Alberta), α-Tubulin (1:1000 dilution, Santa Cruz), and α-HA (1:500 dilution, Covance)

3.2.9 Immunoprecipitation with conjugated HA-antibody

100 µg of lysates from S2 cells transfected with CrPV 1A-HA, CrPV 1AΔ128-HA, CrPV 1A R146A-HA, and dsRED RNA (control) were immunoprecipitated with 50 µL of Anti-HA Affinity Matrix as described by the manufacturer (Roche). Immunoprecipitates were mixed with 100 µL 2X SDS loading dye at 95°C for 10 min, centrifuged and the supernatant was loaded on an SDS-PAGE for immunoblotting analysis using anti-HA antibody (Section 3.7).

3.2.10 [^{35}S]-pulse-labelling in cells

As described previously (Garrey et al., 2010), cells were pulse labeled with [^{35}S]-Met/Cys (Perkin-Elmer) for 20 min, washed with cold PBS twice and harvested with lysis buffer. Equal amounts of lysates were resolved on a SDS-PAGE and the SDS-

PAGE gel was dried. Radioactive bands were imaged with a phosphorimager (Amersham Pharmacia Biotech).

3.2.11 Confocal analysis of stress granules

Rox8-GFP RNAs (1 μg) were co-transfected with the indicated RNAs (1 μg) (lipofectamine 2000, Invitrogen) into S2 cells (3.0 X 10^6 cells per mL; 6-well plates) as described by the manufacturer (Invitrogen). All RNAs were capped and polyadenylated. In preparation for microscopy, a total of 1 X 10^6 S2 cells was plated for one hour on coverslips pre-coated with concanavalin A 0.5 mg/ml (Calbiochem). Cells were subsequently fixed with 3% paraformaldehyde in PBS and permeabilized in 0.5% Tween in PBS. Coverslips were mounted on slides with Prolong Gold Antifade Reagent (Invitrogen). Images were acquired with a confocal microscope (Olympus FV1000 using Olympus Fluoview Ver.2.0a) with a 60X oil immersion lens. Images shown are a representative single Z-section. Photoshop CS2 software was used to process the images. SGs was measured by manually counting the number of Rox8 positive granules for each cell (>100 cells counted for each condition). The results are displayed as a box plot (Figure 3.7).

3.2.12 Northern blot analysis

Total RNA from cells was purified using TRIzol (Invitrogen). 5 μg of each sample was loaded onto a 1% denaturing agarose gel (1X MOPS and 20% formaldehyde v/v). RNA was transferred and crosslinked to Zeta-probe membrane (Bio-Rad, UV Stratalinker 1800TM by Strategene). Transfer of RNA was confirmed by methylene-blue

staining. The membrane was pre-hybridized with 5 mL hybridization buffer (0.5 M Na_2HPO_4 (pH 7.2) , 1 mM EDTA (pH 8.0), 7% SDS w/v) at 65°C for at least 30 min. [α-32P] dATP-labeled DNA probes were generated using the Radprimer kit (Invitrogen) and subsequently purified using the QIAquick Nucleotide Removal Kit (Qiagen). Probes were heated at 95C before adding to the pre-hybridized membranes. After incubating overnight at 65°C, the membranes were washed three times with 15 mL of Wash Buffer (0.1% SDS w/v, 0.1X SSC) at 50°C. The members were analyzed by phosphoryimager analysis (Typhoon, GE Healthcare).

3.3 Results

3.3.1 Expression of CrPV-1A-HA in *Drosophila* S2 cells induces cell death and inhibits transcription

To explore if CrPV-1A has other roles besides inhibiting RNAi, I transiently transfected an expression plasmid that contains a C-terminal hemagglutitin (HA)-tagged CrPV-1A (CrPV-1A-HA) under the control of the actin promoter into *Drosophila* S2 cells and monitored its effects on gene expression by co-transfecting a firefly luciferase expression plasmid that is also under the control of the actin promoter. Expression of CrPV-1A-HA in transfected cells was detected by Western blot analysis using α-HA antibody (Figure 3.1A). Although two bands were detected in transfected cells, the slower migrating band matches the predicted molecular weight of CrPV 1A-HA at 22.8kDa. Currently, we do not know the origin of the faster migrating band, however, this band was also detected by Nayak et al. (2010). We also co-transfected 1A-HA from other Dicistroviruses, Kashmir Bee Virus (KBV) and Acute Bee Paralysis Virus (ABPV)

and a control plasmid that expresses dsRED (Figure 3.1A) with the firefly luciferase expression plasmid. Fourty-eight hours after transfection, S2 cells were harvested, lysed and the lysates were assayed for luciferase activity. In cells expressing CrPV-1A-HA, luciferase activity was 10-fold less compared to cells transfected with expression plasmids expressing KBV 1A, ABPV 1A or dsRED (Figure 3.1B). The loss of luciferase activity can be attributed to inhibition of cellular transcription and/or translation. To distinguish among these possibilities, I isolated total RNA and measured the steady-state reporter RNA levels by Northern blot analysis. Firefly luciferase mRNA levels were dramatically lower in cells expressing 1A compared to cells expressing dsRED (Figure 3.1C). These results suggest that the lower luciferase activities observed in CrPV-1A-HA expressing cells are due to inhibition of transcription or an increase in degradation rates of reporter RNAs.

I next addressed whether expression of CrPV-1A-HA is toxic in S2 cells. (Figure 3.1B, C). I performed a trypan blue exclusion assay 48 hours after transfection. Trypan blue is a large molecule that is impermeable to living cells but is permeable to cells that are undergoing apoptosis or necrosis (Strober, 2001). 26.5% of cells transfected with the CrPV 1A-HA plasmid were permeable. This is ~ two fold higher compared to cells transfected with KBV 1A, ABPV 1A or dsRED expression plasmids (Figure 3.1D). These results indicate that expression of CrPV-1A-HA induces cell death, which may explain the decrease in steady-state reporter RNA levels.

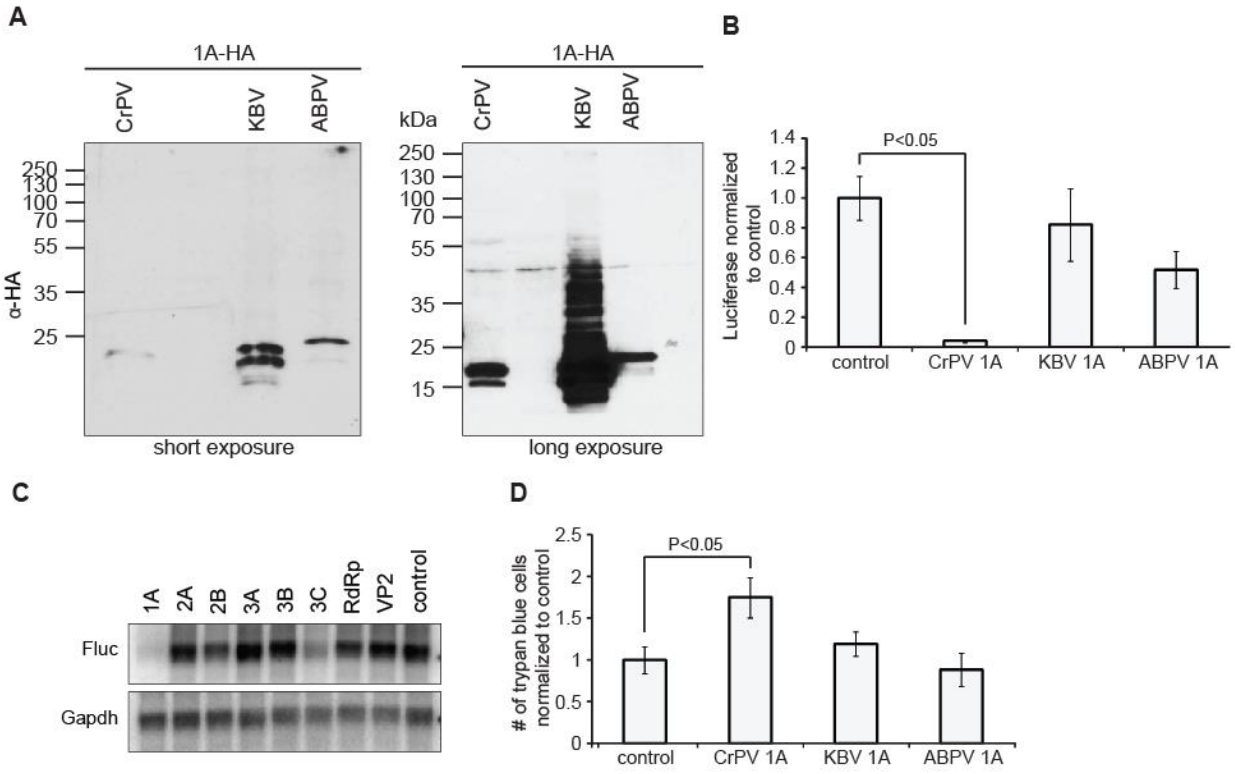

Figure 3.2 CrPV-1A induces cell death and inhibits transcription. (A) α-HA western blot analysis as described in section 3.2.8 and (B) firefly luciferase activities from cells transfected for two days with HA-tagged CrPV-1A, KBV-1A or ABPV-1A plasmid as described in section 3.2.3. (C) Northern blot analysis of Firefly luciferase and GAPDH RNA as described in section 3.2.12. (D) Trypan blue staining of cells as described in section of 3.2.3. The results are normalized to the cells expressing dsRED. Data from b and d are averages and standard deviation from three independent experiments. Western and Northern blots are representative from two independent experiments.

3.3.2 CrPV-1A stimulates 5'-dependent translation

I decided to characterize 1A further. Explicity, I wanted to test if 1A stimulates viral translation. Since 1A is toxic to cells, as defined by trypan blue assay, and inhibits the transcription of DNA luciferase reporters, I examined viral and cellular translation by transfecting RNA luciferase reporters instead. Specifically, I co-transfected *in vitro*

transcribed 5'-capped and polyadenylated RNAs encoding 1A-HA with an *in vitro* transcribed polyadenylated CrPV minigenome reporter RNA (minigenome). The reporter RNA resembles the CrPV genome except that ORF1 and ORF2 are replaced with Renilla and firefly luciferase genes, respectively (Figure 3.3A). As a control, I also co-transfected *in vitro* transcribed 5'-capped and polyadenylated dsRED RNAs (control). I first monitored Renilla and firefly luciferase activities after transfection of the CrPV minigenome RNA. Both luciferase activities increased linearly over time from zero to six hours after transfection (Figure 4.3A and 4.3B), thus demonstrating that this reporter mRNA is engaged in translation during this time. I chose four hours after transfection for further analysis (Figure 3.2B). To confirm that CrPV-1A-HA is expressed (Figure 3.5C), I immunoprecipitated CrPV-1A with an α-HA antibody. 1A-HA was readily detected by immunoblotting using α-HA antibody in the HA-immunoprecipitates demonstrating that 1A-HA is expressed at this time point after transfection (Figure 3.5C). Interestingly, Renilla but not firefly luciferase activity was increased in cells transfected with 1A-HA RNA as compared to that of cells transfected with the control RNA (dsRED) (Figure 3.2B). Nayak *et al.* (2010) demonstrated that the C-terminal region (amino acids H129-V167) of 1A is important for its RNAi suppressor activity. To address if this region has an effect on the translation of the CrPV minigenome RNA, I generated *in vitro* transcribed RNAs encoding a mutant 1A where the C-terminal is truncated down to D128 (1AΔ128). In contrast to the effects of the wild-type 1A-HA, transfection of 1AΔ128 RNA did not affect Renilla or firefly luciferase activities (Figure 3.2B), thus suggesting that expression of full-length 1A stimulates the 5'-UTR IRES but not IGR IRES translation.

The results suggest 1A may have an effect on 5'-UTR IRES translation. To test whether this is specific, I co-transfected the 1A-HA RNA with a bicistronic RNA that monitors cap-dependent translation and IGR IRES-dependent translation or a monocistronic firefly luciferase RNA (monocistronic) (Figure 3.3A). The bicistronic RNA is similar to the minigenome except the 5'-UTR IRES is replaced with the 5'-UTR from *Drosophila* GAPDH (GAPDH bicistronic). All reporters are capped and polyadenylated. Transfection of the 1A-HA RNA but not 1AΔ128-HA RNA stimulated Renilla luciferase activity of the GAPDH bicistronic RNA and the firefly luciferase activity of the monocistronic RNA (Figure 3.2C and D), suggesting that the stimulatory effects of 1A expression are 5'-end dependent. The increase in firefly luciferase activity is similar to the stimulation observed in 5'-UTR-IRES dependent translation and like the minigenome reporter, IGR IRES activity was not stimulated in the GAPDH bicistronic reporter.

3.3.3 CrPV-1A stimulation of 5'-dependent translation is dependent on Ago2.

Since Ago2 interacts with CrPV 1A (Nayak et al., 2010), I tested if Ago2 is important for the 1A-mediated stimulation of 5'-dependent translation by depleting Ago2 from S2 cells. Specifically, I pretreated S2 cells for five days with double-stranded RNAs (dsRNAs) targeting GFP RNA (dsGFP) or with dsRNAs targeting Ago2 RNA (dsAgo2). Two independent experiments confirmed that Ago2 is depleted when treated with dsAgo2 (10.7% and 6.3% compared to cells pretreated with dsGFP) (Figure 3.4D). After treating the cells with the dsRNAs, I co-transfected minigenome RNA with control RNA (dsRED), 1A-HA RNA or 1AΔ128 RNA into S2 cells. As shown in Figure 3.4, 5'-dependent translation but not IGR IRES translation was stimulated in dsGFP-treated

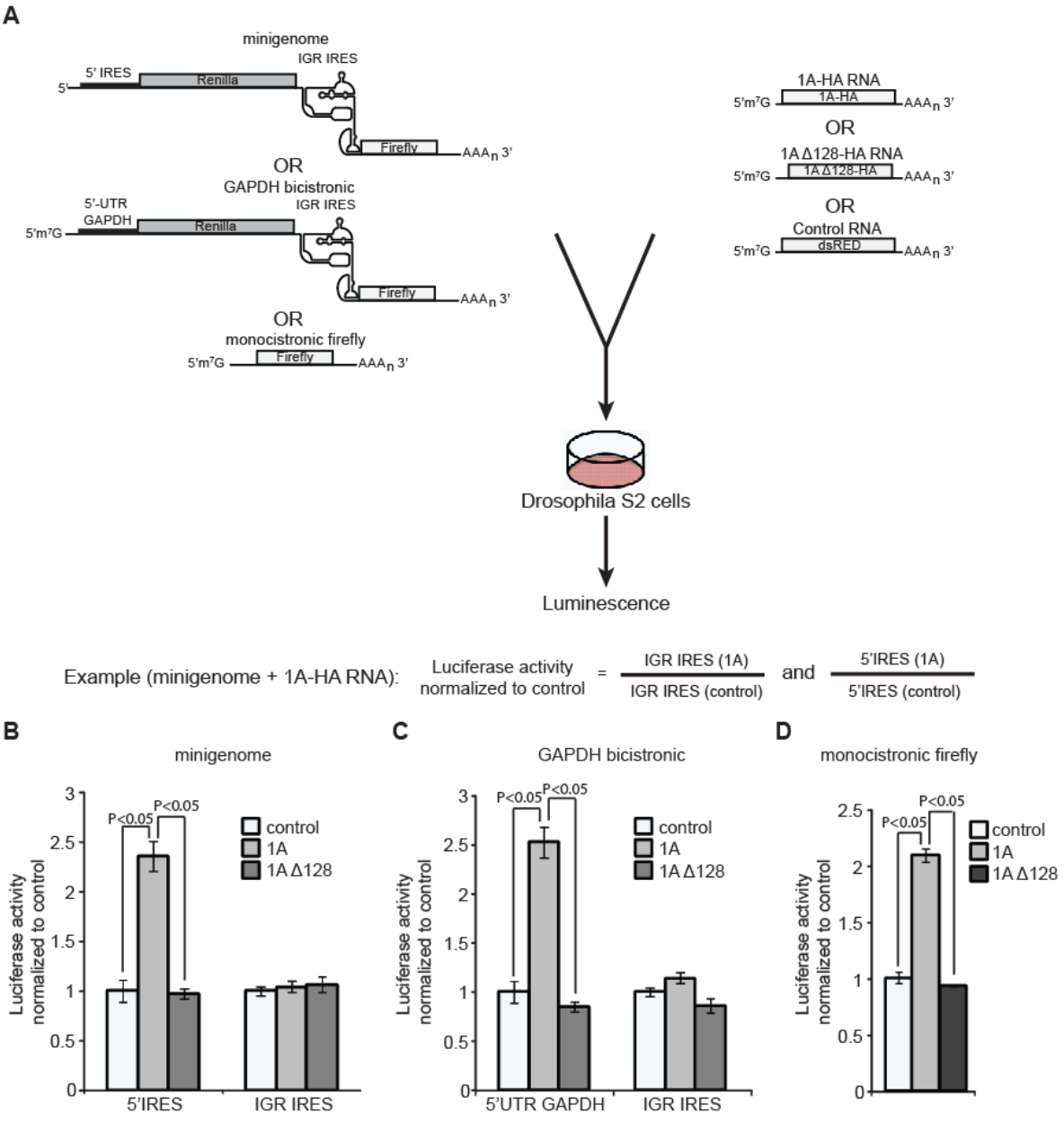

Figure 3.3 CrPV-1A stimulates 5'-dependent translation. (A) Experimental flowchart. CrPV minigenome RNA reporter (B), GAPDH bicistronic RNA reporter (C), or monocistronic RNA reporter (D) were cotransfected with dsRED RNA (control), 1A-HA RNA, or 1AΔ128-HA RNA into S2 cells. Firefly and Renilla luciferase activities were collected and the results are normalized against firefly and Renilla luciferase activities respectively from S2 cells cotransfected with control RNA. Cells were harvested at four hours post transfection and assayed for luciferase activities as described in section

3.2.7. Data in b, c, and d indicate averages and standard deviations from three independent experiments.

---

cells transfected with wild-type 1A but not with control or 1AΔ128 (Figure 3.4A). In contrast, the 5'-dependent stimulation by 1A was partially decreased in cells pretreated with dsAgo2 (Figure 3.4A). I also monitored these effects by using the GAPDH bicistronic RNA and monocistronic RNA (Figure 3.4B, C). I observed similar effects by depleting Ago2, indicating that Ago2 is required for the 1A-mediated 5'-dependent translation of reporter RNAs.

3.3.4 Scanning alanine mutagenesis identifies R146 as important for 5'-dependent stimulation

Our results indicate that the expression of the mutant 1AΔ128 protein does not stimulate 5'-dependent translation, suggesting that the C-terminal 40 amino acid domain may be required for its activity. To pinpoint which amino acids may be important, I performed scanning alanine mutagenesis by generating mutations within the 1A-HA expression plasmid replacing each amino acid residue with alanine from residue 129 to 146. I co-transfected *in vitro* transcribed capped and polyadenylated RNA containing the scanning alanine 1A-HA mutants with the minigenome reporter RNA. As shown in Figure 3.2-3.3, co-transfection with wild-type 1A but not deletion mutant 1AΔ128 resulted in an approximate 2.5-fold stimulation of the 5'-UTR IRES translation (Figure 3.4A). Of all the scanning alanine mutants, mutant R146A, Q134A and N124A failed to stimulate 5'-UTR IRES translation (Figure 3.5A). Q134A and N142A mutations are not as statistically significant ($P>0.05$ and $P=0.044$ respectively) compared to R146A

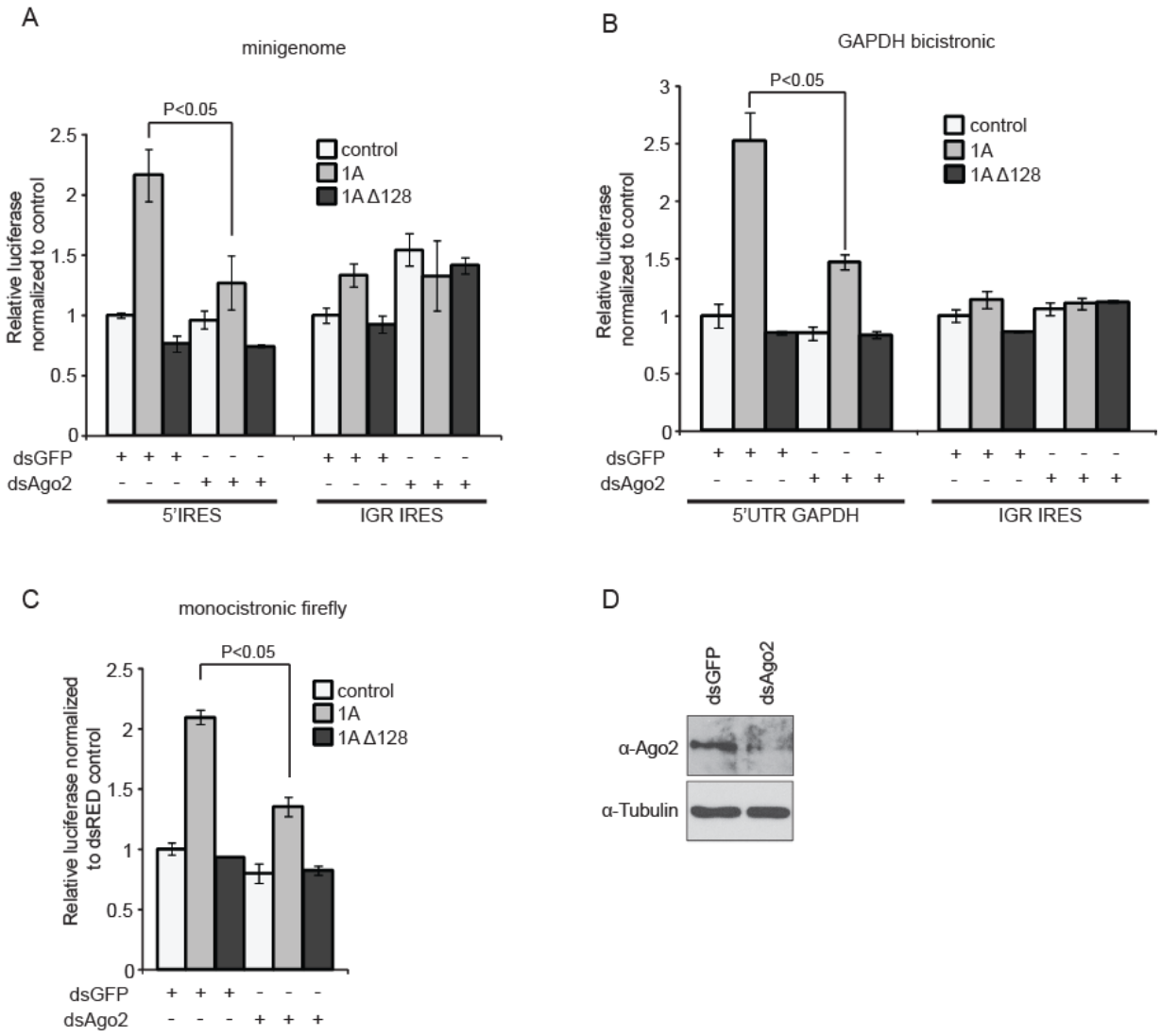

Figure 3.4 Stimulation of 5'-dependent translation by CrPV-1A is dependent on Ago2. Renilla and firefly and luciferase activities from S2 cells cotransfected with minigenome RNA (A) , GAPDH bicistronic RNA (B), or monocistronic RNA(C) with dsRED RNA (control), 1A-HA RNA, or 1AΔ128-HA RNA as described in section 3.2.7. S2 cells were pretreated for 5 days with dsGFP or dsAGO2 as described in section 3.2.6. Cells were harvested at four hours post transfection and assayed for luciferase activities as described in section 3.2.7. (D) Representative α-Ago2 and α-Tubulin blot from S2 cells pretreated with dsGFP or dsAGO2 for 5 days as described in section 3.2.8. Data in a, b, and c indicate averages and standard deviations from three independent experiments. The data represented in Figure 3.3 b, c, d are identical to the

data represented in figure 3.4 a, b, and c respectively except in figure 3.4, S2 cells pretreated with dsAgo2 RNA were included.

(P=0.0006). Mutant 1A R146A-HA was detected by immunoblotting for HA from HA immunoprecipitates indicating that it was expressed (Figure 3.5C). Thus, I identified a single point mutant (R146A) within 1A that substantially inactivated its ability to stimulate 5'-dependent translation.

Since the 1A R146A mutant does not stimulate 5'-dependent translation of reporter RNAs, I next tested whether this mutant could inhibit 1A's ability to suppress the RNAi silencing pathway. To address this, I pre-treated S2 cells for two days with dsRNAs targeting either firefly luciferase RNA (dsFL) or dsGFP and then subsequently co-transfected 1A-HA RNA, 1A R146A RNA, or control RNA with monocistronic RNA. I expected that cells pretreated with dsFL would significantly lower the expression of firefly luciferase activity. Indeed, pretreating cells with dsFL but not dsGFP RNA significantly inhibited firefly luciferase activity (~20 fold) in cells transfected with control RNA (compare cells expressing control RNA), demonstrating that suppression of firefly luciferase was due to silencing by dsFL (Figure 3.5B). In contrast, pretreating with dsFL resulted in only a slight decrease in luciferase activity (~2 fold) in cells transfected with 1A-HA RNA or 1A R146A RNA (compare to cells pretreated with dsGFP) (Figure 3.5B). Thus, these results indicate that R146 is required for 5'-end-dependent stimulation of reporter RNAs but not for 1A's ability to suppress RNAi.

3.3.5 CrPV infection stimulates reporter RNA translation

Our results suggest that expression of 1A stimulates 5'-dependent translation. To determine if this phenomenon occurs during infection, I monitored the translation of transfected reporter mRNAs in CrPV-infected cells. Briefly, I infected S2 cells with CrPV followed by transfecting a bicistronic RNA (Wang and Jan, 2014) that monitors cap-dependent and IGR-IRES mediated translation via Renilla and firefly luciferase activities, respectively. I harvested the cells at different time points after infection and monitored luciferase activities. As shown previously (Wang and Jan, 2014), luciferase activities increased linearly from two to six hours after transfection indicating that the reporter RNAs are engaged in translation during these times. Interestingly, CrPV infection at an MOI of 10 resulted in a significant increase in Renilla luciferase activity as compared to mock-infected cells (>12 fold) (Figure 3.6A). As expected, IGR IRES translation also increased significantly in infected cells (Figure 3.6A). Surprisingly, in CrPV-infected cells at a high MOI of 50, Renilla luciferase activity was still stimulated (1.5 fold) (Figure 3.6A). To confirm that host protein synthesis is repressed during infection, cells were pulse-labeled with [^{35}S]-methionine at six hours post infection (Figure 3.6B). As expected, host translation was repressed at an MOI equal or greater than 10 (Figure 3.6B). Therefore, the increase in Renilla luciferase activity observed in CrPV-infected cells transfected with the bicistronic RNA suggests that existing endogenous mRNAs are differentially regulated from transfected exogenous reporter RNAs. In other words, endogenous mRNAs are subject to translational repression whereas the transfected exogenous mRNAs can bypass this translational block.

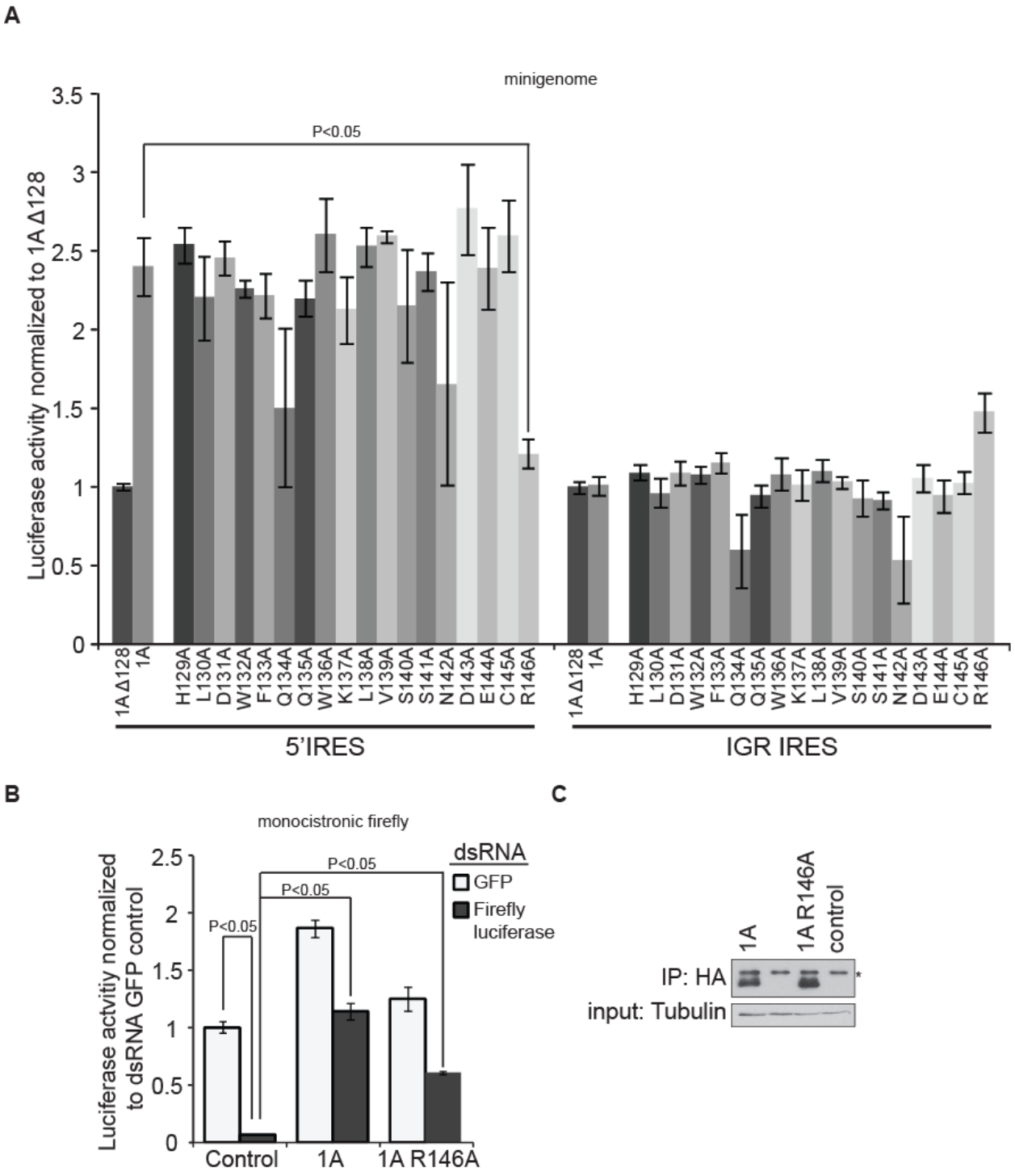

Figure 3.5 Scanning alanine mutagenesis determined residue R146 is critical for 1A dependent stimulation of 5'-UTR translation but not inhibition of RNAi. (A) Each of the amino acid residues in 1A from 128-146 was mutated to alanine as

described in section 3.2.4. Renilla and firefly luciferase activities from S2 cells cotransfected with minigenome RNA and 1A-HA RNA, 1AΔ128 RNA, or 1Amutant RNA. Cells were harvested at four hours post transfection and assayed for luciferase activity as described in section 3.2.7. (B) Firefly luciferase activities from S2 cells pretreated with dsGFP or dsFL for two days as described in section 3.2.6 and cotransfected with 1A RNA, 1A R146A RNA or control RNA (dsRED). Cells were harvested at four hours post transfection and assayed for luciferase activity as described in section 3.2.7. Data in a and b indicate averages and standard deviation from three independent experiments. (C) Representative α-HA western blotting from 100µg HA-immunoprecipitated lysates collected from experiment A as described in section 3.2.9. 10% of the input was immunoblotted against tubulin as shown below as described in section 3.2.8.

To explore this effect more carefully, I examined whether inhibition of host translation via another pathway other than infection can induce cap-dependent translation of reporter RNAs. PatA is a potent compound that inhibits cap-dependent translation by disrupting the helicase activity of eIF4A (Bordeleau et al., 2005). In Chapter 4, PatA treatment of S2 cells resulted in a >95% inhibition of overall cap-dependent translation as measured by [^{35}S]-methionine pulse labeling (Figure 4.6B). In contrast to that observed in CrPV-infected cells, firefly luciferase activity of transfected monocistronic RNA was dramatically inhibited in PatA treated cells (Figure 3.6C). This result suggests that the monocistronic RNA is still responsive to pathways that inhibit cap-dependent translation. Interestingly, when CrPV-infected cells were treated with PatA, firefly luciferase activity of the transfected reporter RNA increased compared to cells treated with PatA alone but not as much as in the absence in the absence of PatA

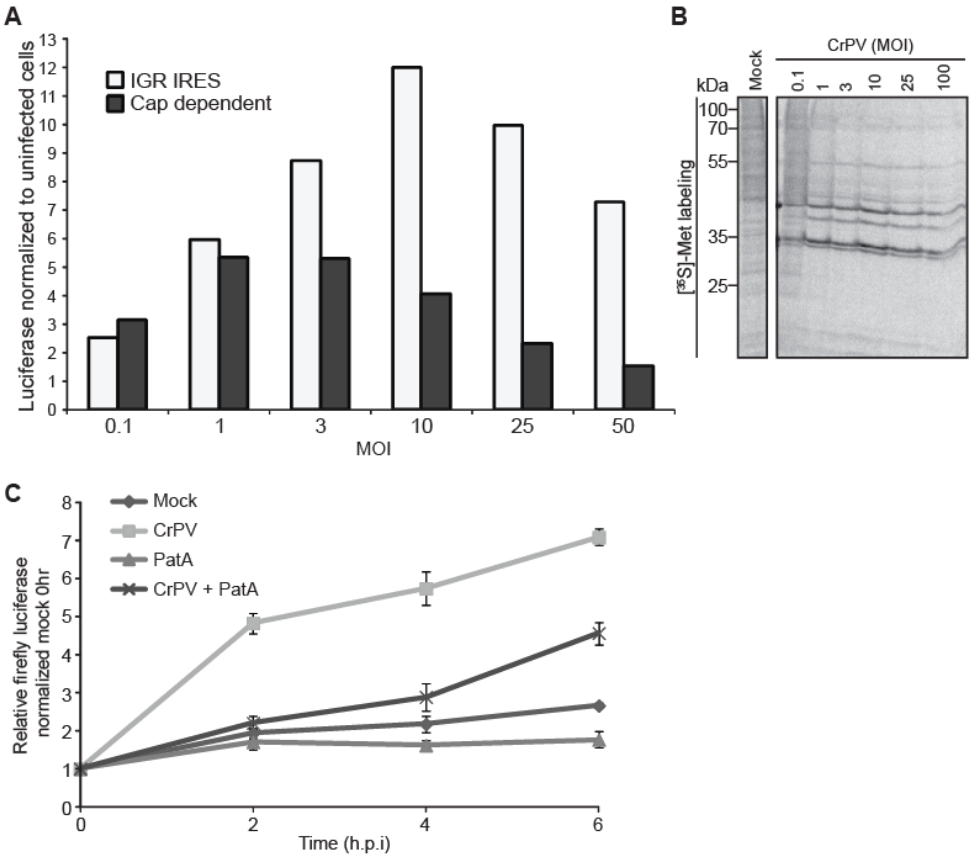

Figure 3.6 CrPV infection stimulates reporter RNA translation. (A) A bicistronic RNA (Wang and Jan, 2014) that monitors cap-dependent translation and IAPV IGR-IRES-mediated translation via Renilla and firefly luciferase activities respectively was transfected into S2 cells for two hours prior to mock- or CrPV infection at an MOI of 0.1, 1, 3, 10, 25, and 50 as described in section 3.2.7. Six hours after infection, S2 cells were lysed and luciferase assays were performed. Renilla and firefly luciferase activities for each MOI were normalized to mock infected cells. (B) Autoradiography of pulse-labelled protein lysates from S2 cells either mock- or CrPV-infected (MOI 0.1, 1, 3, 10, 25, and 50) resolved on a 12% SDS- PAGE gel. The protein lysates were collected from S2 cells at six hours post infection (hpi) and metabolically labeled with [^{35}S]-Met/Cys for 20 min as described in section 3.2.10. (C) Monocistronic RNA were transfected into S2 cells two hours prior to mock, CrPV infection (MOI 10), 50nM PatA treatment, or CrPV infection and 50nM PatA treatment. S2 cells were harvested at the indicated time points after treatment and/or infection and assayed for Firefly luciferase activity as described in section 3.2.7.

(Figure 3.6C). These results suggest that the transfected RNA is behaving differently than host mRNAs and is preferentially translated during CrPV infection.

3.3.6 CrPV 1A inhibits the stress granule pathway

In Chapter 2, I showed that the canonical SG pathway is inhibited during CrPV infection. To determine if 1A is involved, I transfected a Rox8-GFP RNA, which monitors SG formation, with control RNA encoding dsRED, 1A RNA, or 1AΔ128 RNA. 9 hours later, I followed Rox8-containing SG formation in cells that were treated with PatA or arsenite for one hour. Cells were then fixed and examined for GFP expression by confocal imaging analysis (Figure 3.7A). For each experimental condition, the number of visible GFP granules per cell was counted and the results are displayed as a box plot (Figure 3.7B). As shown previously, visible Rox8-GFP SGs were detected in PatA or arsenite-treated cells that were co-transfected with a control mRNAs (Median = 4 SGs). In contrast, a statistically significant decrease in Rox8-GFP SGs per cell was observed in cells transfected with 1A RNA (Median = 1 SG). Furthermore, co-transfection of the mutant 1AΔ128 RNA did not lead to inhibition of SGs mediated by PatA or arsenite (Median = 4SGs). These results suggest that 1A can inhibit the SG pathway, a phenomenon that is observed during CrPV infection.

3.4 Discussion

Prior to these experimental results, 1A was known as a RNAi suppressor (Nayak et al., 2010) and inhibitor of Ago2-dependent microRNA silencing (Besnard-Guerin et al., 2015). However, my experimental results suggest that 1A has other functions. Reporter assays suggest that 1A specifically stimulates 5'-dependent translation of

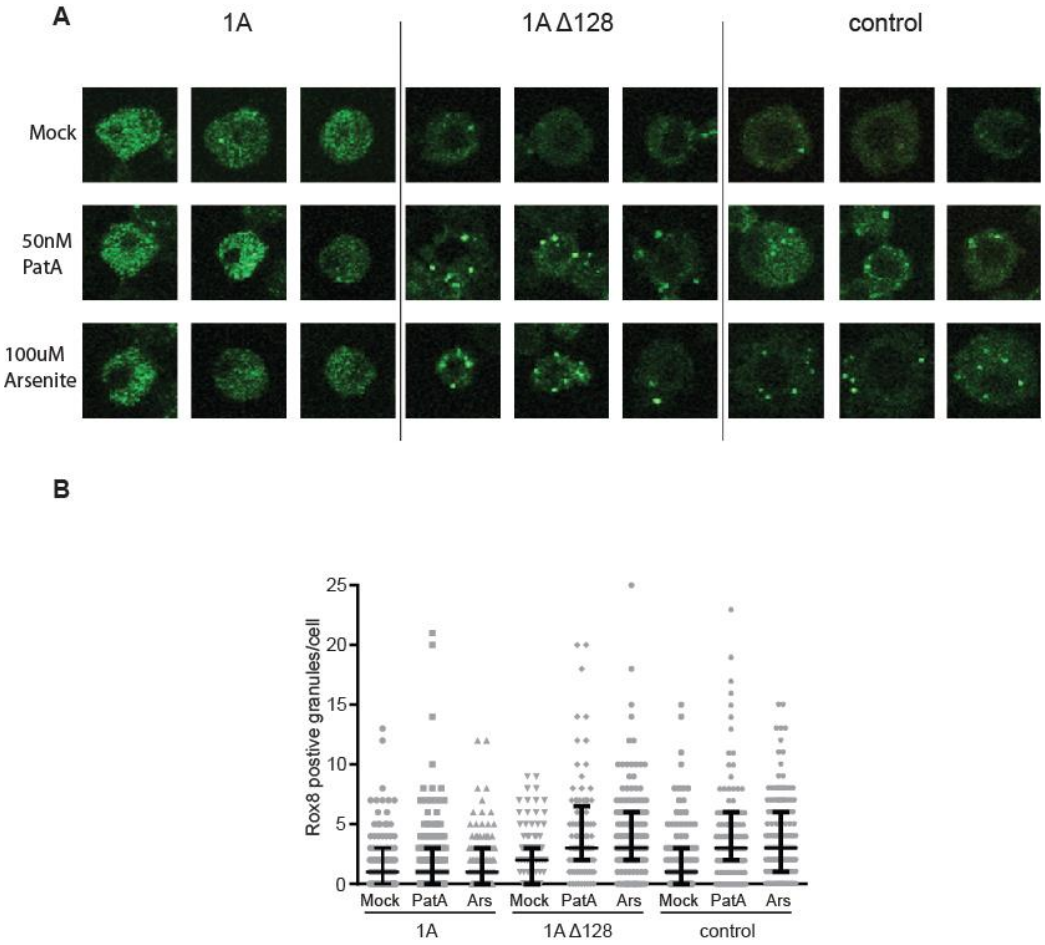

Figure 3.7 CrPV 1A inhibits the stress granule pathway. (A) Single cell images from cells treated with 50nM PatA or 100uM arsenite (ars) and cotransfected with control RNA(dsRED), 1A RNA, or 1AΔ128 RNA with Rox8-GFP RNA as described in section 3.2.7. The cells were fixed and examined by confocal microscopy as described in section 3.2.11. Three representative cells are shown for each experimental condition. (B) Box plot graph showing number of Rox8 positive granules in each cell for each experimental condition. At least 100 cells were counted for each experiment. An unpaired t test was performed on relevant comparitive samples. The following sets pass the t test ($p < 0.05$): mock 1AΔ128 vs PatA 1AΔ128, mock 1AΔ128 vs ars 1AΔ128, mock control vs PatA control, mock control vs ars control, PatA 1A vs PatA 1AΔ128, ars 1A vs ars 1AΔ128, PatA 1A vs PatA control, and ars 1A vs ars control.

transfected reporter RNAs in an Ago2-dependent manner. This effect appears to be specific to 1A as I discovered that R146 is required for 1A's ability to stimulate 5'-end translation. Furthermore, this requirement of R146 is specific for translation and does not affect 1A's ability to suppress the RNAi pathway. Finally, I discovered that 1A represses PatA and arsenite-induced SG formation. All these results suggest 1A has other roles besides suppressing the RNAi pathway.

The robust translational stimulation observed with RNA luciferase reporters during CrPV infection is unexpected. I tested whether CrPV infection stimulates translation of uncapped monocistronic reporter RNAs and discovered the activity is enhanced similarly (data not shown). In addition, I determined that this stimulation is not dependent on the transfection reagent or electroporation (data not shown). These results are unexpected because CrPV infection inhibits host translation between three and four hours post infection in S2 cells (Wilson et al., 2000). How RNA reporters escape translational repression during infection may be explained by a number of scenarios. One scenario is nuclear history. Cellular mRNAs are commonly modified by methylation and exist as a mRNP immediately after being transcribed in the nucleus (reviewed in Lee et al., 2014). The fate of these mRNAs may be different from the *in vitro* transcribed naked RNAs introduced exogenously into cells under CrPV infection. Another scenario is RNA localization. It is possible that transfected RNAs are localized at specific sites that are permissive for translation during infection and that endogenous RNAs are not at these "permitted" translation sites (see poly(A)$^+$ granules in Chapter 2). Supporting this exciting latter hypothesis is the discovery that 1A is responsible for the inhibition of SG induction observed under CrPV infection (Chapter 2). For instance,

CrPV infection may affect where specific mRNAs are localized and translated by disrupting SGs and inducing poly(A) granules. It will be interesting to test if the R146A mutant is inactive in suppressing SGs. If the mutant is inactive, it will strongly suggest the SG disruption is linked to the translational stimulation observed with transfected reporters. In other words, these results, although speculative, suggest that disruption of SGs releases translation factors that enhance reporter translation.

My studies also indicate that Ago2 contributes to the 1A-dependent 5'-dependent translation. One possibility is that Ago2 is required to repress translation of the transfected reporter RNA and that 1A interacts with and antagonizes Ago2, thus relieving the Ago2-dependent repression and resulting in an increase in reporter RNA translation. Alternatively, it is possible that 1A and Ago2 together contribute to the stimulation of 5'-end-dependent translation of reporter RNAs. If the first scenario is true, depletion of Ago2 should lead to a stimulation of 5'-dependent translation; however, this was not observed (Figure 3.4, compare cells treated with dsAgo2 and dsGFP expressing dsRED or 1AΔ128). Therefore, the second scenario is more likely. One outstanding question is the effect of the R146A mutant. It will be interesting to see if R146A can interact with Ago2 and whether Ago2 knockdown affects the effects of R146A on 5'-end-dependent translation.

In general, Ago2 is a repressor of gene expression given its interactions with siRNA and miRNA to repress translation/stability of target mRNAs. However, there is increasing evidence that Ago2 can also lead to increases in translation. Vasudevan *et al*. (2007) demonstrated that during resting phase (G0) in mammalian cells, specific microRNAs such as miR369-3p bind to tumor necrosis factor alpha(TNFα) RNA with the

aid of Ago2 and FXR-iso-a to stimulate TNFα translation (Vasudevan et al., 2007). Another classical example is the translational stimulation of Hepatitis C Virus, HCV, by miR-122. miR-122 complexed with Ago2 binds to two sites within the HCV 5'-UTR to stimulate translation, albeit the increase is only ~1.5 fold (Henke et al., 2008). Furthermore, the authors showed that miR-122 promotes 48S recruitment to the mRNA (Henke et al., 2008; Niepmann, 2009). Although the examples described are in mammalian cells, Ago2 may also stimulate translation in *Drosophila melanogaster*. Iwasaki and Tomari (2009) discovered Ago2 stimulates translation of reporters lacking a poly(A) tail in S2 translation extracts when target microRNAs are added. This was only specific to Ago2 as Ago1 was repressive towards reporters with or without a poly(A) tail (Iwasaki and Tomari, 2009). It is possible CrPV 1A binds to Ago2 and promotes interaction with FXR-iso-a during CrPV infection to stimulate translation. However, the underlying mechanism of Ago2 is that a miRNA or siRNA guides Ago2 to the target mRNA (Henke et al., 2008; Iwasaki and Tomari, 2009; Niepmann, 2009; Vasudevan et al., 2007). Because I showed that different reporter RNAs encoding different genes all were stimulated in a 1A-dependent manner, it is unlikely that a common miRNA is involved in guiding Ago2. To formally rule out this possibility, I can deplete miRNAs and siRNAs by depleting Dicer1 and Dicer2 respectively and test if 1A-dependent stimulation is affected. Alternatively, it is possible that 1A binds to RNA non-specifically and recruits Ago2 to stimulate translation. Although 1A does not bind to dsRNA in an EMSA assay (Nayak et al., 2010), it may still bind to the single-stranded reporter RNA.

In summary, these results suggest that 1A manipulates the host cell in a number of ways through Ago2. Future investigation into how 1A accomplishes this may yield

interesting discoveries on how CrPV facilitate viral infection and may provide us a better understanding on SGs, translation, and the RNAi response in insects.

Chapter 4 Temporal regulation of distinct internal ribosome entry sites of the *Dicistroviridae* cricket paralysis virus

4.1 Introduction

Dicistroviruses are a unique model for characterizing viral protein synthesis because they possess two distinct IRESs that drive the translation of non-structural and structural protein synthesis independently. Unlike picornaviruses that encode a single ORF and express a single polyprotein, dicistroviruses have the potential to regulate the translation of their two ORFs independently. The significance of this strategy is not well understood. I hypothesize that the timing of structural and non-structural protein synthesis is regulated during infection. Many RNA viruses control the timing of viral protein expression in order to facilitate viral replication early in infection and viral packaging later in infection (Miller and Koev, 2000). For example, Alphaviruses translate one of their ORFs (ORF1) that encodes non-structural proteins early in infection and activate translation of another ORF that encodes structural proteins later in infection (Miller and Koev, 2000).

The dicistroviral structural proteins encoded within ORF2 are expressed in supramolar excess over non-structural proteins, which suggests differences in translation activity between the 5'-UTR IRES and the IGR IRES during CrPV infection (Garrey et al., 2010; Moore et al., 1980; Wilson et al., 2000). Indeed, it has been shown that the 5'-UTR IRES directs lower translation than the IGR IRES (Wilson et al., 2000). However, the temporal regulation of these IRESs has not been examined in detail during infection.

In this Chapter, I monitored and compared 5'-UTR and IGR IRES activities during infection by using a combination of metabolic [^{35}S]-pulse-labeling and luciferase reporter assays. My results suggest viral protein synthesis is temporally regulated during infection. Specifically, viral structural protein synthesis increases significantly at later time points during infection relative to viral non-structural protein synthesis. This regulation can be described by two broad hypothesis: a passive form of regulation where a combination of cellular translational repression, differing IRES affinities for ribosomes, differing requirements for translation initiation factors, and a vast increase in viral genomic RNA leads to greater structural protein synthesis or an active form of regulation where viral proteins or changes in the structure of the 5'IRES and the IGR IRES during infection facilitate the increase in IGR IRES-dependent translation. Data presented herein suggests the latter hypothesis. In summary, CrPV likely uses this strategy to promote virus infection, possibly to ensure that packaging of the virus does not occur prematurely.

4.2 Materials and methods

4.2.1 Cell culture, virus infection, and viral titers

Drosophila S2 cells were maintained as described in section 3.2.1.

4.2.2 Reporter constructs

The construction of the minigenome reporter construct was described in section 3.2.2.

4.2.3 RNA transfection, and luciferase assay

In vitro transcription reactions using T7 RNA polymerase were performed as described previously (Wang and Jan, 2014). RNA was polyadenylated (CellScript), purified (RNeasy kit, Qiagen) and the integrity of the RNA was determined by visualizing it on an agarose gel. The quantity of RNA was determined by Nanodrop (Thermo Scientific).

Transfection of 1 μg RNA (lipofectamine 2000, Invitrogen) into S2 cells (1.5 X 10^6 cells per mL; 12-well plates) was performed as described by the manufacturer (Invitrogen). Cells were harvested with passive lysis buffer (Promega) and assayed for luciferase activity (Promega) using a microplate luminometer (Berthold Technologies, Centro LB 960).

4.2.4 Western blotting

As described previously (Garrey et al., 2010), cells were washed once with 20 mL 1X PBS and harvested with 50 μL lysis buffer (20 mM HEPES, 150 mM NaCl, 1% Triton X-100, 10% glycerol, 1 mM EDTA, 10 mM tetrapyrophosphate, 100 mM NaF, 17.5 mM β-glycerophosphate, and protease inhibitors (Roche)). Equal amounts of lysates, as determined by Bradford assay, were resolved on a 10-15% acrylamide SDS-PAGE gel. Proteins were electrophoretically transferred from the gel to a PVDF membrane (Millipore), blocked in 20 mL of 5% skim milk 1X TBST (20mM Tris, 150mM NaCl, 0.1% Tween) for one hour and then probed with 1:10,000 CrPV VP2 antibody (PL Laboratories), 1:10,000 CrPV RdRP antibody (PL Laboratories), or 1:500 phospho-eIF2α antibody (Cell Signaling) and then followed with secondary antibody incubation

(1:20,000 goat anti-rabbit IgG horseradish peroxidase (GE Healthcare Life Sciences) or 1:20,000 goat anti-mouse IgG horseradish peroxidase (Santa Cruz Biotechnology) in 5 mL of 5% skim milk 1X TBST. Detection was performed by enhanced chemiluminescence (Millipore).

4.2.5 Pulse-labelling

As described previously (Garrey et al., 2010), 5 x 10^6 cells were pulse labeled with 250 µCi [^{35}S]-Met/Cys (Perkin-Elmer) for 20 min, washed with 0.5 mL cold PBS twice and harvested with 50 µL lysis buffer. Equal amounts of lysates were resolved on a SDS-PAGE and the SDS-PAGE gel was dried. Radioactive bands from the gel were imaged by a phosphorimager (Amersham Pharmacia Biotech). Densitometric analysis on the pulse-labelled bands was performed using Image J software (http://rsbweb.nih.gov/ij/index.html).

4.2.6 Immunoprecipitation

Up to 1.5mg of S2 lysates were incubated with a fixed amount of 30 uL CrPV RdRp or VP2 rabbit polyclonal primary antibodies respectively in immunoprecipitation lysis buffer (50mM Tris-HCL, pH7.5, 150mM NaCl, 1% Nonidet P40, 0.5% sodium deoxycholate, and protease inhibitors (Roche)) for one hour at 4°C with gentle agitation. 50 µL of protein G-agarose (Roche) were incubated with the reaction overnight at 4°C. Mixtures were centrifuged at 2 krpm for one minute and the precipitate was washed twice with the immunoprecipitation lysis buffer, twice with wash buffer 1 (50mM Tris-HCL, pH 7.5, 500mM NaCl, 0.1% Nonidet P40, and 0.05% sodium deoxycholate), and

once with wash buffer 2 (50mM Tris-HCL, 0.1% Nonidet P40, and 0.05% sodium deoxycholate). The precipitate was resuspended in 50 μL SDS loading dye and removed from the beads by heating at 95°C for 10 min and centrifugation at 13.2 krpm. The samples were resolved by SDS-PAGE. The gel was dried and imaged with a phosphoimager (Amersham Pharmacia Biotech). Densitometric analysis on the pulse-labelled bands was performed using Image J software (http://rsbweb.nih.gov/ij/index.html).

4.2.7 dsRNA-mediated knockdown

dPERK (437-853 nucleotides, NM_141281.3) and dGCN2 (492-1034 nucleotides, NM_057882.4) was RT-PCR amplified from total RNA of *Drosophila* S2 cells using primers that contain the T7 promoter at both ends. The PCR products were used as templates for *in vitro* transcription reactions using T7 RNA polymerase. dsRNA was purified and the integrity was verified by gel analysis. dsRNA (13 μg/million cells) was incubated with S2 cells in serum-free SSM3 media for one h, followed by the addition of complete SSM3 media.

4.2.8 S2 translation extracts and *in vitro* translation assay

The protocol for S2 translation extracts was adapted from published sources (Brasey et al., 2003; Roy et al., 2004). Specifically, 2.0 x 10^9 mock-infected or 6 hour CrPV-infected (MOI 10) S2 cells were pelleted at 1,000 g for 8 min, washed once with PBS and resuspened in 2 mL hypotonic buffer (10mM HEPES-KOH [pH 7.4], 10mM KOAc, 0.5mM MgOAc, 1mM DTT). After incubation in hypotonic buffer on ice for five

min, the cells were lysed by extrusion 25 times through a 23-gauge needle. The extracts were then adjusted to 50 mM KOAc. The supernatant (S2 translation extract) was collected upon clearing all cell debris by centrifugation at 16,000g for 5 min at 4 degrees, aliquoted, and stored at -80C.

Prior to use, the S2 translation extract was supplemented with 0.2 U creatine phosphokinase/uL. Each translation assay was carried out in a final volume of 10 uL containing 6.5 uL S2 translation extract, 2 uL 5X master mix (10 0uM complete amino acids, 40 mM creatine phosphate, 100 mM HEPES-KOH (pH 7.6), 5 mM ATP, 1 mM GTP, 2.5 mM spermidine, 500 mM KOAc, and 5 mM MgOAc), 0.5 uL Ribolock RNase Inhibitor (40 U/uL, Thermo Fisher), and 9 nM template RNA for 30 min at 30°C. After incubation, half of the reaction was assayed for luciferase activity (Promega, section 4.2.3).

4.2.9 Uridine labeling of RNA

$5X10^6$ cells were pretreated with actinomycin D for 15 min, followed by the addition of 5 µCi of [^{3}H]-uridine (Perkin Elmer) for 15 min. Total RNA was extracted (Trizol, Invitrogen). Equal amounts of RNA were separated in a denaturing agarose gel and transferred to nylon membrane. Levels of radioactivity were detected by phosphorimaging and quantified using ImageQuant software.

4.2.10 Northern blot analysis

Northern blot analysis was described in section 3.2.12.

4.3 Results

4.3.1 Expression of non-structural and structural proteins in CrPV-infected S2 cells

Although it is well established that viral structural proteins are expressed in molar excess over the viral non-structural proteins during CrPV infection in *Drosophila* S2 cells (Garrey et al., 2010; Moore et al., 1980; Wilson et al., 2000), it is not known whether the expression of viral proteins is temporally regulated during infection. Therefore, I re-examined viral protein synthesis during CrPV infection by metabolic [^{35}S]-Met/Cys pulse-labeling at different times after infection (Figure 4.1A). As observed previously (Garrey et al., 2010; Moore et al., 1980; Wilson et al., 2000), host translation decreases dramatically two to three hours post infection (hpi), which is concomitant with the synthesis of CrPV proteins. The processed and unprocessed viral structural and non-structural proteins were identified based on previous studies (Garrey et al., 2010; Moore et al., 1980; Wilson et al., 2000) and from immunoblots using antibodies that recognize RNA-dependent RNA polymerase (RdRp) and VP2 structural protein (Figure 4.1A) (Garrey et al., 2010). The RdRp antibody detected unprocessed RdRp non-structural proteins at 120 (RdRp*), 105 (RdRp**), and 100 kDA (RdRp***) and the mature 3D at 60 kDa. A close inspection of the pulse-labeled proteins showed that the non-structural proteins such as the unprocessed 120 kDa RdRp and 2C are detected first at two hpi whereas the structural proteins are not detected until after three hpi. (Figure 4.1A). I quantified the individual viral proteins from three independent protein pulse-labelling experiments and confirmed that the non-structural proteins were first expressed by two hpi and increased steadily at later times of infection and that the viral structural proteins

were not detected until three to four hpi (Figure 4.1B). Thus, the pulse-labeling experiments suggest that translation of the downstream ORF driven by the IGR IRES is delayed until three to four hpi.

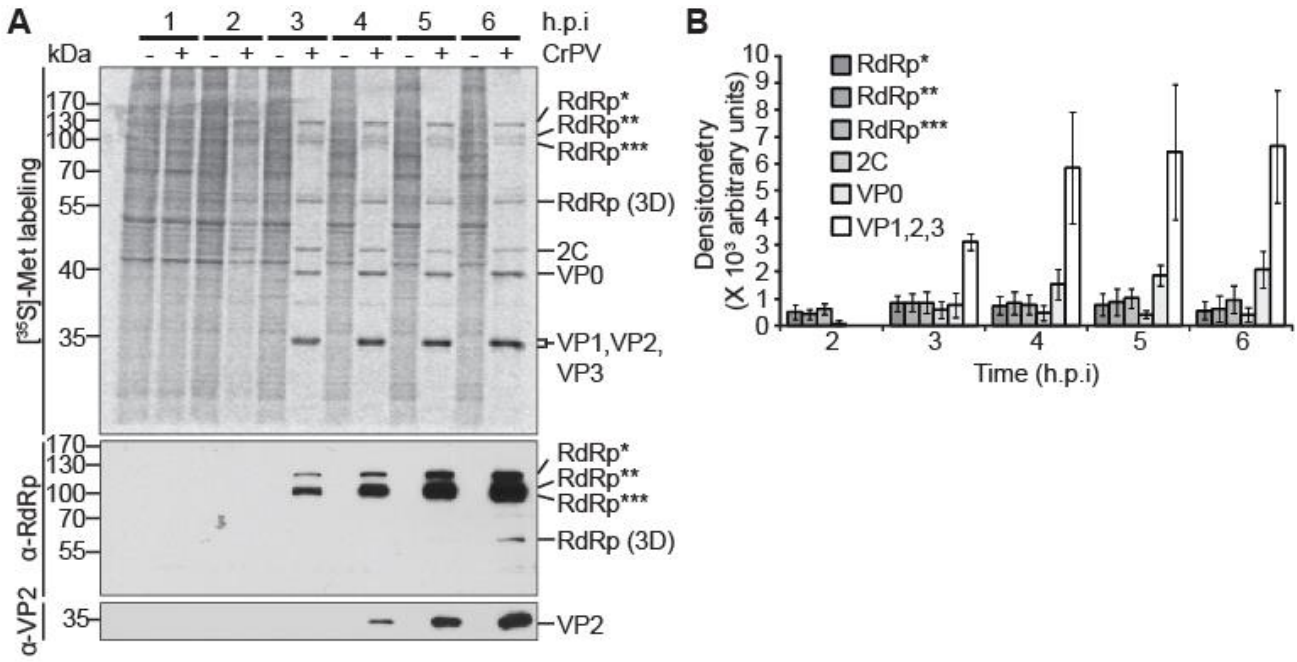

Figure 4.1. Non-structural viral proteins are predominantly expressed early in infection while structural viral proteins are predominantly expressed later in infection. (A) Autoradiography of pulse-labelled protein lysates from S2 cells either mock- or CrPV-infected with CrPV resolved on a 12% SDS- PAGE gel. The protein lysates were collected from S2 cells at the indicated times hours post-infection (hpi) and metabolically labeled with [^{35}S]-Met/Cys for 20 min at the end of each time point as described in section 4.2.5. The identities of specific CrPV viral proteins, as shown on the right of the gel, were previously described (Garrey et al., 2010; Moore et al., 1980), determined by immunoblotting with α-RdRp and α-VP2 peptide antibodies as described in section 4.2.4 or predicted by molecular weight. (B) Raw densitometric quantitation of [^{35}S]-Met/Cys pulse-labelled RdRp*, RdRp**, RdRp***, 2C, VP0, and VP1, 2, and 3

during CrPV infection from three independent experiments (± s.d.). RdRp*, RdRp**, and RdRp*** denote polyproteins containing RdRp at the approximate sizes of 120kDa, 105kDa, and 100kDa respectively.

4.3.2 Translation of ORF1 and ORF2 during CrPV infection

Accurate quantification of the non-structural proteins, especially at two hpi, is difficult due to ongoing host protein synthesis (Figure 4.1A). To detect the non-structural proteins more accurately, I monitored protein synthesis by immunoprecipitation of pulse-labeled structural and non-structural proteins from virus infected cell lysates (Figure 4.2). Specifically, I pulse-labeled cells for one hour starting at various times post infection followed by lysis and immunoprecipitation using α-RdRp and α-VP2 antibodies. I initially optimized the immunoprecipitation conditions by incubating increasing amounts of [^{35}S]-Met/Cys labeled lysates with a constant amount of antibody to ensure that the amount of antibody used is in excess (Figure 4.2A and 4.2B). Immunoprecipitation with α-RdRp antibody pulled down unprocessed and mature RdRp from infected lysates whereas α-VP2 immunoprecipitated all four structural proteins, likely as a packaged virion (Figure 4.2A-C). At two hpi, non-structural proteins were readily detected by α-RdRp pulldowns. In contrast, the structural proteins were not detected until three hpi (Figure 4.2C and 5.2D). Furthermore, whereas the pulse-labelled RdRp increases 1.5 times throughout infection, the immunoprecipitated structural protein increases up to 4-fold at four hour and then decreases slightly during infection, supporting the notion that translation of the two ORFs are distinctly and temporally regulated (Figure 4.2C and 5.2D).

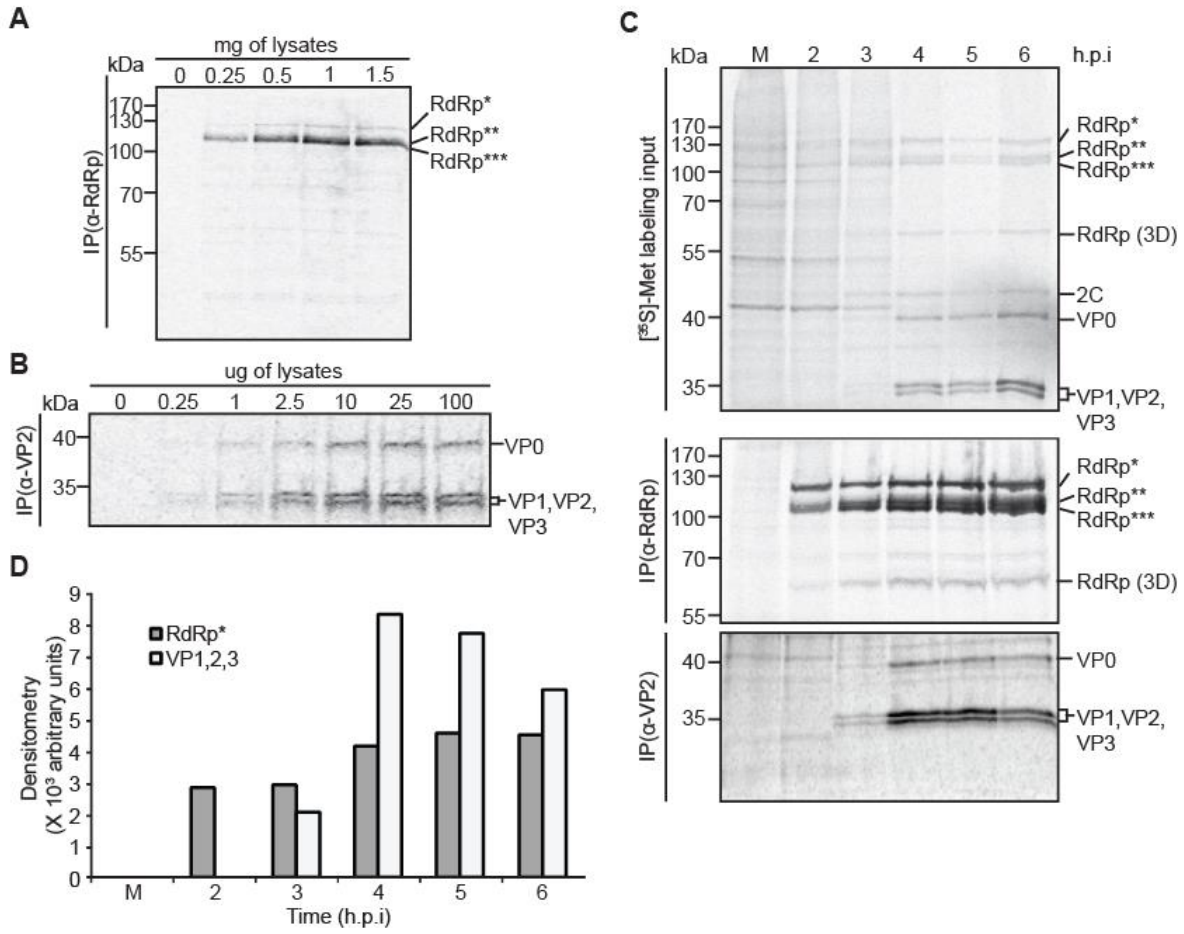

Figure 4.2. CrPV protein synthesis by immunoprecipitation analysis. Increasing amounts of pulse labelled protein lysates from CrPV- infected S2 cells (MOI 10, six h.p.i) were immunoprecipitated with a fixed amount of (A) α-RdRp or (B) α-VP2 antibodies as described in section 4.2.6. Pulldowns were resolved on an 12% SDS-PAGE. (C) 0.25 mg and 2.5 µg of protein lysates isolated from mock- or CrPV-infected (MOI 10) cells for the indicated times (hpi) were immunoprecipitated with α-RdRp or α-VP2 antibodies respectively. (D) Raw densitometric quantitation of immunoprecipitated pulse-labelled RdRp* protein and structural proteins VP1, VP2, and VP3 from (C). Cells were metabolically labelled with [^{35}S]-Met/Cys for one hour prior to the end of each time point. Shown are representative autoradiographs from 2 experiments. RdRp*, RdRp**, and RdRp*** denote polyproteins containing RdRp at the approximate sizes of 120kDa, 105kDa, and 100kDa respectively.

4.3.3 Measuring IRES-dependent translation during CrPV infection with the minigenome reporter

The distinct temporal expression of non-structural and structural proteins may be explained by one of two broad hypothesis. 1) The increase in structural protein synthesis can be described by passive regulation during infection - a combination of ribosome availability upon host translational repression, different intrinsic affinities for ribosomes and requirements for translation initiation factors between the 5'IRES and the IGR IRES, and an increase in viral RNAs drives the increase in viral structural protein synthesis over viral non-structural protein synthesis. 2) Alternatively, the increase in viral structural protein synthesis is driven by some active form of regulation during infection; In other words, IRES activities are regulated by one or more viral or cellular proteins during infection. To address these two broad hypothesis, I examined IRES activities directly with the minigenome construct (Figure 3.2A). As described in Chapter 3, we generated a CrPV minigenome construct whereby the viral ORF1 and ORF2 are replaced with Renilla and firefly luciferase genes, respectively (Figure 3.2A). Therefore, Renilla and firefly luciferase activities monitor 5'-UTR and IGR IRES-mediated translation, respectively. I assume this construct is not able to replicate during infection because the minigenome reporter encodes fewer than 20% of the sequences from the CrPV genome. *In vitro* transcribed polyadenylated minigenome reporter RNA (minigenome) was transfected into S2 cells and then infected with CrPV an hour later. Previously, we showed that luciferase activity increased linearly in the first six hours after transfection, indicating that the reporter RNA is engaged in translation during this time (Wang et al., 2013). Thus, cells were harvested at times after infection and

assayed for luciferase activity (Figure 4.3). As expected, in cells transfected with the minigenome, Renilla luciferase activity increased over time in the first six hours after transfection. In CrPV-infected cells, Renilla luciferase activity increased over time at similar rates as in mock-infected cells, suggesting that the 5'-UTR IRES translation is relatively constant during infection (Figure 4.3A). In contrast, the firefly luciferase activity accumulated gradually early in infection and sharply increased after two hpi as compared to mock-infected cells, suggesting that IGR IRES translation is delayed at early times of infection and is stimulated at later time points (Figure 4.3B). Transfection of a minigenome reporter containing a mutation that inactivates IGR IRES activity (ΔPK1) abolished firefly luciferase activity, indicating that the increase in firefly luciferase is due to IRES translation (Figure 4.3B).

Supporting this, I compared IGR IRES activity in S2 translation extracts that were mock-infected or infected for six hpi. To validate my translation extracts, I tested translation of reporter RNAs that were capped and polyadenylated, properties that promote translation of mRNAs. Incubation of monocistronic firefly luciferase reporter RNA that was 5'-capped (m^7G-FL) or 5'-capped and polyadenylated (m^7G-FL-Poly(A)) in S2 extracts resulted in 38-fold and 133-fold increases in translation, respectively, as compared to an uncapped, nonpolyadenylated reporter RNA (Figure 4.3C). In CrPV-infected extracts, smaller-21 fold and 40 fold increases in luciferase activity were observed with m^7G-FL and m^7G-FL-Poly(A) RNA respectively (Figure 4.3C). This result is expected because CrPV infection inhibits cellular translation. To address if IGR IRES activity differs in extracts from mock-infected or infected cells, I added minigenome RNA (Figure 3.3) and assayed for Renilla and firefly luciferase activity. Similar to the *in vivo*

results, the six hpi CrPV-infected extracts displayed higher IGR IRES activity (Figure 4.3D). On the other hand, the 5'-UTR IRES activity is similar in mock and infected extracts (Figure 4.3D). In summary, these results demonstrate that the

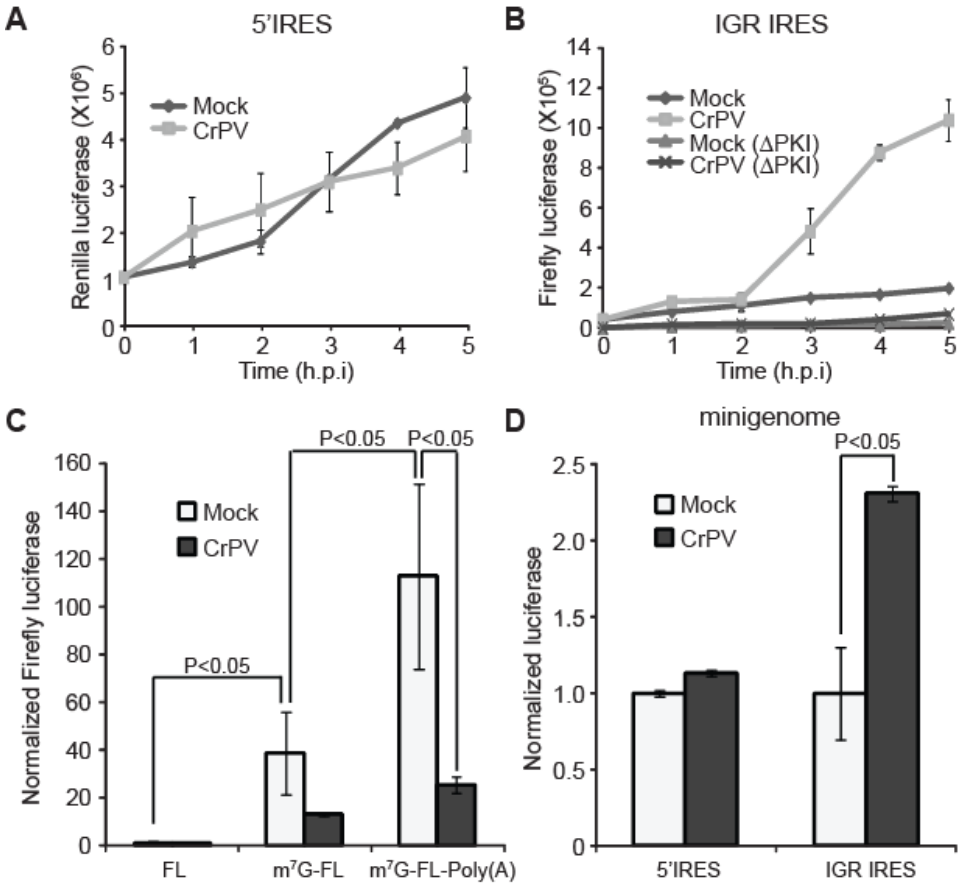

Figure 4.3. IGR IRES activity correlates with increased structural protein synthesis during infection. Minigenome RNA was transfected into S2 cells one hour prior to mock or CrPV infection. Cells were harvested at the indicated time points and assayed for Renilla (A) or firefly luciferase (B) activity as described in section 4.2.3. A mutation within the IGR IRES (ΔPKI), which disrupts pseudoknot I of the IRES, was used to validate that IGR IRES activity was monitored. (C) Monocistronic firefly RNA (FL), 5'-capped monocistronic firefly RNA (m^7G-FL), and 5'-capped and polyadenylated monocistronic firefly RNA (m^7G-FL-poly(A)) were incubated in S2 translation extracts for 30 min and assayed for firefly luciferase activity as described in section 4.2.8. The results are normalized to FL incubated in mock extracts. (D) Minigenome RNA was

incubated in S2 translation extracts from mock or infected cells for 30 min and assayed for Renilla and firefly luciferase activity as described in section 4.2.8. The results are normalized to mock extracts. Shown are results from an average of at least three independent experiments (± s.d.).

---

activities of CrPV 5'-UTR and IGR IRES are distinctly and temporally regulated during CrPV infection and in *in vitro* translation extracts. Although this data suggest IGR IRES is actively regulated, it is possible that some form of passive regulation is also important for increasing structural protein synthesis. To address this, I examined if transcriptional and translational repression induced during CrPV infection stimulates viral structural protein synthesis (Section 4.3.4 to 4.3.6).

4.3.4 Role of transcriptional repression in viral protein synthesis under CrPV infection

A number of viruses inhibit transcription during infection (Kundu et al., 2005; Maldonado et al., 2002; Vogt et al., 2008). The increase in structural protein synthesis may be due to perturbations in host transcription. However, cellular transcription during CrPV infection has not been examined carefully. To address this, I monitored overall transcription by a pulse-labeling approach. Specifically, mock and CrPV-infected S2 cells were pulse-labeled with [^{3}H]-uridine for 15 min at specific time points after infection (Figure 4.4A). RNA was extracted, resolved on an agarose gel, and transferred to a nylon membrane. Methylene blue staining readily detected the 18S/28S rRNA, which migrated at a size of ~2 kb, confirming that the RNA is intact (Figure 4.4B). In *Drosophila*, the mature 28S rRNA undergoes cleavage producing two products of

approximately equal size that migrate with the 18S rRNA (Jordan, 1975). Labeling with [^{3}H]-uridine in mock-infected cells produced two predominant radiolabeled bands that migrated at ~8 kb and ~5 kb (Figure 4.4A). Because we only labeled with [^{3}H]-uridine for a short period, these labeled RNAs represent immature, unprocessed rRNA precursors (data not shown). As expected, treatment of mock-infected cells with actinomycin D largely inhibited host transcription (Figure 4.4A). CrPV infection at an MOI of 10 resulted in labeling of a ~9 kb RNA, which increased during the course of infection demonstrating viral replication (Figure 4.4A). To distinguish between host and viral transcription, host transcription was inhibited by treating cells with actinomycin D (5 ug/mL) prior to [^{3}H]-uridine-labeling. As predicted, radiolabeled viral RNA was only detected in actinomycin D-treated infected cells (Figure 4.4A and 5.4C). Viral RNA synthesis increased during the first 4 hours of infection before leveling off and correlated with the increase in viral RNA as measured by Northern blot analysis (Figure 4.4D). In contrast, host transcription was rapidly inhibited within one hour of infection (~80% inhibition) and remained shut off during infection (Figure 4.4A and 5.4C). Host transcription was calculated by subtracting the amount of [^{3}H]-uridine labeled RNA in cells treated with actinomycin D from that in cells without actinomycin D. The quantitations of both viral and host transcription is shown in Figure 4.4A and 5.4C.

Since CrPV infection inhibits host transcription, I tested if this effect impacts CrPV protein synthesis. I pretreated cells in the absence or presence of actinomycin D for three hours prior to infection and compared the rate of viral protein synthesis in S2 cells by [^{35}S]-Met/Cys pulse labelling. If repression of transcription is necessary for the enhanced structural protein synthesis at three h.p.i, IGR IRES translation may be

prematurely stimulated. No significant changes in viral non-structural and structural protein synthesis were observed between cells pretreated with actinomycin D, demonstrating that host transcriptional repression does not contribute to the temporal regulation of viral ORF protein synthesis (Figure 4.4F and 5.4G).

4.3.5 Role of eIF2α phosphorylation in viral protein synthesis under CrPV infection

Virus-mediated translational repression is a strategy used by many RNA viruses to increase the cellular pool of ribosomes for viral protein synthesis and to inhibit antiviral innate responses during infection (Roberts et al., 2009; Walsh and Mohr, 2011). CrPV infection leads to a significant repression of translation at two to three hpi, which is approximately the time during infection when IGR IRES translation is stimulated. We previously showed that eIF2α is phosphorylated at approximately 3 hpi (Garrey et al., 2010). Previous studies (Deniz et al., 2009; Fernandez et al., 2002; Thompson et al., 2001; Wang and Jan, 2014) have shown that eIF2α phosphorylation stimulates IGR IRES translation; thus, it is possible that phosphorylation of eIF2α is the switch that stimulates IGR IRES translation. Previously, we overexpressed dGADD34 in infected cells. This protein interacts with and activates protein phosphatase I to keep eIF2a dephosphorylated (Garrey et al., 2010). Although this experiment did not alter the temporal regulation of non-structural and structural viral protein synthesis (Garrey et al., 2010), I opted for another approach to examine in more detail whether phosphorylation of eIF2α during CrPV infection has an effect on the regulation of 5'-UTR and IGR IRES translation. Towards this, I inhibited eIF2α phosphorylation by targeting the eIF2α

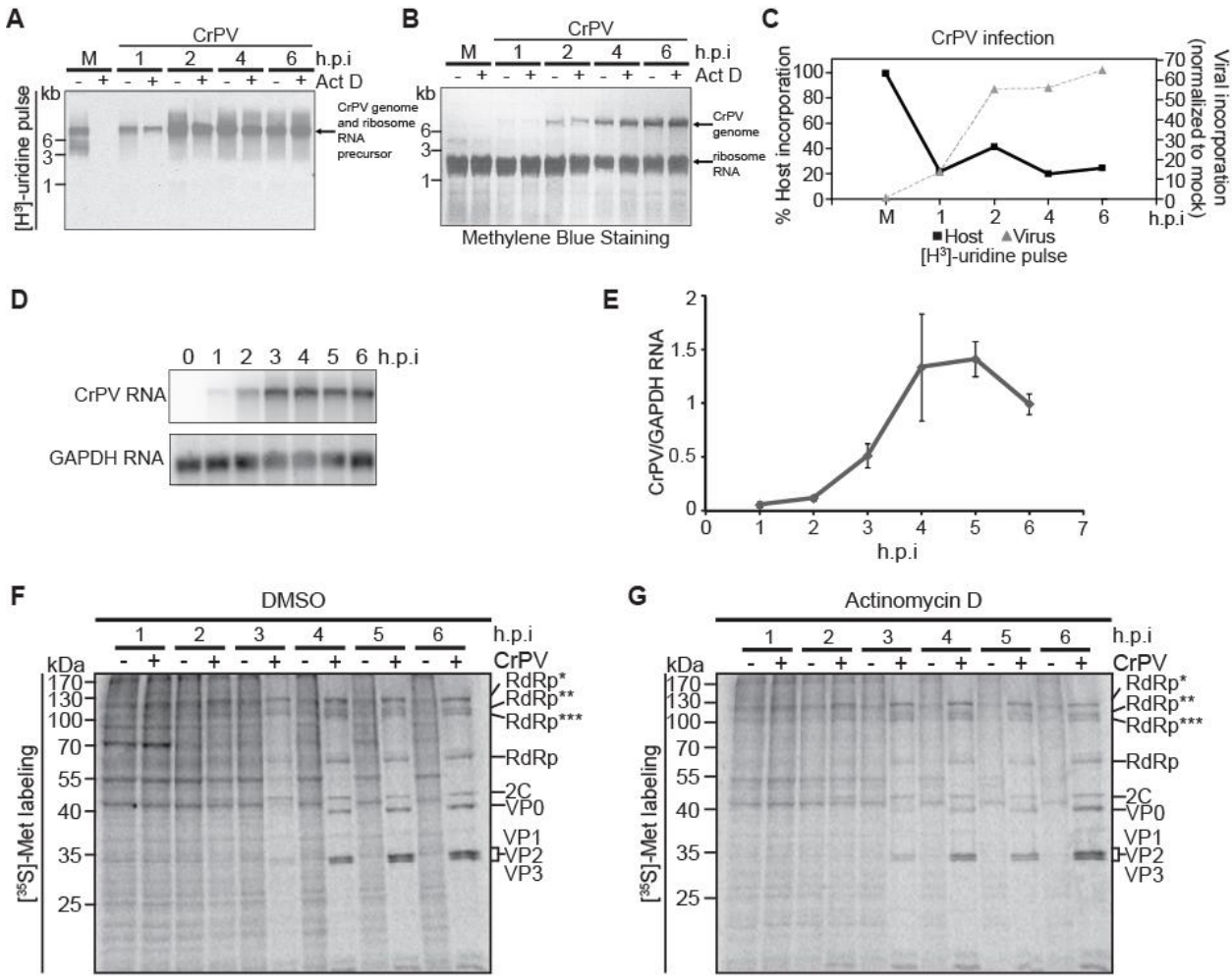

Figure 4.4. Host transcriptional repression in CrPV-infected S2 cells on viral translation. (A) Mock- and CrPV-infected S2 cells were pulse-labeled with [^{3}H]-uridine for 10 min at the indicated hours post infection (hpi) before harvesting as described in section 4.2.9. Where indicated, the cells were left untreated or treated with actinomycin D (Act D, 5 µg/mL) for 15 min prior to pulse-labeling. RNA was extracted, loaded on a denaturing agarose gel, transferred to a nylon membrane, and analyzed by phosphorimager analysis. Representative autoradiograms and a corresponding methylene blue stain are shown in (A) and (B) respectively. (C) Quantitation of host and viral transcription rates in CrPV-infected cells. The rate of host transcription at each time point was calculated using the formula [(Total radioactivity in lane -ActD)-(Total

radioactivity in lane + ActD)]/(Total radioactivity in lane -Act D). The rate of host transcription was normalized to that in mock-infected cells given as 100%. The rate of viral transcription was calculated at each hpi by using the formula [(Total radioactivity in lane + ActD)/(Total radioactivity in lane - ActD)]. The rate of viral transcription was normalized to that in mock-infected cells given as 0%. Shown are representative gels and averages from at least 2 independent experiments. (D) Viral RNA levels were detected by Northern blot analysis as described in section 4.2.10. (E) Viral RNA levels were quantified using Image quant and plotted to show levels of viral RNA/GAPDH RNA at different time points post infection. (F-G) Autoradiography of pulse-labelled protein lysates resolved on a 12% SDS-PAGE gel from S2 cells mock- or CrPV-infected (MOI 10) and treated with DMSO (F) or 50 nM ActD (G) three hours prior to infection as described in section 4.2.5. RdRp*, RdRp**, and RdRp*** denote polyproteins containing RdRp at the approximate sizes of 120kDa, 105kDa, and 100kDa respectively.

---

kinases using an RNAi approach. Unlike Gadd34 overexpression, this technique does not require transfection. Briefly, I incubated S2 cells with dsRNAs directed against the two known eIF2α kinases in *Drosophila*, dPERK and dGCN2. Since both dPERK and dGCN2 are required for eIF2α phosphorylation in arsenite-treated S2 cells, dsRNA knockdown efficiencies can be assessed indirectly by immunoblotting for eIF2α phosphorylation in arsenite-treated dPERK and dGCN2-depleted S2 cells (Farny et al., 2009). Treating cells with both dPERK and dGCN2 dsRNAs but not singly inhibited arsenite-induced eIF2α phosphorylation completely according to P-eIF2α western blot analysis, which is similar to that observed previously (Figure 4.5A), thus validating our knockdown conditions. Next, I determined which kinase is responsible for eIF2α phosphorylation in CrPV-infected S2 cells. I incubated GFP dsRNAs as a control or dPERK or dGCN2 dsRNAs individually or together to S2 cells prior to mock- or CrPV-

infection. While CrPV-infected S2 cells treated with GFP, GCN2 or PERK dsRNAs resulted in phosphorylation of eIF2α, treating infected cells with both PERK and GCN2 dsRNAs abolished eIF2α phosphorylation (Figure 4.5A). Thus, my result suggests that both GCN2 and PERK are activated in CrPV-infected S2 cells to induce eIF2α phosphorylation. To determine whether host or viral protein synthesis is perturbed, I monitored protein synthesis by pulse-labeling in CrPV-infected S2 cells treated with GFP dsRNAs (Figure 4.5B) or with PERK and GCN2 dsRNAs (Figure 4.5C). Despite inhibiting eIF2α phosphorylation, host translational repression and viral protein synthesis occurred to the same extent and at roughly the same time as in cells treated with a nonspecific GFP dsRNAs (Figure 4.5B and 4.5C). Thus, in agreement with previous findings, eIF2α phosphorylation is not responsible for host translation repression or viral protein synthesis and does not contribute to the temporal regulation of IGR IRES-mediated translation of CrPV ORF2 in CrPV-infected S2 cells.

4.3.6 Premature translational repression and CrPV IRES translation

Next I asked whether prematurely repressing host cap-dependent translation during CrPV infection can alter the temporal regulation of ORF1 and ORF2 expression. I reasoned that premature global repression of translation may stimulate IGR IRES translation early in infected cells because ribosomes that would otherwise be trapped on translating mRNAs can now be recruited by the viral genome for viral protein synthesis. Treatment of mammalian cells with PatA results in a rapid decrease in cap-dependent translation and stimulates IGR IRES-mediated translation (Bordeleau et al., 2005). I

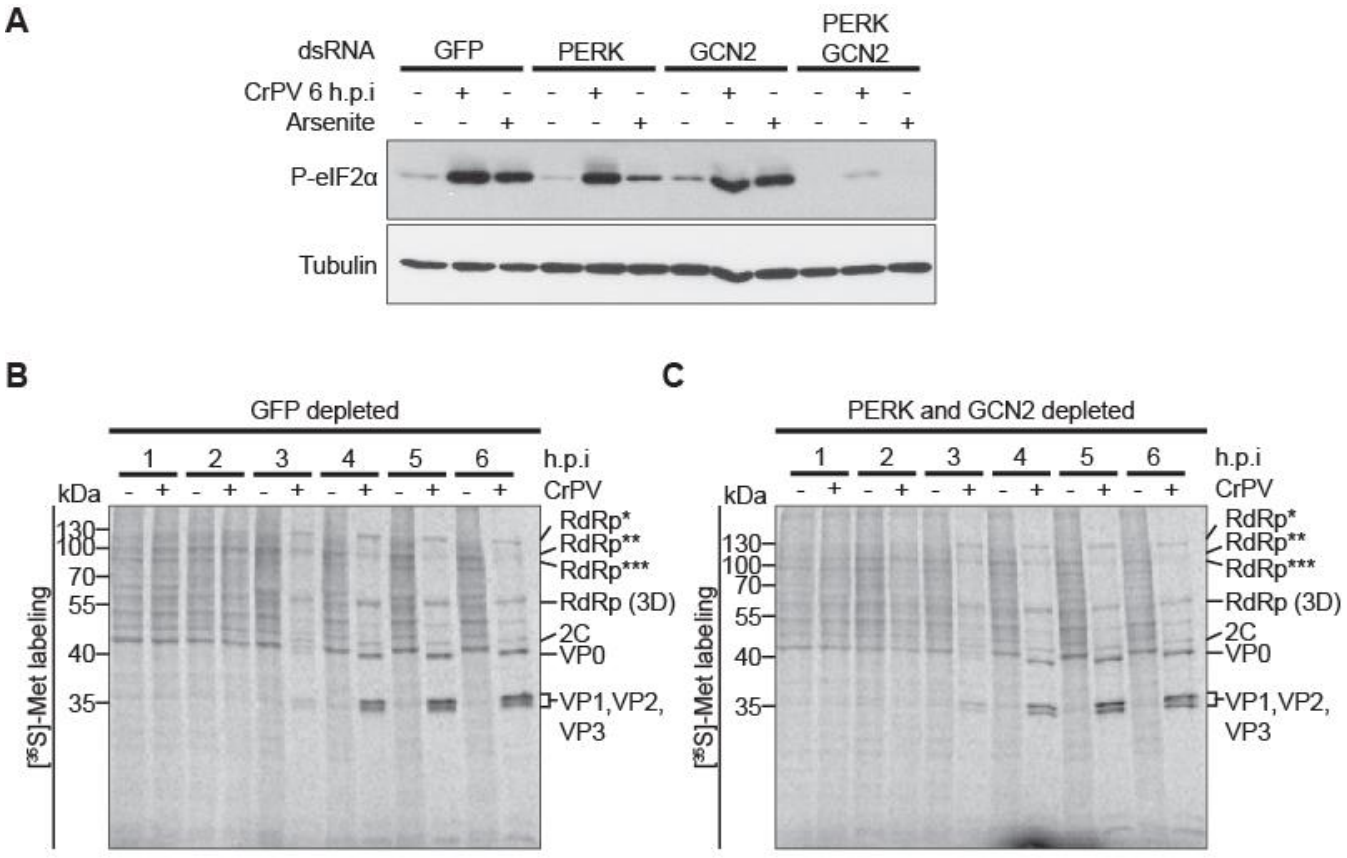

Figure 4.5. eIF2α phosphorylation during CrPV infection. (A) Representative phospho-eIF2α and tubulin western blots of lysates from cells depleted with dPERK and/or dGCN2 using dsRNAs treated with arsenite or infected with CrPV (MOI 10) as described in section 4.2.7 and 4.2.4. Pulse-labelled protein lysates from untreated (B) or dPERK and dGCN2 dsRNA-treated (C) S2 cells that were either mock or CrPV-infected were resolved on a 12% SDS- PAGE gel as described in section 4.2.5. The protein lysates were collected from S2 cells that were mock infected or CrPV infected (MOI 10) for the indicated times (hpi) and metabolically labeled with [^{35}S]-Met/Cys for 20 min at the end of each time point. Shown are representative autoradiographs from at least three independent experiments. RdRp*, RdRp**, and RdRp*** denote polyproteins containing RdRp at the approximate sizes of 120kDa, 105kDa, and 100kDa respectively.

treated mock- or CrPV-infected S2 cells with PatA at one hpi and monitored protein synthesis by pulse-labeling. As expected, PatA inhibited overall host protein synthesis after only one hour of treatment (Figure 4.6B, lanes 1 and 3). The effects of PatA continue to block translation after 5 hours of treatment (Figure 4.6B, lanes, 5, 7, 9 and 11). Compared to DMSO treated cells (Figure 4.6A), PatA treatment of CrPV-infected cells resulted in a premature dramatic shut off of host protein synthesis by 2 hpi (Figure 4.6B). Interestingly, although overall host translation is repressed at 2 hpi, in PatA treated infected cells, only the CrPV non-structural proteins could be visibly detected at this time point (Figure 4.6B, lane 4). It is not until 3 hpi that synthesis of the structural proteins is detected, which is similar to the time that of their detection in DMSO-treated infected cells (Figure 4.6A and 4.6B). Moreover, the extents of viral non-structural and structural protein synthesis and RNA synthesis were similar between DMSO- and PatA-treatments over the course of infection (Figure 4.6B). Finally, PatA treatment affected CrPV viral titres slightly (Figure 4.6C). To ensure that these results are not specific to PatA, I also prematurely inhibited cellular translation with DTT, a treatment that induces eIF2α phosphorylation and is also known to stimulate IGR IRES translation (Figure 4.6D and 4.6E). Like PatA treatment, I observed no differences in the timing or extent of viral non-structural and structural protein synthesis in DMSO- and DTT-treated infected cells (Figure 4.6D and 4.6E). Thus, premature shut-off of protein synthesis does not disrupt the temporal regulation of IGR IRES-mediated translation.

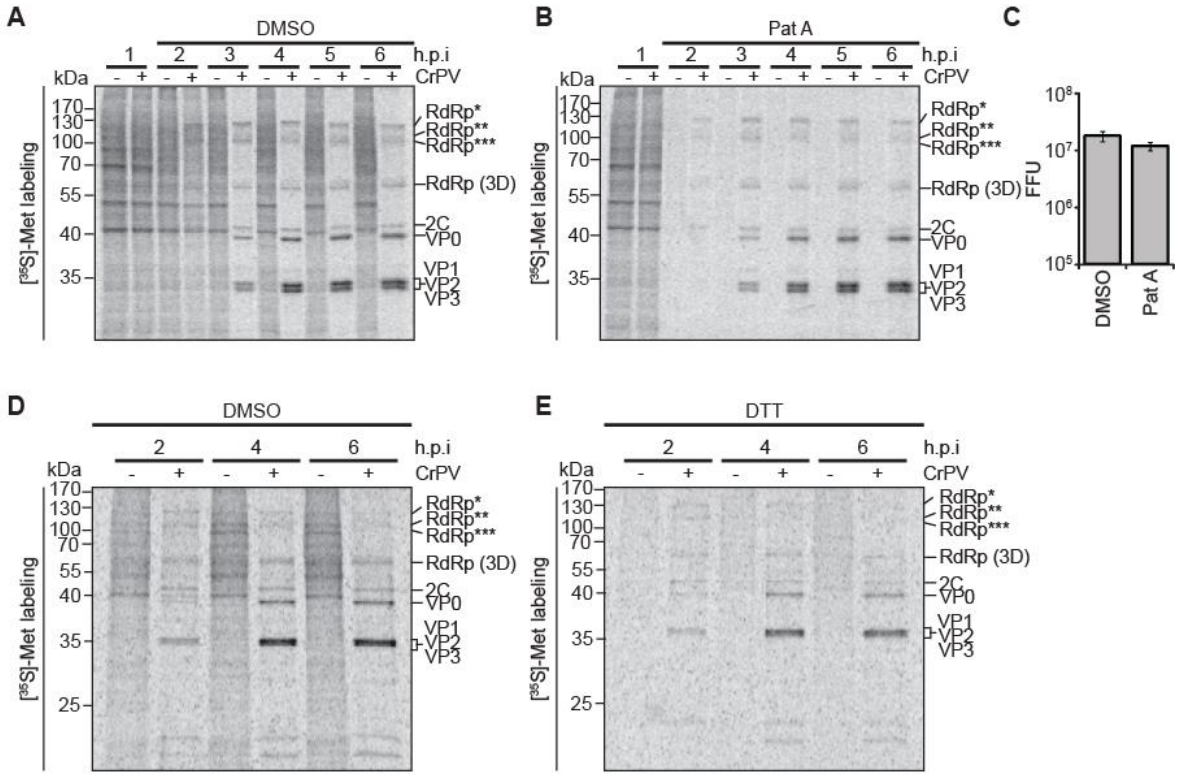

Figure 4.6. Effects of pateamine A and DTT on CrPV translation. Pulse-labelled protein lysates from mock- or CrPV-infected (MOI 10) S2 cells treated with either (A) DMSO or (B) 50nM PatA were resolved on a 12% SDS-PAGE gel as described in section 4.2.5. The cells were metabolically labeled with [^{35}S]-Met/Cys for 20 min at the end of each time point. Shown are representative autoradiographs from at least three independent experiments. (C) Viral titers from infected lysates treated with DMSO or Pat A after 10 hpi as described in section 4.2.1. (D and E) Autoradiography of pulse-labelled protein lysates resolved on a 12% SDS-PAGE gel from S2 cells mock infected or CrPV infected (MOI 10) and treated with DMSO (D) or 50nM DTT (E) one h.p.i as described in section 4.2.5. 20 min prior to each timepoint, the cells were metabolically labeled with [^{35}S]-Met and [^{35}S]-Cys. RdRp*, RdRp**, and RdRp*** denote polyproteins containing RdRp at the approximate sizes of 120kDa, 105kDa, and 100kDa respectively.

4.4 Discussion

Unlike some RNA viruses such as picornaviruses that use an IRES to direct translation of one main ORF to produce stoichiometric amounts of mature viral proteins, Dicistroviruses utilize a strategy whereby two different IRESs independently regulate translation of non-structural and structural proteins. While it has been well established that the viral structural proteins are produced in supramolar excess over non-structural proteins (Garrey et al., 2010; Moore et al., 1980; Wilson et al., 2000), I discovered that non-structural and structural protein synthesis are temporally regulated during infection by metabolic pulse labelling. To explore if this regulation involves a direct stimulation of the IGR IRES, I used reporters that measure IGR IRES and 5'-UTR IRES translation directly during infection and in mock or infected extracts. I discovered a significant relative increase in IGR IRES activity with the minigenome reporter during infection and in extracts from infected cells. Nevertheless, it is possible that the increase seen in structural protein synthesis relative to non-structural protein synthesis is in large part due to a repression of cellular transcription and translation. To investigate this, I attempted to affect the temporal regulation of IGR IRES activity by perturbing transcription and translation. In each case, I showed that temporal regulation of non-structural protein synthesis was not affected. These results suggest a novel strategy utilized by Dicistroviruses to ensure the optimal ratio of viral structural to non-structural proteins for virus infection.

It is presumed that the temporal regulation of the 5'-UTR and IGR IRES translation during CrPV infection is due to the differential requirements for translation. IGR IRES translation does not require factors for initiation (Deniz et al., 2009; Jan and

Sarnow, 2002; Wilson et al., 2000) whereas the CrPV 5'-UTR IRES likely uses a subset of initiation factors including eIF4A (Terenin et al., 2013). Although the factors required for the related dicistrovirus RhPV 5'-UTR have been identified, the specific factors required by the CrPV 5'-UTR IRES have not been examined in detail. Based on these observations, I predicted that premature inhibition of translation via modification of initiation factors may drive IGR IRES translation earlier during infection. Surprisingly, attempts to disrupt overall host translation by either inhibiting eIF2α phosphorylation or prematurely inhibiting translation during infection did not affect the timing of 5'-UTR and IGR IRES translation (Figure 4.5, 4.6). Although it has been shown that CrPV IGR IRES translation is stimulated when eIF2α is phosphorylated or eIF4A activity is disrupted (Wang and Jan, 2014), it is clear that translational repression is not a prerequisite for IGR IRES activation during CrPV infection. There are a number of potential mechanisms that may explain how IGR IRES activity is temporally regulated during infection by non-structural viral proteins. It is possible that the slight delay in IGR IRES translation in CrPV-infected cells is due to either an inhibition of IGR IRES translation at early time points of infection or that IGR IRES translation is activated at later times. Two potential candidates for this are ITAFs or ITIF (IRES trans inactivating factor). Specifically, an ITAF or ITIF could bind to the IGR IRES and either stimulate or inhibit IRES activity (Spriggs et al., 2005) (Lin et al., 2009). One possibility is that a non-structural viral protein(s) is involved, which would be feasible and may explain the delay in IGR IRES translation as non-structural proteins have to be expressed prior to IGR IRES activation.

In a recent report, Wu *et al.* (2014) determined that Pelo is required for structural protein synthesis during Dicistrovirus infection.Pelo is the homolog of Dom34 in *Drosophila melanogaster* and is responsible for the recycling of stalled 80S ribosomes on mRNAs (Tsuboi et al., 2012). Wu et al. (2014) speculated that the action of pelo during infection provides Dicistrovirus genomes greater access to ribosomes for high level synthesis of viral structural proteins. Whether pelo itself is regulated during infection and affects IGR IRES activity remains unexplored. Nevertheless, despite significant depletion of pelo protein, structural proteins are still expressed in supramolar excess over non-structural proteins (Wu et al., 2014). Thus, ribosome recycling is likely not the sole reason why structural protein synthesis is observed late in infection.

Another possible target for viral non-structural proteins is the ribosome. Depletion of specific ribosomal proteins can inhibit IRES-dependent but not cap-dependent translation (Cherry et al., 2005), suggesting that heterogeneity of ribosomes may have an effect on IRES activities. For example, depletion of rpS25 inhibits IGR IRES translation and lowers CrPV titer (Landry et al., 2009). Similarly, depletion of RACK1 inhibits 5'-UTR IRES-dependent but not IGR IRES-dependent translation (Majzoub et al., 2014) and infection. It is possible that post-translational modifications of key ribosomal proteins during CrPV infection may be responsible for the temporal regulation of IGR IRES activity.

A number of viruses express structural proteins later than non-structural proteins during infection. This strategy presumably allows translation and replication to occur before the viral genomes are packaged. For example, SBV and coronavirus control the timing of viral structural protein synthesis through subgenomic mRNAs (sgRNAs).

SgRNA synthesis requires replication and is therefore always translated later than the genomic RNA (Miller and Koev, 2000). Further work will be required to address if the delay in structural protein synthesis observed after CrPV infection is critical for the viral life cycle and can be generalized to the family *Dicistroviridae*.

Chapter 5: Summary and future directions

How dicistroviruses usurp the translational machinery and inhibit antiviral responses is still not well described. In my thesis, using dicistrovirus infection in *Drosophila* S2 cells as a model, I examined the interplay between SGs and dicistroviruses, identified a viral protein, 1A, which blocks SG formation and observed temporal regulation of viral non-structural and structural protein synthesis during CrPV infection (Figure 5.1). Furthermore, upon further characterization of 1A, I discovered that 1A can stimulate 5'-dependent translation. Therefore, I speculate 1A may enhance 5'IRES-dependent translation during infection (Figure 5.1).

Investigations into dicistroviruses' life cycle and viral-host interactions are important for many reasons. First, the study of dicistroviruses may lead to treatments for agricuturally beneficial anthropods afflicted by these viruses (Cox-Foster et al., 2007; Lightner, 1996; Lightner et al., 1997). Second, dicistroviruses may be important in many ecosystems because recent metagonomic surveys suggest that Dicistroviruses are ubiquitous (Culley et al., 2006; Ng et al., 2012; Victoria et al., 2009). Third, since dicistroviruses infect arthropods, investigation into this family of viruses can facilitate a deeper understanding of insect and crustacean innate immunity. More importantly, unlike other insect viruses like West Nile virus and Dengue virus, there is no added pressure for dicistroviruses to evolve mechanisms to evade or suppress mammalian innate immunity. Therefore, the study of dicistrovirus-host interaction provides a unique perspective for investigating ancient antiviral mechanisms that are conserved in the kingdom Animalia.

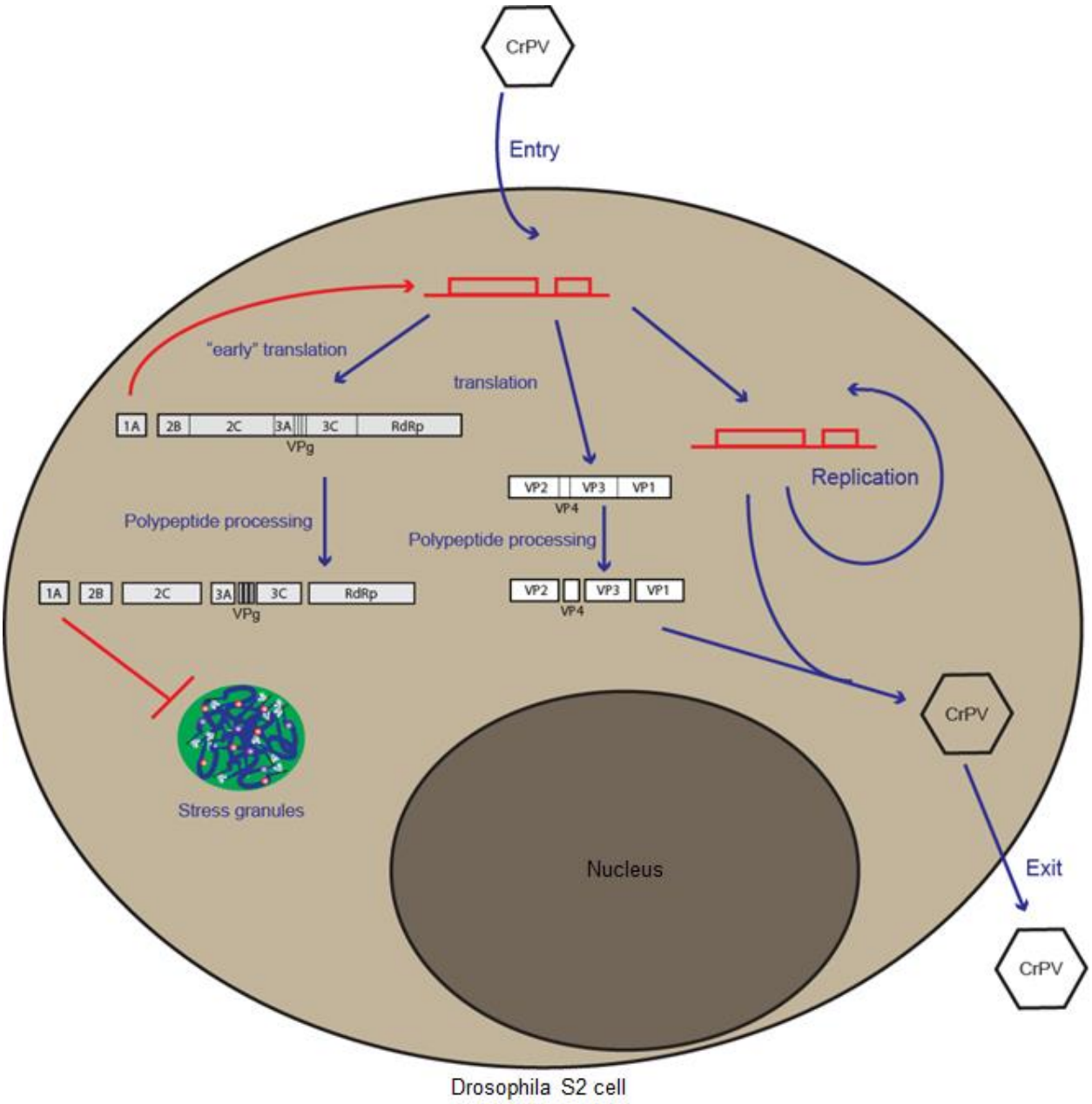

Figure 5.1. Model of cricket paralysis virus life cycle and virus host-interaction. Upon entry into Drosophila S2 cells, viral translation begins. Specfically, non-structural viral proteins are predominatly expressed early in infection whereas structural viral proteins are predominatly expressed later in infection (Chapter 4). One of the non-structural viral protein, CrPV 1A, stimulates 5'-dependent translation (Chapter 3) and suppresses SG aggregation (Chapter 2 and 3). It is not well understood how CrPV enters S2 cells, replicates its genome, and leaves the cell.

There are many exciting, unresolved, major questions in the dicistrovirus field. Several questions can be derived directly from my thesis. One of the major findings in this thesis is the suppression by CrPV 1A of the SG induction pathway (Chapter 3). Although I was not able to elucidate how 1A accomplishes this, one future aim will be to immuoprecipitate 1A and identify interacting partners by mass spectrometry. This pull-down approach may identify one or more factors essential for formation and/or maintenance of SGs. Follow-up experiments by using RNAi to deplete these factors may unravel their role in SGs during dicistrovirus infection. In Chapter 2, I also discovered that the related dicistrovirus DCV inhibits the SG pathway. Although DCV 1A inhibits RNAi differently than CrPV 1A, by binding to dsRNA and sequestering the viral RNA from the RNAi machinery, it will be interesting to test if DCV 1A and other dicistrovirus 1A gene products also suppress SGs. Alternatively, It is possible that other dicistrovirus proteins in addition to CrPV 1A are involved in SG suppression. Expressing these recombinant viral proteins and assaying for inhibition of SG induction in S2 cells is another avenue to pursue.

Besides addressing how SGs are suppressed by CrPV infection, another major question is why SGs are disrupted during CrPV infection. Although I speculate it is to keep viral proteins from being trapped in SGs, there may be other reasons. First, like many other viral examples, SG factors like Rox8 or Rin may be required for viral replication. To address this hypothesis, biotinylated viral RNAs can be prepared and interacting partners can be identified by mass spectrometry. Second, SGs may activate an innate immune response. This was observed recently in mammalian cells (Reineke and Lloyd, 2015) and it will be interesting to test if this process is observed in

Drosophila. To test this, we can induce SGs by overexpressing SG markers and performing SILAC, stable isotape labeling of amino acids in cell culture. To elaborate, cells are differentially labelled with normal arginine or with heavy arginine in normal cells or cells overexpressing RinGFP respectively. After labelling for a day, the cells are lysed and the samples are pooled. Mass spectrometry is performed on the samples and any significant differences in the ratio of peak intensities between light and heavy labelled peptides are noted. If overexpression of SG markers activates an innate immune response, we should see an enrichment of heavy peptides from insect innate immune proteins in cells overexpressing RinGFP. If we confirm that SGs activate an innate immune antiviral response in insects, we can test if this is functionally important in the context of CrPV infection. Specifically, we can compare viral yield in CrPV-infected cells with CrPV-infected cells overexpressing RinGFP.

Another major unresolved question in Chapter 2 is what the poly(A)$^+$ granules represent in CrPV-infected cells. Thorough examination ruled out CrPV viral RNA and PBs, thus I suspect the poly(A)$^+$ granules are cellular RNAs that are no longer engaged with the translational machinery. Detection of specific abundant host mRNAs such as actin and GAPDH using fluorescent *In situ* hybridization would address this hypothesis. How these poly(A)$^+$ granules are aggregating is another interesting important question as these poly(A)$^+$ granules lack any traditional SG and PB markers. Identification of the proteins involved in the assembly of poly(A)$^+$ granules during CrPV infection may be difficult because RNA granules in general are highly dynamic and most proteins in RNA granules are weakly interacting (Souquere et al., 2009) (section 1.6). A recently developed technique called BioID may help identify factors present in poly(A)$^+$ granules

(Roux, Kim, Raida, & Burke, 2012). Specifically, by expressing a chimeric protein containing a protein-of-interest fused with a promiscious biotin ligase in cells incubated with biotin, the fusion protein can biotinylate proximal endogenous proteins. The proximal labelled proteins can be isolated with streptavidin and identified by mass spectrometry. Since this approach is *in vivo*, this technique will not disrupt RNA granules. By fusing PABP with this biotin ligase, we can use this approach to identify other factors that are enriched in poly(A)$^+$ granules which may lead to a better understanding of how these granules form.

A large part of my thesis is devoted to CrPV 1A (Chapter 3). Besides inhibiting Ago2 (Nayak et al., 2010) and inhibiting SG induction, I discovered that 1A has other functions including stimulating translation of reporter RNAs and the 5'-UTR IRES. In addition, I discovered CrPV 1A is toxic to S2 cells. To address all these different functions it will be interesting to solve the structure of CrPV 1A by x-ray crystallography. The 1A structure can be used as a tool to identify critical elements important for all these different functions. Another approach to address these diverse 1A functions is to identify interacting viral or cellular proteins. As described earlier, 1A can be immunoprecipitated and interacting partners can be identified by mass spectrometry. Follow-up experiments with RNAi to deplete these interacting factors may identify binding proteins involved in these various 1A functions.

Another important unanswered question in Chapter 3 is how are reporter RNAs translated differently than cellular RNAs during CrPV infection. One possibility is that cellular RNAs are commonly modified and exist as an mRNP (Fu et al., 2014). These differences might be the reason why exogenous reporter RNAs are still translated

during infection. To test this hypothesis, one can transfect *in vitro* synthesized luciferase RNA with modified nucleotides like m^6A and determine if CrPV infection inhibits or enhance expression of this particular RNA. Supporting this interesting hypothesis is the observation that modified RNAs behave differently than unmodified RNAs; For example, modified RNAs can bypass innate immune responses (Kormann et al., 2011). Perhaps unmodified RNAs behave like the CrPV viral genomic RNA and can avoid the translational repression observed during infection.

Another interesting and complementary perspective that may explain why exogenous RNAs are stimulated during CrPV infection stems from the observation that cellular mRNAs are sequestered to poly(A)$^+$ granules. Since a recent report suggests that cellular mRNAs that are heavily modified with m^6A are trapped in SGs and PBs (Fu et al., 2014), it is interesting to speculate if m^6A modified mRNAs are also trapped in poly(A)$^+$ granules. Therefore it is not a stretch to suggest that exogenous unmodified RNAs such as transfected reporter RNAs or viral RNAs are not trapped in poly(A)$^+$ granules and thus can recruit the translational machinery during infection.

Another hypothesis that may explain why exogenously introduced RNAs are behaving differently than cellular RNAs is a block in nuclear export during infection. Specifically, CrPV infection might block the transport of cellular mRNAs from the nucleus to the cytoplasm and therefore inhibit cellular protein synthesis. Presumably, this will indirectly stimulate translation of exogenously introduced RNA. To test this hypothesis, we can add drugs like leptomycin B, an antibiotic that blocks nuclear export, to cells and test if reporter RNAs are stimulated.

In Chapter 4, I discovered that viral structural proteins are expressed later than non-structural viral proteins. An unanswered question in that Chapter is how IGR IRES activity is regulated *in vivo.* One possibility is that the IGR IRES may interact with specific factors during CrPV infection. To address this, a pull down coupled with mass spectrometry with biotinylated IGR IRES in S2 extracts may identify host or viral factors that bind to the IRES that enhance or repress translation. Alternatively, an siRNA genome-wide approach may identify cellular factors that are important for this regulation. Specifically, an siRNA screen can be performed on stable cell lines expressing a bicistronic reporter that monitors 5'IRES and IGR IRES activity by red fluorescent protein and green fluorescent protein respectively. If IGR IRES activity but not 5'IRES activity is significantly affected during infection in a particular siRNA treated S2 cell, the depleted protein may be important for this regulation. These two complementary approaches should address how IGR IRES activity is regulated *in vivo*.

Finally, there are many features in dicistroviruses that are not well characterized. For example, most dicistrovirus proteins are not well described. In order to gain a better understanding of this viral family, it is imperative to understand how each individual viral protein interacts with each other and with host proteins. To determine interactions, we can use BioID to find interacting partners *in vivo.* This can be done by fusing the biotin ligase with a particular viral protein of interest in the recently created CrPV infectious clone (Kerr et al., 2015). Upon identifying interacting partners, we can start to deduce what each dicistroviral protein is doing during infection. The next step is to introduce key mutations in the viral protein within the infectious clone and observe its effects on the viral life cycle.

Another relatively uncharacterized dicistrovirus feature is the 5'IRES. Although RhPV requires eIF1, eIF2 and eIF3 for translation initiation and is stimulated by eIF1A, eIF4F, and eIF4A (Terenin et al., 2013), the 5'IRES sequence is not well conserved in dicistroviruses (reviewed in Roberts and Groppelli, 2009). Therefore, it is unclear if the 5'-IRES from other dicistroviruses require the same factors. To examine this, one can reconstitute 48S initiation complexes on the CrPV 5'IRES with purified components, an approach similar to that used for the RhPV 5'IRES and perform single component omission experiment. Alternatively, specific translation inhibitors like PatA or 4ER1cat, a compound that blocks eIF4E:eIF4G interaction (Cencic et al., 2011), can be used to test if a particular translation factor is required or not required for 5'-IRES-dependent translation *in vitro*.

In summary, I discovered many interesting features during dicistrovirus infection. The studies on SGs, 1A, and temporal regulation of viral non-structural and structural protein synthesis during CrPV infection enclosed in this thesis should provide an excellent foundation for deeper investigation into dicistrovirus-host interaction. Moreover, these studies also expand on fundamental viral-host interactions and may lead to the development of drugs to treat agriculturally important dicistroviruses.

References

Algire, M.A., Maag, D., and Lorsch, J.R. (2005). Pi release from eIF2, not GTP hydrolysis, is the step controlled by start-site selection during eukaryotic translation initiation. Molecular cell *20*, 251-262.

Ameres, S.L., and Zamore, P.D. (2013). Diversifying microRNA sequence and function. Nature reviews Molecular cell biology *14*, 475-488.

Anderson, P., and Kedersha, N. (2009). RNA granules: post-transcriptional and epigenetic modulators of gene expression. Nature reviews Molecular cell biology *10*, 430-436.

Arimoto, K., Fukuda, H., Imajoh-Ohmi, S., Saito, H., and Takekawa, M. (2008). Formation of stress granules inhibits apoptosis by suppressing stress-responsive MAPK pathways. Nature cell biology *10*, 1324-1332.

Ariumi, Y., Kuroki, M., Kushima, Y., Osugi, K., Hijikata, M., Maki, M., Ikeda, M., and Kato, N. (2011). Hepatitis C virus hijacks P-body and stress granule components around lipid droplets. Journal of virology *85*, 6882-6892.

Baird, N.L., York, J., and Nunberg, J.H. (2012). Arenavirus infection induces discrete cytosolic structures for RNA replication. Journal of virology *86*, 11301-11310.

Behm-Ansmant, I., Rehwinkel, J., Doerks, T., Stark, A., Bork, P., and Izaurralde, E. (2006). mRNA degradation by miRNAs and GW182 requires both CCR4:NOT deadenylase and DCP1:DCP2 decapping complexes. Genes Dev *20*, 1885-1898.

Berthelot, K., Muldoon, M., Rajkowitsch, L., Hughes, J., and McCarthy, J.E. (2004). Dynamics and processivity of 40S ribosome scanning on mRNA in yeast. Molecular microbiology *51*, 987-1001.

Besnard-Guerin, C., Jacquier, C., Pidoux, J., Deddouche, S., and Antoniewsk, C. (2015). The Cricket Paralysis Virus Suppressor Inhibits microRNA Silencing Mediated by the Drosophila Argonaute-2 Protein. PloS one *10*, e0120205.

Bonning, B.C., and Miller, W.A. (2010). Dicistroviruses. Annual review of entomology *55*, 129-150.

Bordeleau, M.E., Matthews, J., Wojnar, J.M., Lindqvist, L., Novac, O., Jankowsky, E., Sonenberg, N., Northcote, P., Teesdale-Spittle, P., and Pelletier, J. (2005).

Stimulation of mammalian translation initiation factor eIF4A activity by a small molecule inhibitor of eukaryotic translation. Proceedings of the National Academy of Sciences of the United States of America *102*, 10460-10465.

Borman, A., and Jackson, R.J. (1992). Initiation of translation of human rhinovirus RNA: mapping the internal ribosome entry site. Virology *188*, 685-696.

Brasey, A., Lopez-Lastra, M., Ohlmann, T., Beerens, N., Berkhout, B., Darlix, J.L., and Sonenberg, N. (2003). The leader of human immunodeficiency virus type 1 genomic RNA harbors an internal ribosome entry segment that is active during the G2/M phase of the cell cycle. Journal of virology *77*, 3939-3949.

Bronkhorst, A.W., van Cleef, K.W., Venselaar, H., and van Rij, R.P. (2014). A dsRNA-binding protein of a complex invertebrate DNA virus suppresses the Drosophila RNAi response. Nucleic acids research *42*, 12237-12248.

Buchan, J.R., Muhlrad, D., and Parker, R. (2008). P bodies promote stress granule assembly in Saccharomyces cerevisiae. The Journal of cell biology *183*, 441-455.

Buchan, J.R., and Parker, R. (2009). Eukaryotic stress granules: the ins and outs of translation. Molecular cell *36*, 932-941.

Burgui, I., Yanguez, E., Sonenberg, N., and Nieto, A. (2007). Influenza virus mRNA translation revisited: is the eIF4E cap-binding factor required for viral mRNA translation? Journal of virology *81*, 12427-12438.

Cencic, R., Hall, D.R., Robert, F., Du, Y., Min, J., Li, L., Qui, M., Lewis, I., Kurtkaya, S., Dingledine, R.*, et al.* (2011). Reversing chemoresistance by small molecule inhibition of the translation initiation complex eIF4F. Proceedings of the National Academy of Sciences of the United States of America *108*, 1046-1051.

Chang, H.W., and Jacobs, B.L. (1993). Identification of a conserved motif that is necessary for binding of the vaccinia virus E3L gene products to double-stranded RNA. Virology *194*, 537-547.

Cherry, S., Doukas, T., Armknecht, S., Whelan, S., Wang, H., Sarnow, P., and Perrimon, N. (2005). Genome-wide RNAi screen reveals a specific sensitivity of IRES-containing RNA viruses to host translation inhibition. Genes & development *19*, 445-452.

Cherry, S., and Perrimon, N. (2004). Entry is a rate-limiting step for viral infection in a Drosophila melanogaster model of pathogenesis. Nature immunology *5*, 81-87.

Cheung, Y.N., Maag, D., Mitchell, S.F., Fekete, C.A., Algire, M.A., Takacs, J.E., Shirokikh, N., Pestova, T., Lorsch, J.R., and Hinnebusch, A.G. (2007). Dissociation of eIF1 from the 40S ribosomal subunit is a key step in start codon selection in vivo. Genes & development *21*, 1217-1230.

Connor, J.H., and Lyles, D.S. (2002). Vesicular stomatitis virus infection alters the eIF4F translation initiation complex and causes dephosphorylation of the eIF4E binding protein 4E-BP1. Journal of virology *76*, 10177-10187.

Costantino, D.A., Pfingsten, J.S., Rambo, R.P., and Kieft, J.S. (2008). tRNA-mRNA mimicry drives translation initiation from a viral IRES. Nature structural & molecular biology *15*, 57-64.

Cox-Foster, D.L., Conlan, S., Holmes, E.C., Palacios, G., Evans, J.D., Moran, N.A., Quan, P.L., Briese, T., Hornig, M., Geiser, D.M.*, et al.* (2007). A metagenomic survey of microbes in honey bee colony collapse disorder. Science *318*, 283-287.

Cristea, I.M., Rozjabek, H., Molloy, K.R., Karki, S., White, L.L., Rice, C.M., Rout, M.P., Chait, B.T., and MacDonald, M.R. (2010). Host factors associated with the Sindbis virus RNA-dependent RNA polymerase: role for G3BP1 and G3BP2 in virus replication. Journal of virology *84*, 6720-6732.

Culley, A.I., Lang, A.S., and Suttle, C.A. (2006). Metagenomic analysis of coastal RNA virus communities. Science *312*, 1795-1798.

Dang, Y., Kedersha, N., Low, W.K., Romo, D., Gorospe, M., Kaufman, R., Anderson, P., and Liu, J.O. (2006). Eukaryotic initiation factor 2alpha-independent pathway of stress granule induction by the natural product pateamine A. J Biol Chem *281*, 32870-32878.

Deniz, N., Lenarcic, E.M., Landry, D.M., and Thompson, S.R. (2009). Translation initiation factors are not required for Dicistroviridae IRES function in vivo. Rna *15*, 932-946.

Dias, A., Bouvier, D., Crepin, T., McCarthy, A.A., Hart, D.J., Baudin, F., Cusack, S., and Ruigrok, R.W. (2009). The cap-snatching endonuclease of influenza virus polymerase resides in the PA subunit. Nature *458*, 914-918.

Dunn, E.F., and Connor, J.H. (2011). Dominant inhibition of Akt/protein kinase B signaling by the matrix protein of a negative-strand RNA virus. Journal of virology *85*, 422-431.

Eaton, B.T., and Steacie, A.D. (1980). Cricket Paralysis Virus RNA has a 3' Terminal Poly(A). J Gen Virol *50*, 167-171.

Emara, M.M., and Brinton, M.A. (2007). Interaction of TIA-1/TIAR with West Nile and dengue virus products in infected cells interferes with stress granule formation and processing body assembly. Proceedings of the National Academy of Sciences of the United States of America *104*, 9041-9046.

Eulalio, A., Behm-Ansmant, I., and Izaurralde, E. (2007). P bodies: at the crossroads of post-transcriptional pathways. Nat Rev Mol Cell Biol *8*, 9-22.

Eystathioy, T., Chan, E.K., Tenenbaum, S.A., Keene, J.D., Griffith, K., and Fritzler, M.J. (2002). A phosphorylated cytoplasmic autoantigen, GW182, associates with a unique population of human mRNAs within novel cytoplasmic speckles. Mol Biol Cell *13*, 1338-1351.

Farny, N.G., Kedersha, N.L., and Silver, P.A. (2009). Metazoan stress granule assembly is mediated by P-eIF2alpha-dependent and -independent mechanisms. Rna *15*, 1814-1821.

Fekete, C.A., Mitchell, S.F., Cherkasova, V.A., Applefield, D., Algire, M.A., Maag, D., Saini, A.K., Lorsch, J.R., and Hinnebusch, A.G. (2007). N- and C-terminal residues of eIF1A have opposing effects on the fidelity of start codon selection. The EMBO journal *26*, 1602-1614.

Fernandez, I.S., Bai, X.C., Murshudov, G., Scheres, S.H., and Ramakrishnan, V. (2014). Initiation of translation by cricket paralysis virus IRES requires its translocation in the ribosome. Cell *157*, 823-831.

Fernandez, J., Yaman, I., Merrick, W.C., Koromilas, A., Wek, R.C., Sood, R., Hensold, J., and Hatzoglou, M. (2002). Regulation of internal ribosome entry site-mediated translation by eukaryotic initiation factor-2alpha phosphorylation and translation of a small upstream open reading frame. The Journal of biological chemistry *277*, 2050-2058.

Flint, S.J., Racaniello, V.R., Enquist, L.W., and Skalka, A.M. (2009). Principles of Virology Third Edition (ASM Press).

Fros, J.J., Domeradzka, N.E., Baggen, J., Geertsema, C., Flipse, J., Vlak, J.M., and Pijlman, G.P. (2012). Chikungunya virus nsP3 blocks stress granule assembly by recruitment of G3BP into cytoplasmic foci. Journal of virology *86*, 10873-10879.

Fu, Y., Dominissini, D., Rechavi, G., and He, C. (2014). Gene expression regulation mediated through reversible m(6)A RNA methylation. Nature reviews Genetics *15*, 293-306.

Fujimura, K., Kano, F., and Murata, M. (2008). Identification of PCBP2, a facilitator of IRES-mediated translation, as a novel constituent of stress granules and processing bodies. Rna *14*, 425-431.

Garaigorta, U., Heim, M.H., Boyd, B., Wieland, S., and Chisari, F.V. (2012). Hepatitis C virus (HCV) induces formation of stress granules whose proteins regulate HCV RNA replication and virus assembly and egress. Journal of virology *86*, 11043-11056.

Garrey, J.L., Lee, Y.Y., Au, H.H., Bushell, M., and Jan, E. (2010). Host and viral translational mechanisms during cricket paralysis virus infection. Journal of virology *84*, 1124-1138.

Ghadge, G.D., Malhotra, P., Furtado, M.R., Dhar, R., and Thimmapaya, B. (1994). In vitro analysis of virus-associated RNA I (VAI RNA): inhibition of the double-stranded RNA-activated protein kinase PKR by VAI RNA mutants correlates with the in vivo phenotype and the structural integrity of the central domain. Journal of virology *68*, 4137-4151.

Gibbings, D.J., Ciaudo, C., Erhardt, M., and Voinnet, O. (2009). Multivesicular bodies associate with components of miRNA effector complexes and modulate miRNA activity. Nat Cell Biol *11*, 1143-1149.

Gilks, N., Kedersha, N., Ayodele, M., Shen, L., Stoecklin, G., Dember, L.M., and Anderson, P. (2004). Stress granule assembly is mediated by prion-like aggregation of TIA-1. Molecular biology of the cell *15*, 5383-5398.

Gingras, A.C., Svitkin, Y., Belsham, G.J., Pause, A., and Sonenberg, N. (1996). Activation of the translational suppressor 4E-BP1 following infection with

encephalomyocarditis virus and poliovirus. Proceedings of the National Academy of Sciences of the United States of America *93*, 5578-5583.

Glass, M.J., and Summers, D.F. (1992). A cis-acting element within the hepatitis A virus 5'-non-coding region required for in vitro translation. Virus research *26*, 15-31.

Guil, S., Long, J.C., and Caceres, J.F. (2006). hnRNP A1 relocalization to the stress granules reflects a role in the stress response. Molecular and cellular biology *26*, 5744-5758.

Guo, Z.X., He, J.G., Xu, H.D., and Weng, S.P. (2013). Pathogenicity and complete genome sequence analysis of the mud crab dicistrovirus-1. Virus research *171*, 8-14.

Han, T.W., Kato, M., Xie, S., Wu, L.C., Mirzaei, H., Pei, J., Chen, M., Xie, Y., Allen, J., Xiao, G.*, et al.* (2012). Cell-free formation of RNA granules: bound RNAs identify features and components of cellular assemblies. Cell *149*, 768-779.

Hashem, Y., des Georges, A., Fu, J., Buss, S.N., Jossinet, F., Jobe, A., Zhang, Q., Liao, H.Y., Grassucci, R.A., Bajaj, C.*, et al.* (2013). High-resolution cryo-electron microscopy structure of the Trypanosoma brucei ribosome. Nature *494*, 385-389.

Henke, J.I., Goergen, D., Zheng, J., Song, Y., Schuttler, C.G., Fehr, C., Junemann, C., and Niepmann, M. (2008). microRNA-122 stimulates translation of hepatitis C virus RNA. The EMBO journal *27*, 3300-3310.

Hilbert, M., Kebbel, F., Gubaev, A., and Klostermeier, D. (2011). eIF4G stimulates the activity of the DEAD box protein eIF4A by a conformational guidance mechanism. Nucleic acids research *39*, 2260-2270.

Hilgers, V., Teixeira, D., and Parker, R. (2006). Translation-independent inhibition of mRNA deadenylation during stress in Saccharomyces cerevisiae. Rna *12*, 1835-1845.

Hinnebusch, A.G., and Lorsch, J.R. (2012). The mechanism of eukaryotic translation initiation: new insights and challenges. Cold Spring Harbor perspectives in biology *4*.

Hussain, T., Llacer, J.L., Fernandez, I.S., Munoz, A., Martin-Marcos, P., Savva, C.G., Lorsch, J.R., Hinnebusch, A.G., and Ramakrishnan, V. (2014). Structural

changes enable start codon recognition by the eukaryotic translation initiation complex. Cell *159*, 597-607.

Ingelfinger, D., Arndt-Jovin, D.J., Luhrmann, R., and Achsel, T. (2002). The human LSm1-7 proteins colocalize with the mRNA-degrading enzymes Dcp1/2 and Xrnl in distinct cytoplasmic foci. Rna *8*, 1489-1501.

Irvine, K., Stirling, R., Hume, D., and Kennedy, D. (2004). Rasputin, more promiscuous than ever: a review of G3BP. The International journal of developmental biology *48*, 1065-1077.

Iwasaki, S., and Tomari, Y. (2009). Argonaute-mediated translational repression (and activation). Fly *3*, 204-206.

Jackson, R.J., Hellen, C.U., and Pestova, T.V. (2010). The mechanism of eukaryotic translation initiation and principles of its regulation. Nature reviews Molecular cell biology *11*, 113-127.

Jan, E. (2006). Divergent IRES elements in invertebrates. Virus research *119*, 16-28.

Jan, E., and Sarnow, P. (2002). Factorless ribosome assembly on the internal ribosome entry site of cricket paralysis virus. Journal of molecular biology *324*, 889-902.

Jang, C.J., and Jan, E. (2010). Modular domains of the Dicistroviridae intergenic internal ribosome entry site. Rna *16*, 1182-1195.

Jang, C.J., Lo, M.C., and Jan, E. (2009). Conserved element of the dicistrovirus IGR IRES that mimics an E-site tRNA/ribosome interaction mediates multiple functions. Journal of molecular biology *387*, 42-58.

Jang, S.K., Krausslich, H.G., Nicklin, M.J., Duke, G.M., Palmenberg, A.C., and Wimmer, E. (1988). A segment of the 5' nontranslated region of encephalomyocarditis virus RNA directs internal entry of ribosomes during in vitro translation. Journal of virology *62*, 2636-2643.

Jordan, B.R. (1975). Demonstration of intact 26 S ribosomal RNA molecules in Drosophila cells. Journal of molecular biology *98*, 277-280.

Kapp, L.D., and Lorsch, J.R. (2004). GTP-dependent recognition of the methionine moiety on initiator tRNA by translation factor eIF2. Journal of molecular biology *335*, 923-936.

Kedersha, N., Chen, S., Gilks, N., Li, W., Miller, I.J., Stahl, J., and Anderson, P. (2002). Evidence that ternary complex (eIF2-GTP-tRNA(i)(Met))-deficient preinitiation complexes are core constituents of mammalian stress granules. Molecular biology of the cell *13*, 195-210.

Kedersha, N., Cho, M.R., Li, W., Yacono, P.W., Chen, S., Gilks, N., Golan, D.E., and Anderson, P. (2000). Dynamic shuttling of TIA-1 accompanies the recruitment of mRNA to mammalian stress granules. J Cell Biol *151*, 1257-1268.

Kedersha, N., Stoecklin, G., Ayodele, M., Yacono, P., Lykke-Andersen, J., Fritzler, M.J., Scheuner, D., Kaufman, R.J., Golan, D.E., and Anderson, P. (2005). Stress granules and processing bodies are dynamically linked sites of mRNP remodeling. The Journal of cell biology *169*, 871-884.

Kedersha, N.L., Gupta, M., Li, W., Miller, I., and Anderson, P. (1999). RNA-binding proteins TIA-1 and TIAR link the phosphorylation of eIF-2 alpha to the assembly of mammalian stress granules. J Cell Biol *147*, 1431-1442.

Kerr, C.H., Wang, Q.S., Keatings, K., Khong, A., Allan, D., Yip, C.K., Foster, L.J., and Jan, E. (2015). The 5' untranslated region of a novel infectious molecular clone of the dicistrovirus Cricket paralysis virus modulates infection. Journal of virology.

Khaperskyy, D.A., Emara, M.M., Johnston, B.P., Anderson, P., Hatchette, T.F., and McCormick, C. (2014). Influenza a virus host shutoff disables antiviral stress-induced translation arrest. PLoS pathogens *10*, e1004217.

Khaperskyy, D.A., Hatchette, T.F., and McCormick, C. (2012). Influenza A virus inhibits cytoplasmic stress granule formation. FASEB journal : official publication of the Federation of American Societies for Experimental Biology *26*, 1629-1639.

Khong, A., and Jan, E. (2011). Modulation of stress granules and P bodies during dicistrovirus infection. Journal of virology *85*, 1439-1451.

Kieft, J.S. (2008). Viral IRES RNA structures and ribosome interactions. Trends in biochemical sciences *33*, 274-283.

Kimball, S.R., Horetsky, R.L., Ron, D., Jefferson, L.S., and Harding, H.P. (2003). Mammalian stress granules represent sites of accumulation of stalled translation initiation complexes. American journal of physiology Cell physiology *284*, C273-284.

Koh, C.S., Brilot, A.F., Grigorieff, N., and Korostelev, A.A. (2014). Taura syndrome virus IRES initiates translation by binding its tRNA-mRNA-like structural element in the ribosomal decoding center. Proceedings of the National Academy of Sciences of the United States of America *111*, 9139-9144.

Komar, A.A., and Hatzoglou, M. (2011). Cellular IRES-mediated translation: the war of ITAFs in pathophysiological states. Cell cycle *10*, 229-240.

Komarova, A.V., Real, E., Borman, A.M., Brocard, M., England, P., Tordo, N., Hershey, J.W., Kean, K.M., and Jacob, Y. (2007). Rabies virus matrix protein interplay with eIF3, new insights into rabies virus pathogenesis. Nucleic acids research *35*, 1522-1532.

Kormann, M.S., Hasenpusch, G., Aneja, M.K., Nica, G., Flemmer, A.W., Herber-Jonat, S., Huppmann, M., Mays, L.E., Illenyi, M., Schams, A.*, et al.* (2011). Expression of therapeutic proteins after delivery of chemically modified mRNA in mice. Nature biotechnology *29*, 154-157.

Kozak, M. (1984). Point mutations close to the AUG initiator codon affect the efficiency of translation of rat preproinsulin in vivo. Nature *308*, 241-246.

Kozak, M. (1986). Point mutations define a sequence flanking the AUG initiator codon that modulates translation by eukaryotic ribosomes. Cell *44*, 283-292.

Kozak, M. (2003). Alternative ways to think about mRNA sequences and proteins that appear to promote internal initiation of translation. Gene *318*, 1-23.

Kozak, M. (2005). A second look at cellular mRNA sequences said to function as internal ribosome entry sites. Nucleic acids research *33*, 6593-6602.

Kuhn, R., Luz, N., and Beck, E. (1990). Functional analysis of the internal translation initiation site of foot-and-mouth disease virus. Journal of virology *64*, 4625-4631.

Kundu, P., Raychaudhuri, S., Tsai, W., and Dasgupta, A. (2005). Shutoff of RNA polymerase II transcription by poliovirus involves 3C protease-mediated cleavage of the TATA-binding protein at an alternative site: incomplete shutoff of transcription interferes with efficient viral replication. Journal of virology *79*, 9702-9713.

Kwon, S., Zhang, Y., and Matthias, P. (2007). The deacetylase HDAC6 is a novel critical component of stress granules involved in the stress response. Genes & development *21*, 3381-3394.

Landry, D.M., Hertz, M.I., and Thompson, S.R. (2009). RPS25 is essential for translation initiation by the Dicistroviridae and hepatitis C viral IRESs. Genes & development *23*, 2753-2764.

Lee, M., Kim, B., and Kim, V.N. (2014). Emerging roles of RNA modification: m(6)A and U-tail. Cell *158*, 980-987.

Lemaitre, B., Nicolas, E., Michaut, L., Reichhart, J.M., and Hoffmann, J.A. (1996). The dorsoventral regulatory gene cassette spatzle/Toll/cactus controls the potent antifungal response in Drosophila adults. Cell *86*, 973-983.

Leung, A.K., Calabrese, J.M., and Sharp, P.A. (2006). Quantitative analysis of Argonaute protein reveals microRNA-dependent localization to stress granules. Proc Natl Acad Sci U S A *103*, 18125-18130.

Li, C.H., Ohn, T., Ivanov, P., Tisdale, S., and Anderson, P. (2009). eIF5A promotes translation elongation, polysome disassembly and stress granule assembly. PLoS One *5*, e9942.

Li, P., Banjade, S., Cheng, H.C., Kim, S., Chen, B., Guo, L., Llaguno, M., Hollingsworth, J.V., King, D.S., Banani, S.F.*, et al.* (2012). Phase transitions in the assembly of multivalent signalling proteins. Nature *483*, 336-340.

Lightner, D.V. (1996). Epizootiology, distribution and the impact on international trade of two penaeid shrimp viruses in the Americas. Revue scientifique et technique *15*, 579-601.

Lightner, D.V., Redman, R.M., Poulos, B.T., Nunan, L.M., Mari, J.L., and Hasson, K.W. (1997). Risk of spread of penaeid shrimp viruses in the Americas by the international movement of live and frozen shrimp. Revue scientifique et technique *16*, 146-160.

Lin, J.Y., Li, M.L., and Shih, S.R. (2009). Far upstream element binding protein 2 interacts with enterovirus 71 internal ribosomal entry site and negatively regulates viral translation. Nucleic acids research *37*, 47-59.

Linero, F.N., Thomas, M.G., Boccaccio, G.L., and Scolaro, L.A. (2011). Junin virus infection impairs stress-granule formation in Vero cells treated with arsenite via inhibition of eIF2alpha phosphorylation. The Journal of general virology *92*, 2889-2899.

Liu, J., Rivas, F.V., Wohlschlegel, J., Yates, J.R., 3rd, Parker, R., and Hannon, G.J. (2005). A role for the P-body component GW182 in microRNA function. Nat Cell Biol *7*, 1261-1266.

Lloyd, R.E. (2013). Regulation of stress granules and P-bodies during RNA virus infection. Wiley interdisciplinary reviews RNA *4*, 317-331.

Loschi, M., Leishman, C.C., Berardone, N., and Boccaccio, G.L. (2009). Dynein and kinesin regulate stress-granule and P-body dynamics. Journal of cell science *122*, 3973-3982.

Lu, R., Maduro, M., Li, F., Li, H.W., Broitman-Maduro, G., Li, W.X., and Ding, S.W. (2005). Animal virus replication and RNAi-mediated antiviral silencing in Caenorhabditis elegans. Nature *436*, 1040-1043.

Lu, Y., Wambach, M., Katze, M.G., and Krug, R.M. (1995). Binding of the influenza virus NS1 protein to double-stranded RNA inhibits the activation of the protein kinase that phosphorylates the eIF-2 translation initiation factor. Virology *214*, 222-228.

Maag, D., Fekete, C.A., Gryczynski, Z., and Lorsch, J.R. (2005). A conformational change in the eukaryotic translation preinitiation complex and release of eIF1 signal recognition of the start codon. Molecular cell *17*, 265-275.

Mader, S., Lee, H., Pause, A., and Sonenberg, N. (1995). The translation initiation factor eIF-4E binds to a common motif shared by the translation factor eIF-4 gamma and the translational repressors 4E-binding proteins. Molecular and cellular biology *15*, 4990-4997.

Majzoub, K., Hafirassou, M.L., Meignin, C., Goto, A., Marzi, S., Fedorova, A., Verdier, Y., Vinh, J., Hoffmann, J.A., Martin, F.*, et al.* (2014). RACK1 controls IRES-mediated translation of viruses. Cell *159*, 1086-1095.

Maldonado, E., Cabrejos, M.E., Banks, L., and Allende, J.E. (2002). Human papillomavirus-16 E7 protein inhibits the DNA interaction of the TATA binding transcription factor. Journal of cellular biochemistry *85*, 663-669.

Mazroui, R., Sukarieh, R., Bordeleau, M.E., Kaufman, R.J., Northcote, P., Tanaka, J., Gallouzi, I., and Pelletier, J. (2006). Inhibition of ribosome recruitment induces stress granule formation independently of eukaryotic initiation factor 2alpha phosphorylation. Molecular biology of the cell *17*, 4212-4219.

Medzhitov, R., Preston-Hurlburt, P., and Janeway, C.A., Jr. (1997). A human homologue of the Drosophila Toll protein signals activation of adaptive immunity. Nature *388*, 394-397.

Meyer, K.D., and Jaffrey, S.R. (2014). The dynamic epitranscriptome: N6-methyladenosine and gene expression control. Nature reviews Molecular cell biology *15*, 313-326.

Miller, W.A., and Koev, G. (2000). Synthesis of subgenomic RNAs by positive-strand RNA viruses. Virology *273*, 1-8.

Miller, W.A., Wang, Z., and Treder, K. (2007). The amazing diversity of cap-independent translation elements in the 3'-untranslated regions of plant viral RNAs. Biochemical Society transactions *35*, 1629-1633.

Mokas, S., Mills, J.R., Garreau, C., Fournier, M.J., Robert, F., Arya, P., Kaufman, R.J., Pelletier, J., and Mazroui, R. (2009). Uncoupling stress granule assembly and translation initiation inhibition. Molecular biology of the cell *20*, 2673-2683.

Mollet, S., Cougot, N., Wilczynska, A., Dautry, F., Kress, M., Bertrand, E., and Weil, D. (2008). Translationally repressed mRNA transiently cycles through stress granules during stress. Molecular biology of the cell *19*, 4469-4479.

Moore, N.F., Kearns, A., and Pullin, J.S. (1980). Characterization of cricket paralysis virus-induced polypeptides in Drosophila cells. Journal of virology *33*, 1-9.

Nayak, A., Berry, B., Tassetto, M., Kunitomi, M., Acevedo, A., Deng, C., Krutchinsky, A., Gross, J., Antoniewski, C., and Andino, R. (2010). Cricket paralysis virus antagonizes Argonaute 2 to modulate antiviral defense in Drosophila. Nature structural & molecular biology *17*, 547-554.

Ng, T.F., Marine, R., Wang, C., Simmonds, P., Kapusinszky, B., Bodhidatta, L., Oderinde, B.S., Wommack, K.E., and Delwart, E. (2012). High variety of known and new RNA and DNA viruses of diverse origins in untreated sewage. Journal of virology *86*, 12161-12175.

Nielsen, K.H., Behrens, M.A., He, Y., Oliveira, C.L., Jensen, L.S., Hoffmann, S.V., Pedersen, J.S., and Andersen, G.R. (2011). Synergistic activation of eIF4A by eIF4B and eIF4G. Nucleic acids research *39*, 2678-2689.

Niepmann, M. (2009). Activation of hepatitis C virus translation by a liver-specific microRNA. Cell cycle *8*, 1473-1477.

O'Neill, L.A., Golenbock, D., and Bowie, A.G. (2013). The history of Toll-like receptors - redefining innate immunity. Nature reviews Immunology *13*, 453-460.

Oberer, M., Marintchev, A., and Wagner, G. (2005). Structural basis for the enhancement of eIF4A helicase activity by eIF4G. Genes & development *19*, 2212-2223.

Ohn, T., Kedersha, N., Hickman, T., Tisdale, S., and Anderson, P. (2008). A functional RNAi screen links O-GlcNAc modification of ribosomal proteins to stress granule and processing body assembly. Nature cell biology *10*, 1224-1231.

Onomoto, K., Jogi, M., Yoo, J.S., Narita, R., Morimoto, S., Takemura, A., Sambhara, S., Kawaguchi, A., Osari, S., Nagata, K.*, et al.* (2012). Critical role of an antiviral stress granule containing RIG-I and PKR in viral detection and innate immunity. PloS one *7*, e43031.

Ozes, A.R., Feoktistova, K., Avanzino, B.C., and Fraser, C.S. (2011). Duplex unwinding and ATPase activities of the DEAD-box helicase eIF4A are coupled by eIF4G and eIF4B. Journal of molecular biology *412*, 674-687.

Pager, C.T., Schutz, S., Abraham, T.M., Luo, G., and Sarnow, P. (2013). Modulation of hepatitis C virus RNA abundance and virus release by dispersion of processing bodies and enrichment of stress granules. Virology *435*, 472-484.

Panas, M.D., Varjak, M., Lulla, A., Eng, K.E., Merits, A., Karlsson Hedestam, G.B., and McInerney, G.M. (2012). Sequestration of G3BP coupled with efficient translation inhibits stress granules in Semliki Forest virus infection. Molecular biology of the cell *23*, 4701-4712.

Parrish, S., and Moss, B. (2007). Characterization of a second vaccinia virus mRNA-decapping enzyme conserved in poxviruses. Journal of virology *81*, 12973 - 12978.

Parrish, S., Resch, W., and Moss, B. (2007). Vaccinia virus D10 protein has mRNA decapping activity, providing a mechanism for control of host and viral gene expression. Proceedings of the National Academy of Sciences of the United States of America *104*, 2139-2144.

Passmore, L.A., Schmeing, T.M., Maag, D., Applefield, D.J., Acker, M.G., Algire, M.A., Lorsch, J.R., and Ramakrishnan, V. (2007). The eukaryotic translation initiation factors eIF1 and eIF1A induce an open conformation of the 40S ribosome. Molecular cell *26*, 41-50.

Pelletier, J., and Sonenberg, N. (1988). Internal initiation of translation of eukaryotic mRNA directed by a sequence derived from poliovirus RNA. Nature *334*, 320-325.

Pestova, T.V., and Kolupaeva, V.G. (2002). The roles of individual eukaryotic translation initiation factors in ribosomal scanning and initiation codon selection. Genes & development *16*, 2906-2922.

Pestova, T.V., Lomakin, I.B., Lee, J.H., Choi, S.K., Dever, T.E., and Hellen, C.U. (2000). The joining of ribosomal subunits in eukaryotes requires eIF5B. Nature *403*, 332-335.

Pfingsten, J.S., Costantino, D.A., and Kieft, J.S. (2006). Structural basis for ribosome recruitment and manipulation by a viral IRES RNA. Science *314*, 1450-1454.

Piotrowska, J., Hansen, S.J., Park, N., Jamka, K., Sarnow, P., and Gustin, K.E. (2010). Stable formation of compositionally unique stress granules in virus-infected cells. Journal of virology *84*, 3654-3665.

Pisarev, A.V., Kolupaeva, V.G., Pisareva, V.P., Merrick, W.C., Hellen, C.U., and Pestova, T.V. (2006). Specific functional interactions of nucleotides at key -3 and +4 positions flanking the initiation codon with components of the mammalian 48S translation initiation complex. Genes & development *20*, 624-636.

Pisareva, V.P., Pisarev, A.V., Komar, A.A., Hellen, C.U., and Pestova, T.V. (2008). Translation initiation on mammalian mRNAs with structured 5'UTRs requires DExH-box protein DHX29. Cell *135*, 1237-1250.

Plotch, S.J., Bouloy, M., Ulmanen, I., and Krug, R.M. (1981). A unique cap(m7GpppXm)-dependent influenza virion endonuclease cleaves capped

RNAs to generate the primers that initiate viral RNA transcription. Cell *23*, 847-858.

Rehwinkel, J., Behm-Ansmant, I., Gatfield, D., and Izaurralde, E. (2005). A crucial role for GW182 and the DCP1:DCP2 decapping complex in miRNA-mediated gene silencing. Rna *11*, 1640-1647.

Reineke, L.C., Dougherty, J.D., Pierre, P., and Lloyd, R.E. (2012). Large G3BP-induced granules trigger eIF2alpha phosphorylation. Molecular biology of the cell *23*, 3499-3510.

Reineke, L.C., Kedersha, N., Langereis, M.A., van Kuppeveld, F.J., and Lloyd, R.E. (2015). Stress Granules Regulate Double-Stranded RNA-Dependent Protein Kinase Activation through a Complex Containing G3BP1 and Caprin1. mBio *6*.

Reineke, L.C., and Lloyd, R.E. (2013). Diversion of stress granules and P-bodies during viral infection. Virology *436*, 255-267.

Reineke, L.C., and Lloyd, R.E. (2015). The Stress Granule Protein G3BP1 Recruits Protein Kinase R To Promote Multiple Innate Immune Antiviral Responses. Journal of virology *89*, 2575-2589.

Reinganum, C. (1975). The isolation of cricket paralysis virus from the emperor gum moth, Antheraea eucalypti Scott, and its infectivity towards a range of insect species. Intervirology *5*, 97-102.

Rijnbrand, R., van der Straaten, T., van Rijn, P.A., Spaan, W.J., and Bredenbeek, P.J. (1997). Internal entry of ribosomes is directed by the 5' noncoding region of classical swine fever virus and is dependent on the presence of an RNA pseudoknot upstream of the initiation codon. Journal of virology *71*, 451-457.

Riley, A., Jordan, L.E., and Holcik, M. (2010). Distinct 5' UTRs regulate XIAP expression under normal growth conditions and during cellular stress. Nucleic acids research *38*, 4665-4674.

Rivas-Estilla, A.M., Svitkin, Y., Lopez Lastra, M., Hatzoglou, M., Sherker, A., and Koromilas, A.E. (2002). PKR-dependent mechanisms of gene expression from a subgenomic hepatitis C virus clone. Journal of virology *76*, 10637-10653.

Roberts, L.O., and Groppelli, E. (2009). An atypical IRES within the 5' UTR of a dicistrovirus genome. Virus research *139*, 157-165.

Roberts, L.O., Jopling, C.L., Jackson, R.J., and Willis, A.E. (2009). Viral strategies to subvert the mammalian translation machinery. Progress in molecular biology and translational science *90*, 313-367.

Rodriguez Pulido, M., Serrano, P., Saiz, M., and Martinez-Salas, E. (2007). Foot-and-mouth disease virus infection induces proteolytic cleavage of PTB, eIF3a,b, and PABP RNA-binding proteins. Virology *364*, 466-474.

Rowlands, A.G., Panniers, R., and Henshaw, E.C. (1988). The catalytic mechanism of guanine nucleotide exchange factor action and competitive inhibition by phosphorylated eukaryotic initiation factor 2. The Journal of biological chemistry *263*, 5526-5533.

Roy, G., Miron, M., Khaleghpour, K., Lasko, P., and Sonenberg, N. (2004). The Drosophila poly(A) binding protein-interacting protein, dPaip2, is a novel effector of cell growth. Molecular and cellular biology *24*, 1143-1154.

Ruggieri, A., Dazert, E., Metz, P., Hofmann, S., Bergeest, J.P., Mazur, J., Bankhead, P., Hiet, M.S., Kallis, S., Alvisi, G.*, et al.* (2012). Dynamic oscillation of translation and stress granule formation mark the cellular response to virus infection. Cell host & microbe *12*, 71-85.

Sabin, L.R., Hanna, S.L., and Cherry, S. (2010). Innate antiviral immunity in Drosophila. Current opinion in immunology *22*, 4-9.

Sasaki, J., and Nakashima, N. (1999). Translation initiation at the CUU codon is mediated by the internal ribosome entry site of an insect picorna-like virus in vitro. Journal of virology *73*, 1219-1226.

Sato, H., Masuda, M., Kanai, M., Tsukiyama-Kohara, K., Yoneda, M., and Kai, C. (2007). Measles virus N protein inhibits host translation by binding to eIF3-p40. Journal of virology *81*, 11569-11576.

Schneider, M.D., Najand, N., Chaker, S., Pare, J.M., Haskins, J., Hughes, S.C., Hobman, T.C., Locke, J., and Simmonds, A.J. (2006). Gawky is a component of cytoplasmic mRNA processing bodies required for early Drosophila development. J Cell Biol *174*, 349-358.

Schnettler, E., Sterken, M.G., Leung, J.Y., Metz, S.W., Geertsema, C., Goldbach, R.W., Vlak, J.M., Kohl, A., Khromykh, A.A., and Pijlman, G.P. (2012). Noncoding

flavivirus RNA displays RNA interference suppressor activity in insect and Mammalian cells. Journal of virology *86*, 13486-13500.

Schuler, M., Connell, S.R., Lescoute, A., Giesebrecht, J., Dabrowski, M., Schroeer, B., Mielke, T., Penczek, P.A., Westhof, E., and Spahn, C.M. (2006). Structure of the ribosome-bound cricket paralysis virus IRES RNA. Nature structural & molecular biology *13*, 1092-1096.

Schutz, P., Bumann, M., Oberholzer, A.E., Bieniossek, C., Trachsel, H., Altmann, M., and Baumann, U. (2008). Crystal structure of the yeast eIF4A-eIF4G complex: an RNA-helicase controlled by protein-protein interactions. Proceedings of the National Academy of Sciences of the United States of America *105*, 9564-9569.

Semler, B.L., and Waterman, M.L. (2008). IRES-mediated pathways to polysomes: nuclear versus cytoplasmic routes. Trends in microbiology *16*, 1-5.

Sharp, T.V., Schwemmle, M., Jeffrey, I., Laing, K., Mellor, H., Proud, C.G., Hilse, K., and Clemens, M.J. (1993). Comparative analysis of the regulation of the interferon-inducible protein kinase PKR by Epstein-Barr virus RNAs EBER-1 and EBER-2 and adenovirus VAI RNA. Nucleic acids research *21*, 4483-4490.

Shuman, S. (1990). Catalytic activity of vaccinia mRNA capping enzyme subunits coexpressed in Escherichia coli. The Journal of biological chemistry *265*, 11960-11966.

Skabkin, M.A., Skabkina, O.V., Dhote, V., Komar, A.A., Hellen, C.U., and Pestova, T.V. (2010). Activities of Ligatin and MCT-1/DENR in eukaryotic translation initiation and ribosomal recycling. Genes & development *24*, 1787-1801.

Sonenberg, N., and Hinnebusch, A.G. (2009). Regulation of translation initiation in eukaryotes: mechanisms and biological targets. Cell *136*, 731-745.

Souquere, S., Mollet, S., Kress, M., Dautry, F., Pierron, G., and Weil, D. (2009). Unravelling the ultrastructure of stress granules and associated P-bodies in human cells. Journal of cell science *122*, 3619-3626.

Spahn, C.M., Jan, E., Mulder, A., Grassucci, R.A., Sarnow, P., and Frank, J. (2004). Cryo-EM visualization of a viral internal ribosome entry site bound to human ribosomes: the IRES functions as an RNA-based translation factor. Cell *118*, 465-475.

Spriggs, K.A., Bushell, M., Mitchell, S.A., and Willis, A.E. (2005). Internal ribosome entry segment-mediated translation during apoptosis: the role of IRES-trans-acting factors. Cell death and differentiation *12*, 585-591.

Stoecklin, G., Stubbs, T., Kedersha, N., Wax, S., Rigby, W.F., Blackwell, T.K., and Anderson, P. (2004). MK2-induced tristetraprolin:14-3-3 complexes prevent stress granule association and ARE-mRNA decay. EMBO J *23*, 1313-1324.

Stoneley, M., Subkhankulova, T., Le Quesne, J.P., Coldwell, M.J., Jopling, C.L., Belsham, G.J., and Willis, A.E. (2000). Analysis of the c-myc IRES; a potential role for cell-type specific trans-acting factors and the nuclear compartment. Nucleic acids research *28*, 687-694.

Strober, W. (2001). Trypan blue exclusion test of cell viability. Current protocols in immunology / edited by John E Coligan [et al] *Appendix 3*, Appendix 3B.

Sullivan, C.S., and Ganem, D. (2005). A virus-encoded inhibitor that blocks RNA interference in mammalian cells. Journal of virology *79*, 7371-7379.

Tate, J., Liljas, L., Scotti, P., Christian, P., Lin, T., and Johnson, J.E. (1999). The crystal structure of cricket paralysis virus: the first view of a new virus family. Nature structural biology *6*, 765-774.

Terenin, I.M., Andreev, D.E., Dmitriev, S.E., and Shatsky, I.N. (2013). A novel mechanism of eukaryotic translation initiation that is neither m7G-cap-, nor IRES-dependent. Nucleic acids research *41*, 1807-1816.

Thomas, M.G., Martinez Tosar, L.J., Desbats, M.A., Leishman, C.C., and Boccaccio, G.L. (2009). Mammalian Staufen 1 is recruited to stress granules and impairs their assembly. J Cell Sci *122*, 563-573.

Thompson, S.R. (2012). So you want to know if your message has an IRES? Wiley interdisciplinary reviews RNA *3*, 697-705.

Thompson, S.R., Gulyas, K.D., and Sarnow, P. (2001). Internal initiation in Saccharomyces cerevisiae mediated by an initiator tRNA/eIF2-independent internal ribosome entry site element. Proceedings of the National Academy of Sciences of the United States of America *98*, 12972-12977.

Tian, Q., Streuli, M., Saito, H., Schlossman, S.F., and Anderson, P. (1991). A polyadenylate binding protein localized to the granules of cytolytic lymphocytes induces DNA fragmentation in target cells. Cell *67*, 629-639.

Tourriere, H., Chebli, K., Zekri, L., Courselaud, B., Blanchard, J.M., Bertrand, E., and Tazi, J. (2003). The RasGAP-associated endoribonuclease G3BP assembles stress granules. The Journal of cell biology *160*, 823-831.

Tsuboi, T., Kuroha, K., Kudo, K., Makino, S., Inoue, E., Kashima, I., and Inada, T. (2012). Dom34:hbs1 plays a general role in quality-control systems by dissociation of a stalled ribosome at the 3' end of aberrant mRNA. Molecular cell *46*, 518-529.

Tsukiyama-Kohara, K., Iizuka, N., Kohara, M., and Nomoto, A. (1992). Internal ribosome entry site within hepatitis C virus RNA. Journal of virology *66*, 1476-1483.

Van Eden, M.E., Byrd, M.P., Sherrill, K.W., and Lloyd, R.E. (2004). Demonstrating internal ribosome entry sites in eukaryotic mRNAs using stringent RNA test procedures. Rna *10*, 720-730.

van Mierlo, J.T., Overheul, G.J., Obadia, B., van Cleef, K.W., Webster, C.L., Saleh, M.C., Obbard, D.J., and van Rij, R.P. (2014). Novel Drosophila viruses encode host-specific suppressors of RNAi. PLoS pathogens *10*, e1004256.

van Rij, R.P., Saleh, M.C., Berry, B., Foo, C., Houk, A., Antoniewski, C., and Andino, R. (2006). The RNA silencing endonuclease Argonaute 2 mediates specific antiviral immunity in Drosophila melanogaster. Genes & development *20*, 2985-2995.

Vasudevan, S., Tong, Y., and Steitz, J.A. (2007). Switching from repression to activation: microRNAs can up-regulate translation. Science *318*, 1931-1934.

Ventoso, I., Sanz, M.A., Molina, S., Berlanga, J.J., Carrasco, L., and Esteban, M. (2006). Translational resistance of late alphavirus mRNA to eIF2alpha phosphorylation: a strategy to overcome the antiviral effect of protein kinase PKR. Genes & development *20*, 87-100.

Victoria, J.G., Kapoor, A., Li, L., Blinkova, O., Slikas, B., Wang, C., Naeem, A., Zaidi, S., and Delwart, E. (2009). Metagenomic analyses of viruses in stool samples from children with acute flaccid paralysis. Journal of virology *83*, 4642-4651.

Vogt, C., Preuss, E., Mayer, D., Weber, F., Schwemmle, M., and Kochs, G. (2008). The interferon antagonist ML protein of thogoto virus targets general transcription factor IIB. Journal of virology *82*, 11446-11453.

Walsh, D., and Mohr, I. (2011). Viral subversion of the host protein synthesis machinery. Nature reviews Microbiology *9*, 860-875.

Wang, Q.S., Au, H.H., and Jan, E. (2013). Methods for studying IRES-mediated translation of positive-strand RNA viruses. Methods *59*, 167-179.

Wang, Q.S., and Jan, E. (2014). Switch from cap- to factorless IRES-dependent 0 and +1 frame translation during cellular stress and dicistrovirus infection. PloS one *9*, e103601.

Wang, X.H., Aliyari, R., Li, W.X., Li, H.W., Kim, K., Carthew, R., Atkinson, P., and Ding, S.W. (2006). RNA interference directs innate immunity against viruses in adult Drosophila. Science *312*, 452-454.

Weber, S.C., and Brangwynne, C.P. (2012). Getting RNA and protein in phase. Cell *149*, 1188-1191.

White, J.P., Cardenas, A.M., Marissen, W.E., and Lloyd, R.E. (2007). Inhibition of cytoplasmic mRNA stress granule formation by a viral proteinase. Cell Host Microbe *2*, 295-305.

White, J.P., and Lloyd, R.E. (2011). Poliovirus unlinks TIA1 aggregation and mRNA stress granule formation. Journal of virology *85*, 12442-12454.

Wilson, J.E., Powell, M.J., Hoover, S.E., and Sarnow, P. (2000). Naturally occurring dicistronic cricket paralysis virus RNA is regulated by two internal ribosome entry sites. Molecular and cellular biology *20*, 4990-4999.

Wu, X., He, W.T., Tian, S., Meng, D., Li, Y., Chen, W., Li, L., Tian, L., Zhong, C.Q., Han, F.*, et al.* (2014). pelo is required for high efficiency viral replication. PLoS pathogens *10*, e1004034.

Yu, Y., Abaeva, I.S., Marintchev, A., Pestova, T.V., and Hellen, C.U. (2011). Common conformational changes induced in type 2 picornavirus IRESs by cognate trans-acting factors. Nucleic acids research *39*, 4851-4865.

Zuo, X., Wang, J., Yu, P., Eyler, D., Xu, H., Starich, M.R., Tiede, D.M., Simon, A.E., Kasprzak, W., Schwieters, C.D.*, et al.* (2010). Solution structure of the cap-

independent translational enhancer and ribosome-binding element in the 3' UTR of turnip crinkle virus. Proceedings of the National Academy of Sciences of the United States of America *107*, 1385-1390.

Appendix

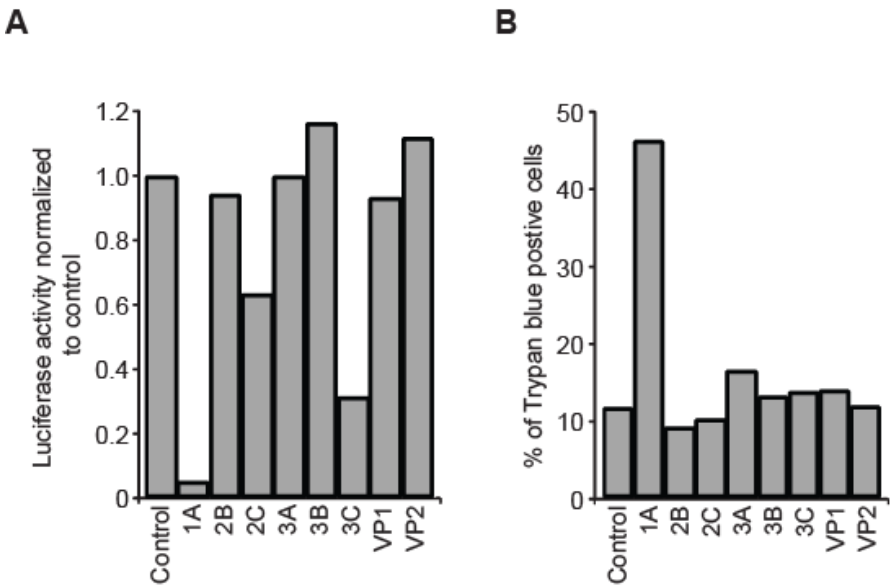

Supplemental figure 1 Luciferase and cell death assays when expressing recombinant CrPV viral proteins in *Drosophila* S2 cells. (A) Firefly luciferase activities from cells transfected for two days with dsRED (control), CrPV-1A, CrPV-2B, CrPV-2C, CrPV-3A, CrPV-3B, CrPV-3C, CrPV-VP1, or CrPV-VP2 expression plasmids. (B) Trypan blue staining of cells.